1976-03

A study of boundary layer and mass bleed in a short length supersonic diffuser for a gas dynamic laser

Habel, Paul Grimmer

Monterey, California. Naval Postgraduate School

A STUDY OF BOUNDARY LAYER AND MASS BLEED IN A SHORT LENGTH SUPERSONIC DIFFUSER FOR A GAS DYNAMIC LASER

Paul Grimmer Habel

NAVAL POSTGRADUATE SCHOOL
Monterey, California

THESIS

A Study of Boundary Layer and Mass Bleed in a Short Length Supersonic Diffuser for a Gas Dynamic Laser

by

Paul Grimmer Habel

March 1976

Thesis Advisor: A. E. Fuhs

SECURITY CLASSIFICATION OF THIS PAGE (When Data Entered)

REPORT DOCUMENTATION PAGE		READ INSTRUCTIONS BEFORE COMPLETING FORM
1. REPORT NUMBER	2. GOVT ACCESSION NO.	3. RECIPIENT'S CATALOG NUMBER
4. TITLE (and Subtitle) A Study of Boundary Layer and Mass Bleed in a Short Length Supersonic Diffuser for a Gas Dynamic Laser		5. TYPE OF REPORT & PERIOD COVERED Master's Thesis; March 1976
		6. PERFORMING ORG. REPORT NUMBER
7. AUTHOR(s) Paul Grimmer Habel		8. CONTRACT OR GRANT NUMBER(s)
9. PERFORMING ORGANIZATION NAME AND ADDRESS Naval Postgraduate School Monterey, California 93940		10. PROGRAM ELEMENT, PROJECT, TASK AREA & WORK UNIT NUMBERS
11. CONTROLLING OFFICE NAME AND ADDRESS Naval Postgraduate School Monterey, California 93940		12. REPORT DATE March 1976
		13. NUMBER OF PAGES 115
14. MONITORING AGENCY NAME & ADDRESS(if different from Controlling Office) Naval Postgraduate School Monterey, California 93940		15. SECURITY CLASS. (of this report) Unclassified
		15a. DECLASSIFICATION/DOWNGRADING SCHEDULE

16. DISTRIBUTION STATEMENT (of this Report)

Approved for public release; distribution unlimited.

17. DISTRIBUTION STATEMENT (of the abstract entered in Block 20, if different from Report)

18. SUPPLEMENTARY NOTES

19. KEY WORDS (Continue on reverse side if necessary and identify by block number)

Laser, Gas Dynamic Laser, Diffuser, Boundary Layer Bleed

20. ABSTRACT (Continue on reverse side if necessary and identify by block number)

This research was conducted to study the effect of boundary layer and mass bleed on the starting (i. e., establishment of supersonic flow) and running of a short length supersonic diffuser for a gas dynamic laser. A one-dimensional diffuser geometry which diffused the flow by an isentropic turn was laid out by the method of characteristics. Extensive boundary layer bleed holes and slots were incorporated in the diffuser walls. Self-actuating, one-way valves installed in the walls bled excess flow during starting. Schlieren flow visualization was obtained through opposite glass diffuser walls. The diffuser was started and Mach 3.5 flow established in a diffuser with a contraction ratio of 1.69. This geometry would not start without utilizing boundary layer and mass bleed. A mode of operation called self bleed was discovered. The lower static pressure in the diffuser entrance, via suitable ducting, was used to bleed the boundary layer in the diffuser throat. This method reduced the minimum operating stagnation pressure 17.0% without utilizing vacuum tanks or pumps. Testing confirmed that boundary layer bleed in the diffuser throat significantly lowers operating stagnation pressure.

A Study of Boundary Layer and Mass Bleed in a Short Length Supersonic Diffuser for a Gas Dynamic Laser

by

Paul Grimmer Habel
Lieutenant, United States Navy
B.S., University of Florida, 1967

Submitted in partial fulfillment of the requirements for the degree of

MASTER OF SCIENCE IN AERONAUTICAL ENGINEERING

from the

NAVAL POSTGRADUATE SCHOOL
March 1976

ABSTRACT

This research was conducted to study the effect of boundary layer and mass bleed on the starting (i.e., establishment of supersonic flow) and running of a short length supersonic diffuser for a gas dynamic laser. A one-dimensional diffuser geometry which diffused the flow by an isentropic turn was laid out by the method of characteristics. Extensive boundary layer bleed holes and slots were incorporated in the diffuser walls. Self-actuating, one-way valves installed in the walls bled excess flow during starting. Schlieren flow visualization was obtained through opposite glass diffuser walls. The diffuser was started and Mach 3.5 flow established in a diffuser with a contraction ratio of 1.69. This geometry would not start without utilizing boundary layer and mass bleed. A mode of operation called self bleed was discovered. The lower static pressure in the diffuser entrance, via suitable ducting, was used to bleed the boundary layer in the diffuser throat. This method reduced the minimum operating stagnation pressure 17.0% without utilizing vacuum tanks or pumps. Testing confirmed that boundary layer bleed in the diffuser throat significantly lowers operating stagnation pressure.

TABLE OF CONTENTS

LIST OF TABLES

LIST OF FIGURES

ACKNOWLEDGEMENT

The author wishes to express his most sincere gratitude and appreciation to Professor Allen E. Fuhs of the Naval Postgraduate School for his help in the preparation and execution of this project. Funding support for this project was provided by Naval Air Systems Command, Code 320; Mr. William Volz was project monitor. The author would also like to express his gratitude to Mr. John Moulton for his advice and the fabrication of the test apparatus, and to my dear wife for her support during this research and her help in the preparation of this report.

I. INTRODUCTION

A supersonic diffuser is an integral part of both gas dynamic and chemical lasers. The gas dynamics in each of these devices is analogous to that of a supersonic wind tunnel. Figure (1) shows schematically the gas flow and some flow parameters for a gas dynamic laser (GDL). Fuels, oxidizers, and additives whose combustion products possess the physical characteristics necessary for lasing under the correct circumstances are injected, mixed, and burned in the combustion chamber. Combustion increases the stagnation temperature in excess of 1500°F and the chamber pressure to greater than 10 atmospheres. The array of short length convergent/divergent nozzles rapidly expands the gases to pressures less than 0.5 psia and to speeds in excess of Mach 4. The lasing occurs just downstream of these nozzles in the lasing cavity at the above mentioned pressure and flow speed. After the lasing has occurred, the gases enter the diffuser where the static pressure is increased to ambient conditions and exhausted to the atmosphere. Figure (2) shows cutaways of actual GDLs.

A supersonic wind tunnel has the same flow regimes as the GDL. High pressure air is accelerated through only one nozzle into the test section and then decelerated with a subsequent pressure increase in the diffuser section. A GDL is very similar to the supersonic wind tunnel and has

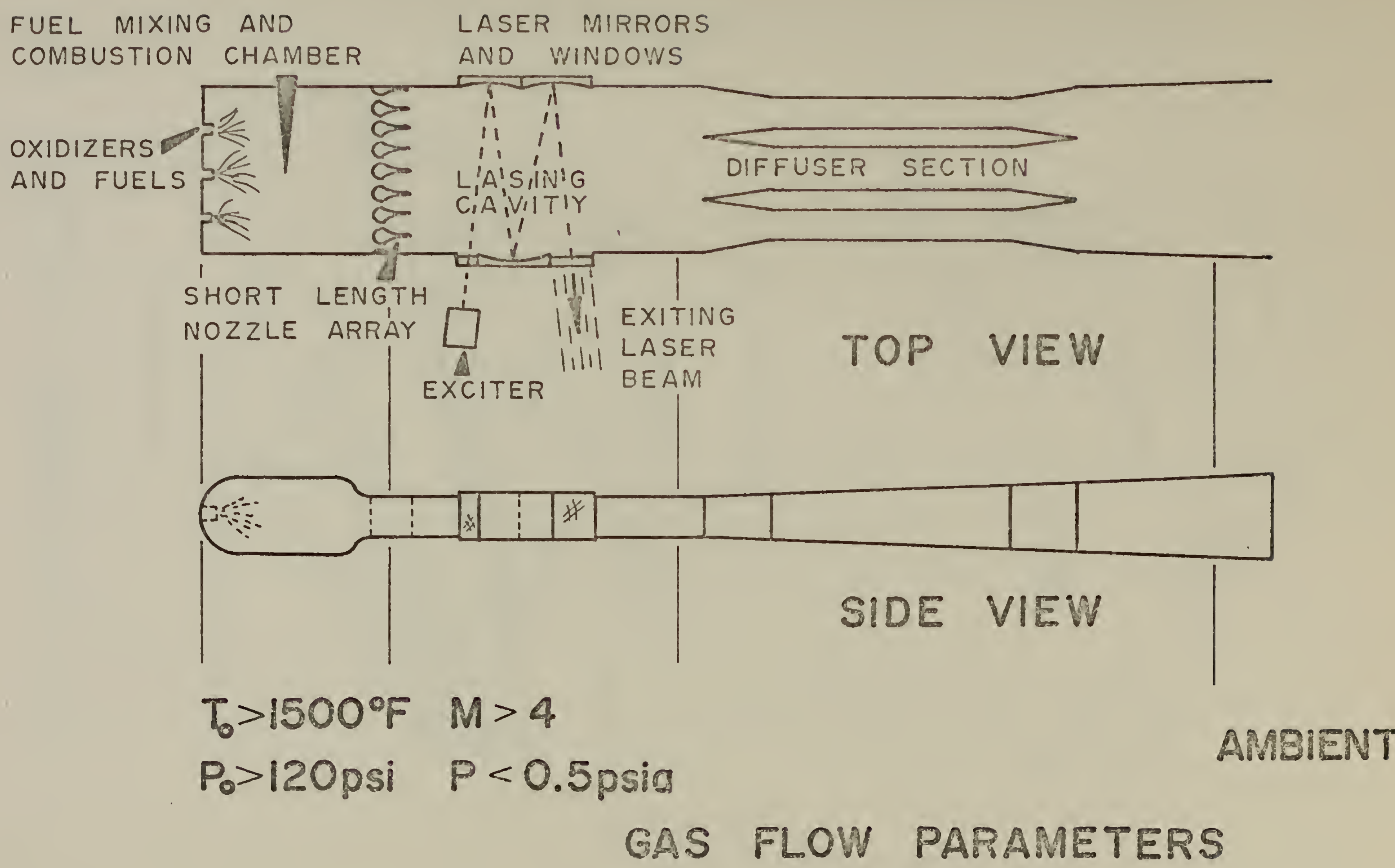

FIGURE (1) SCHEMATIC OF A GAS DYNAMIC LASER

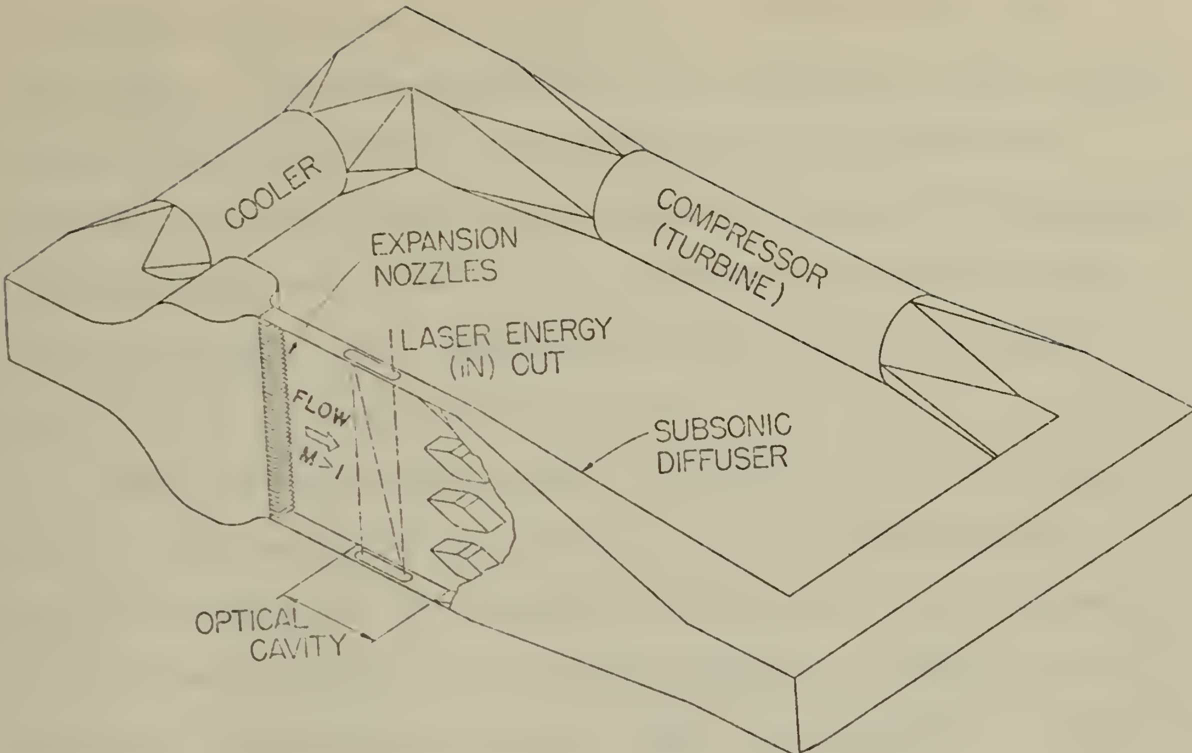

(a) Closed Cycle

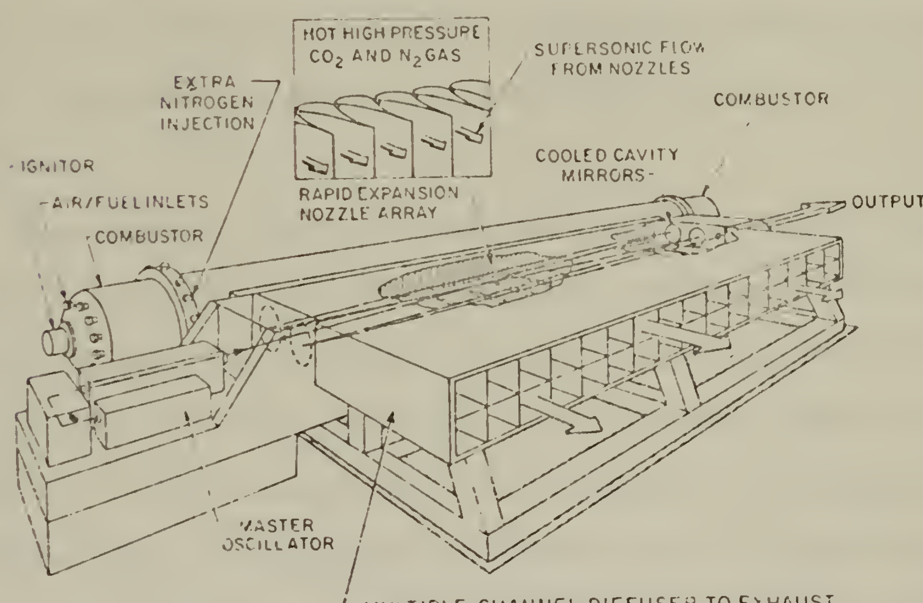

(b) Open Cycle

FIGURE (2) CUTAWAYS OF ACTUAL GDL'S
(FROM REF. 2)

a similar dependence on an effective diffuser for its operation. The efficiency of both of these gas flow devices is directly affected by the efficiency of the diffuser. The GDL diffuser represents a large portion of the apparatus; consequently, any reduction in diffuser size will greatly reduce the GDL size. Weight and volume are especially critical to an airborne GDL system.

Many methods can be used to diffuse a high speed gas flow. This research explored the use of boundary layer bleed on the walls of a supersonic diffuser. The diffusion process was accomplished by the isentropic turning of the flow in a rectangular channel. This configuration, diffusion by turning, was chosen because of its relatively short length and its potential application to high energy lasers. It was hoped that a reduction in starting and running pressures compared to previously published values could be attained.

The overall research was divided into three stages: analytical design, manufacture, and testing of the apparatus. The analytical design used the method of characteristics to lay out the diffuser channel. The boundary layer bleed system, i.e. hole size, hole distribution, and pressure differential, was designed to remove all of the boundary layer; its design was based on suitable boundary layer calculations. The machine shop staff in the Aeronautics Department of the Naval Postgraduate School, Monterey, California fabricated all the components. The apparatus was mounted on a high pressure air manifold in Building 230 of the Aeronautical Laboratories of the Naval Postgraduate School. Pressure readings and Schlieren photography of the flow in the diffuser were obtained. Section II covers pertinent aspects of diffuser operation. Details of the analytical design and boundary layer bleed calculations are covered in Section III. Section IV contains the experimental results and conclusions.

II. PRINCIPLES OF DIFFUSER OPERATION

A. ONE DIMENSIONAL SUPERSONIC DIFFUSERS

A supersonic diffuser cannot be designed as the reverse of a converging-diverging nozzle. Supersonic wind tunnels, GDLs, and chemical lasers all have diffusers preceded by a supersonic nozzle. Viscous effects, e.g. boundary layer displacement thickness and boundary layer separation in the nozzles and the diffuser require that the diffuser throat be somewhat larger than the nozzle throat. Supersonic flow will not be attained in the nozzle if the diffuser throat is made slightly too small. If the diffuser throat is slightly too large there will necessarily be a shock wave or several shock waves somewhere within the diffuser. Equal areas of the two throats in a combined system would be unstable and flow oscillations would occur. More serious problems arise during starting of the system when the flow accelerates from rest to operating velocity. During the starting process shock waves pass through the system. Across a normal shock there is no change in flow rate or stagnation temperature; however, the stagnation pressure is reduced. Reduction of stagnation pressure by a shock wave increases the minimum area through which the flow can be made to pass.

A gas dynamic or chemical laser is composed of converging-diverging nozzles, lasing cavity, and a diffuser. The diffuser exits either to ambient pressure or a lower value established by an exhauster. The ambient or exhauster pressure is fixed, and the stagnation pressure and temperature upstream of the nozzles are increased to constant values when flow is established. Figure (3) shows this arrangement.

B. STARTING CONDITIONS; ONE DIMENSIONAL MODEL

Consider the arrangement of a GDL as shown in Figure (3), and suppose that the exhaust conditions are constant. The stagnation pressure and temperature are increased and shocks move through the diverging sections of the nozzles and into the cavity. During this period the nozzle throats collectively are passing the maximum possible flow. A^* is defined as the sum of the throat areas of the nozzle array. The product P_oA^* is constant across a normal shock. Since P_o decreases due to a shock wave, A^* must increase. The worst condition occurs when the shock is moving through the lasing cavity where the shock occurs at the maximum possible Mach number and, consequently, produces the largest loss in stagnation pressure. For this condition the minimum total area of the diffuser throats is

$$\frac{A_{\text{min. diff. throat}}}{A_{\text{nozzle throat}}} = \frac{A_y^*}{A_x^*} = \frac{P_{ox}}{P_{oy}} \qquad (1)$$

where P_{oy}/P_{ox} is the stagnation pressure ratio for a shock at the lasing cavity or design Mach number. The limiting contraction ratio, ψ, where ψ equals A_x/A_y^* for the diffuser is

$$\psi = \frac{A_x}{A_y^*} = \frac{A_x}{A_x^*}\frac{A_x^*}{A_y^*} = \frac{A_x}{A_x^*}\frac{P_{oy}}{P_{ox}} \qquad (2)$$

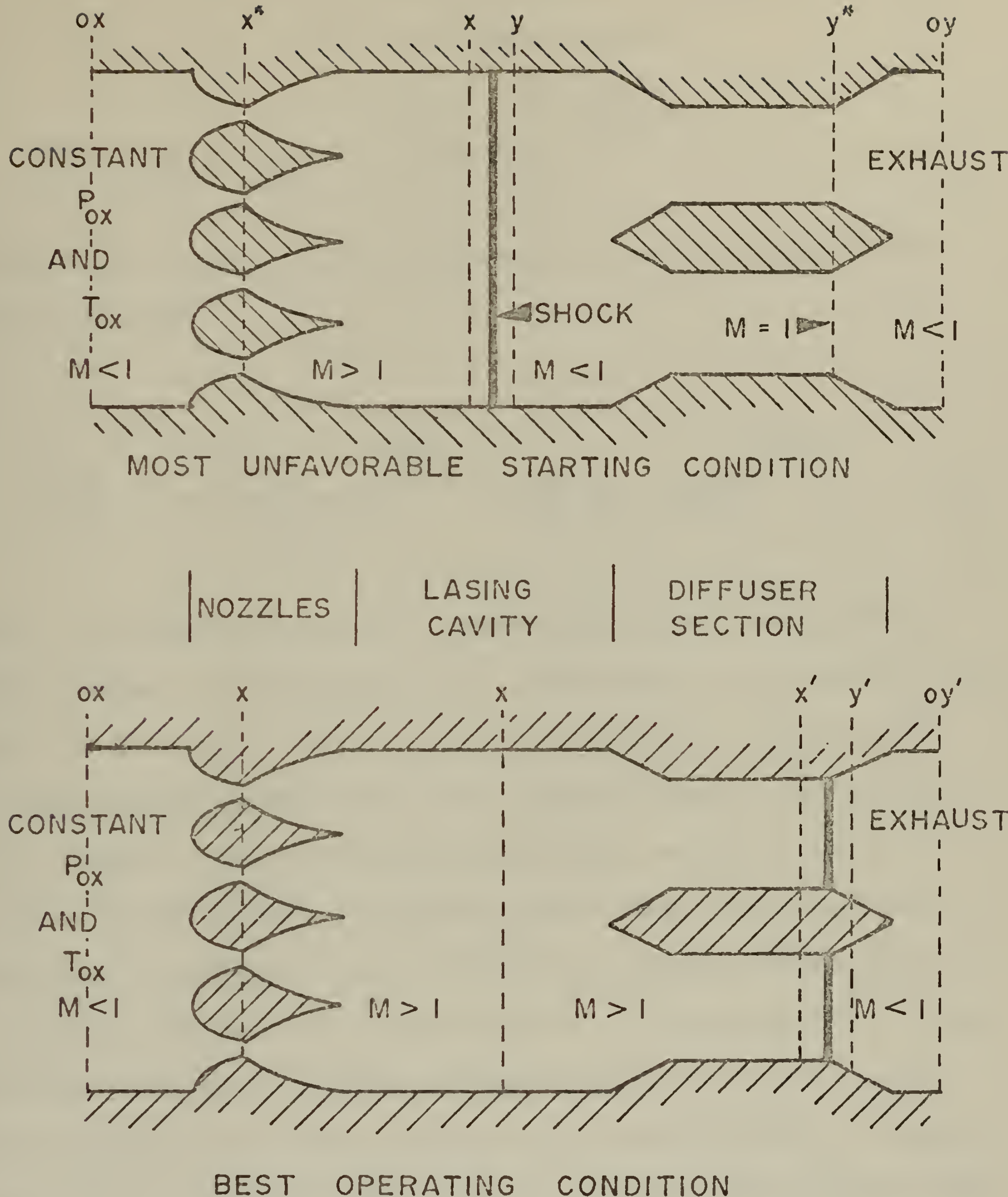

FIGURE (3) STARTING OF A GDL

The area ratio A_x/A_x^* can be expressed in terms of the Mach number at x, M_x, by the isentropic formula

$$\frac{A_x}{A_x^*} = \frac{1}{M_x}\left[\left(\frac{2}{k+1}\right) \left(1 + \frac{k-1}{2} M_x^2\right) \right]^{\frac{k+1}{2(k-1)}} \qquad (3)$$

The ratio P_{oy}/P_{ox} can be expressed in terms of M_x by the shock formula

$$\frac{P_{oy}}{P_{ox}} = \left(\frac{\frac{k+1}{2} M_x^2}{1 + \frac{k-1}{2} M_x^2}\right)^{\frac{k}{(k-1)}} \left(\frac{2k}{k+1} M_x^2 - \frac{k-1}{k+1}\right)^{-\frac{1}{(k-1)}} \qquad (4)$$

The contraction ratio, ψ , depends only on the operating Mach number in the cavity, M_x. This ratio is plotted versus M in Figure (4). With the limiting diffuser throat area corresponding to equation (1), the diffuser is barely able to "swallow" the flow during starting, and the flow at the diffuser throat is exactly sonic when the shock is in the lasing cavity. If the diffuser's total throat area is slightly smaller than that required by equation (1), normal shocks will stand in the diverging portion of the nozzles and subsonic flow will exist in the lasing cavity. Should the total diffuser throat area be considerably smaller than that given by equation (1), the flow will be subsonic throughout the entire system.

Essentially the starting problem is formulated so as to satisfy the continuity equation. After the shock occurs in the starting process and the stagnation pressure is

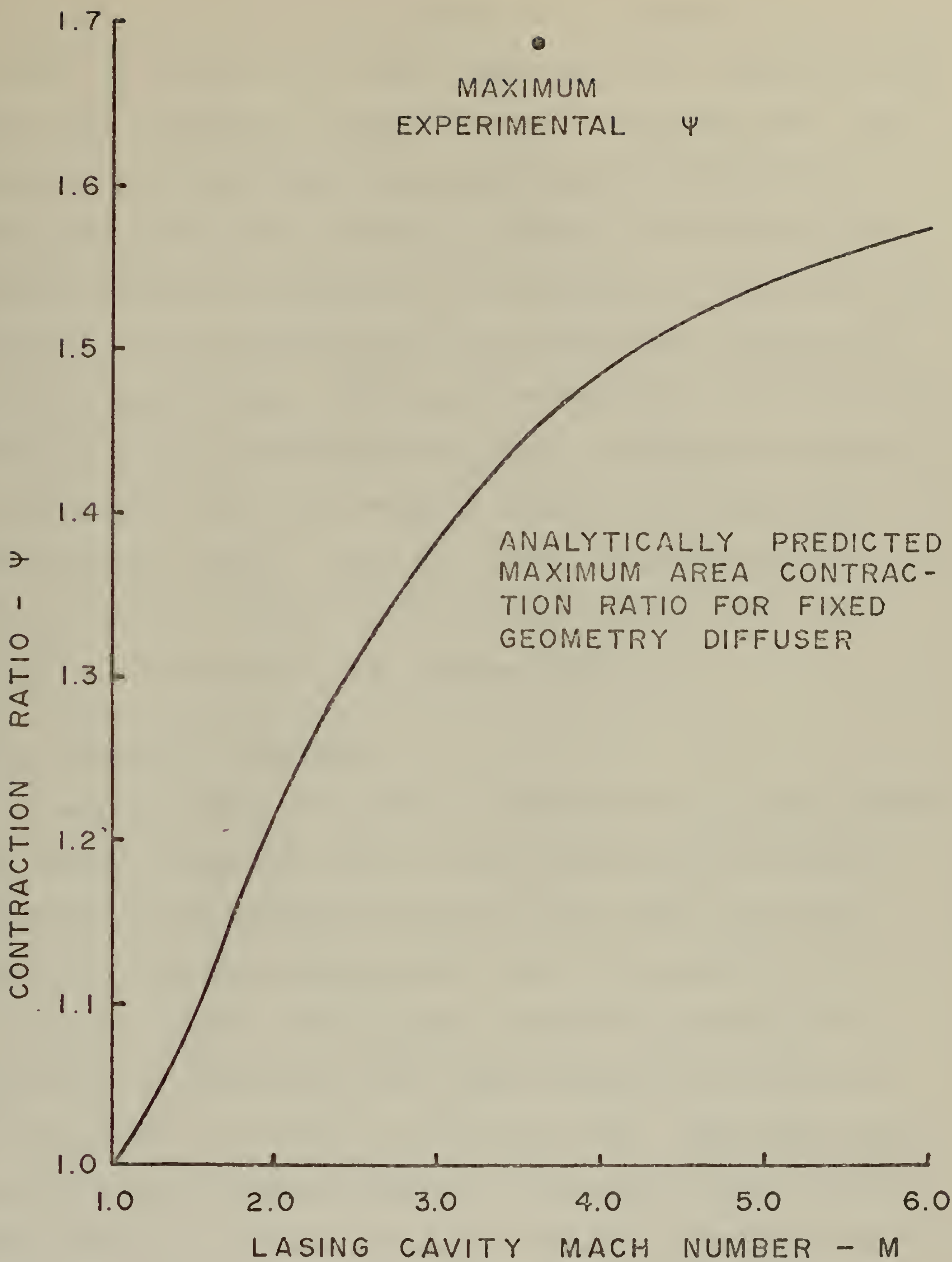

FIGURE (4) PLOT OF MACH NUMBER VERSUS CONTRACTION RATIO decreased, the total flow cannot pass through an area that is equal to the area at a point upstream of the shock and has the same velocity. There are ways to overcome this. One possibility is to use a variable geometry diffuser; a variable area throat opens for starting until the shock passes through the device and then closes to the operating area. A second possibility for solving the starting problem is mass bleed. Bleeding flow upstream of the diffuser throats during starting effectively increases the diffuser throat area; flow with reduced stagnation pressure passes through the device. Once the flow is supersonic and shock free from the nozzles to the diffuser throat, the bleed must be discontinued for optimum operation.

C. OPERATING CONDITIONS

Assuming that the diffuser throat area is large enough to permit supersonic flow in the lasing civity, a sufficiently large combustor pressure will cause the shock to move through the lasing cavity and to be swallowed by the diffuser throats. For minimum combustor pressure, the equilibrium position of the shock should be at the exit of the diffuser throat. See Figure 3(b). The shock will occur at the minimum possible Mach number in the diffuser. The stagnation pressure loss for optimum, steady operation is less than for starting because of the lower Mach number at which the shock occurs. For this reason the maximum ratio of the combustor to ambient or combustor to exhaust pressure is determined by the starting rather than by the operating condition.

The preceding discussion considered the flow to be isentropic in all regions except across shocks. To insure that a supersonic diffuser will start and run, the throat area must be made slightly larger than the theoretical minimum value to account for inaccurate estimates of the boundary layer displacement thickness, boundary layer separation, of the departures from one-dimensionality, and so forth.

D. OTHER VICOUS EFFECTS

The influence of the shock wave has been discussed. Other viscous effects, e.g. boundary layers and nozzle wakes occur in laser diffusers; these phenomena will now be discussed.

It is presumed the reader is familiar with boundary layer concept.

Four aspects of boundary layer phenomena have an effect on diffuser flow: flow separation, the displacement thickness, the retarding force of wall drag, and shock-wave-boundary-layer interaction.

Flow separation occurs as a result of an adverse pressure gradient. The conversion of fluid kinetic energy to static pressure in a diffuser creates an adverse pressure gradient. The extent and magnitude of pressure gradient that can be surmounted by the flow depends critically on the steadiness of the boundary layer. A laminar boundary layer is more susceptible to separation than is a turbulent boundary layer. Figure (5) illustrates the transition of the boundary layer from laminar to turbulent flow. When a region

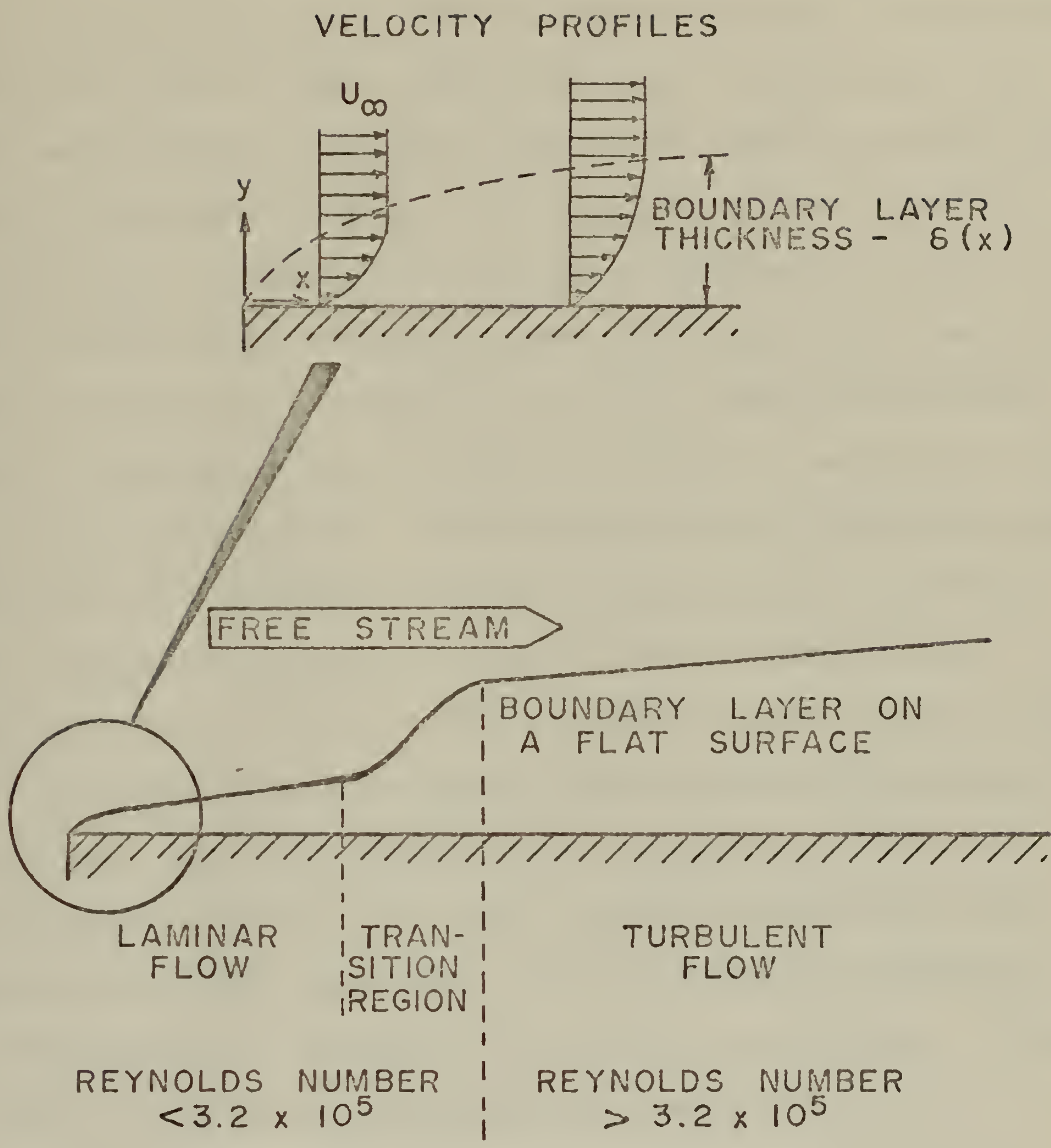

FIGURE (5) BOUNDARY LAYER ILLUSTRATION

with an adverse pressure gradient exists along the wall, the retarded fluid particles cannot, in general, penetrate too far into the region of increasing pressure owing to their small kinetic energy. Thus the boundary layer is deflected sideways from the wall, separates from it, and moves into the main stream. In general the fluid particles behind the point of separation follow the pressure gradient and move in a direction opposite to the external stream. Figure (6) is a schematic of boundary layer separation. One can see that separation is likely to occur in a diffuser because of its inherent adverse pressure gradient. Separation of the boundary layer greatly reduces the effective flow area and geometry of a diffuser, which can cause unstarting from the reduction in area and choking from a normal shock. The diffuser's effective geometry while running can be significantly altered by boundary layer separation and the entrapped region of reverse flow, especially if the flow reattaches itself to the walls further downstream of the point of initial separation. Figure (7) shows boundary layer separation phenomena in a supersonic diffuser. Separation is mostly an undesirable phenomenon because it entails large energy losses and reduction in flow area. Methods have been developed for the artificial prevention of separation. One of the most effective is boundary layer suction or bleed. In this method the decelerated fluid particles in the boundary layer are removed through slits in the walls via a vacuum pump or tank.

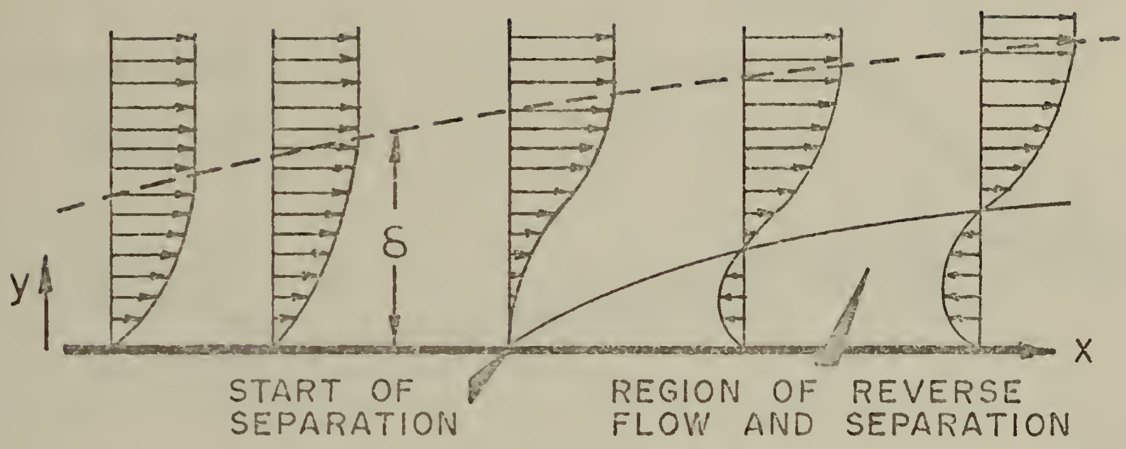

FLOW PAST A WALL WITH SEPARATION

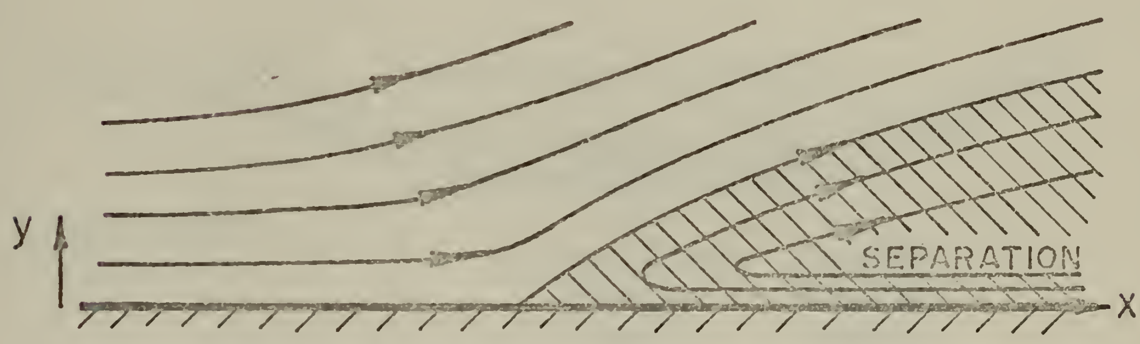

SHAPE OF STREAMLINES WITH SEPARATION

FIGURE (6) BOUNDARY LAYER SEPARATION

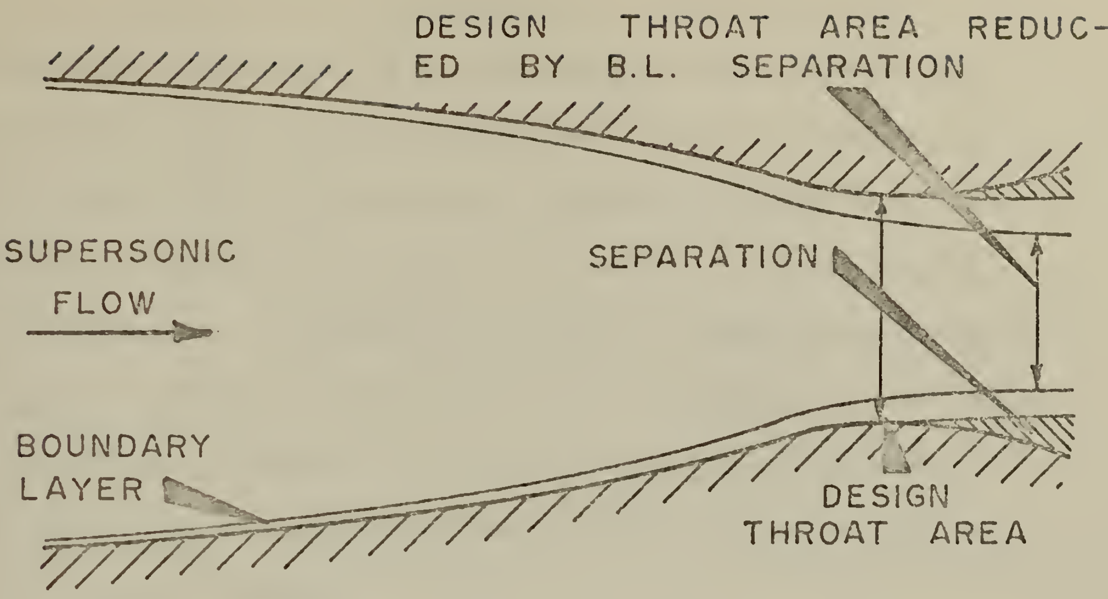

REDUCED THROAT AREA CAN UNSTART DIFFUSER BY CAUSING AN UNSTABLE NORMAL SHOCK IN THE CONVERGING SECTION OF THE DIFFUSER

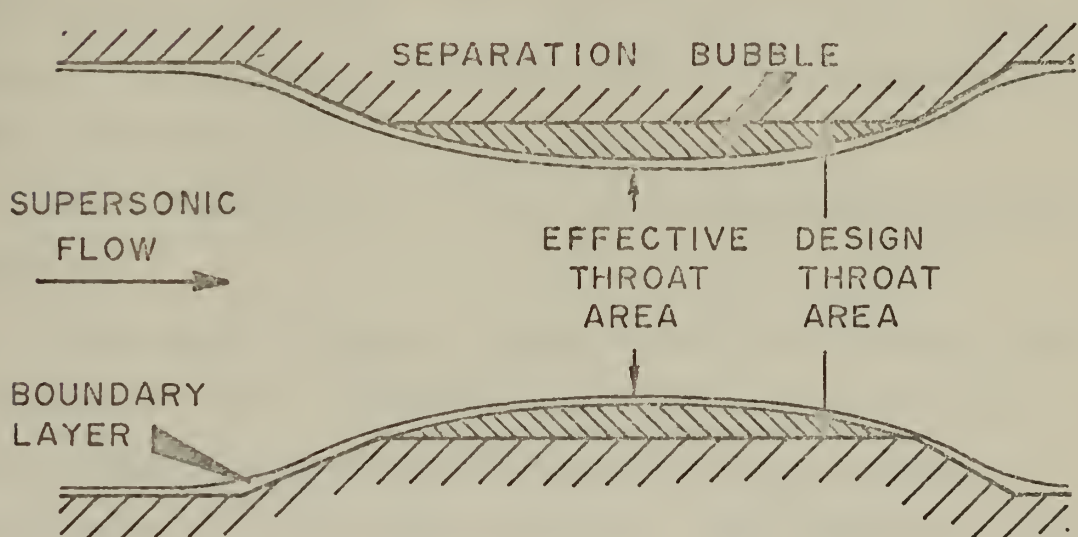

FIGURE (7) SEPARATION PHENOMENA IN SUPERSONIC DIFFUSERS

The displacement thickness, δ_1 , is a term used to describe the distance by which the external streamlines are shifted owing to the formation of the boundary layer. In the case of a flat surface in parallel flow the displacement thickness is about one third of the boundary layer thickness. Figure (8) shows the displacement thickness and its effect on decreasing the effective flow area in a diffuser. Figure (9) illustrates the displacement thickness within a diffuser due to the velocity gradient of the nozzle's wakes.

The wall shear force is influenced by the boundary layer. The shear force on the wall opposes the motion of the fluid. In early phases of the time dependent starting process the boundary layer is thin. This thin boundary layer generates higher than normal shear forces. The starting and running pressures must be larger to compensate for the retarding force.

The retarding force is not discussed further in this thesis.

Shock waves interact strongly with the boundary layer causing increased thickness and/or separation to occur. The extremely high adverse pressure gradient across a shock wave is responsible for this. This disturbance of the boundary layer can occur wherever a shock wave originates, touches, or terminates on the boundary layer. The top photograph in Figure (40) shows such an area of thickened boundary layer. Figure (10) illustrates this phenomenon.

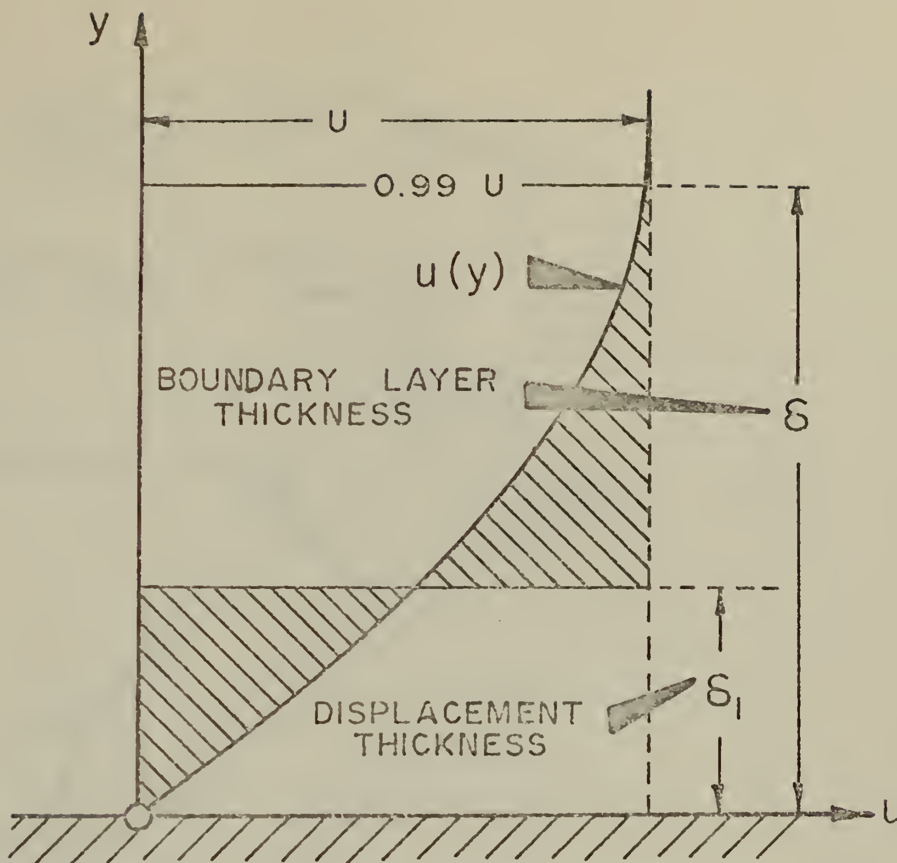

$$\delta_1 \approx \frac{1}{3}\,\delta$$

ILLUSTRATION OF DISPLACEMENT THICKNESS

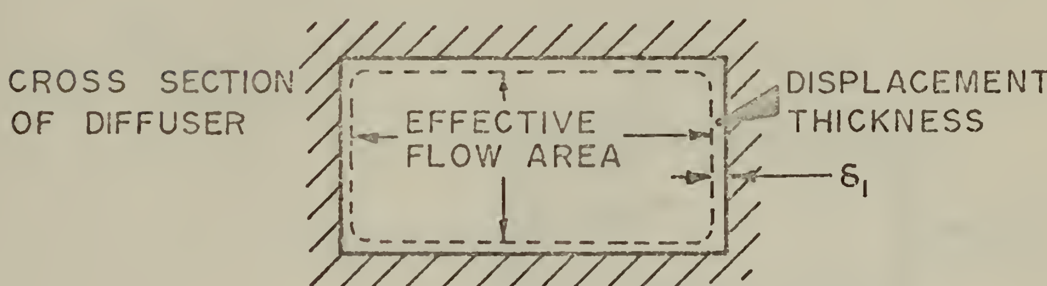

EFFECTIVE FLOW AREA REDUCTION FROM DISPLACEMENT THICKNESS

FIGURE (8) DISPLACEMENT THICKNESS

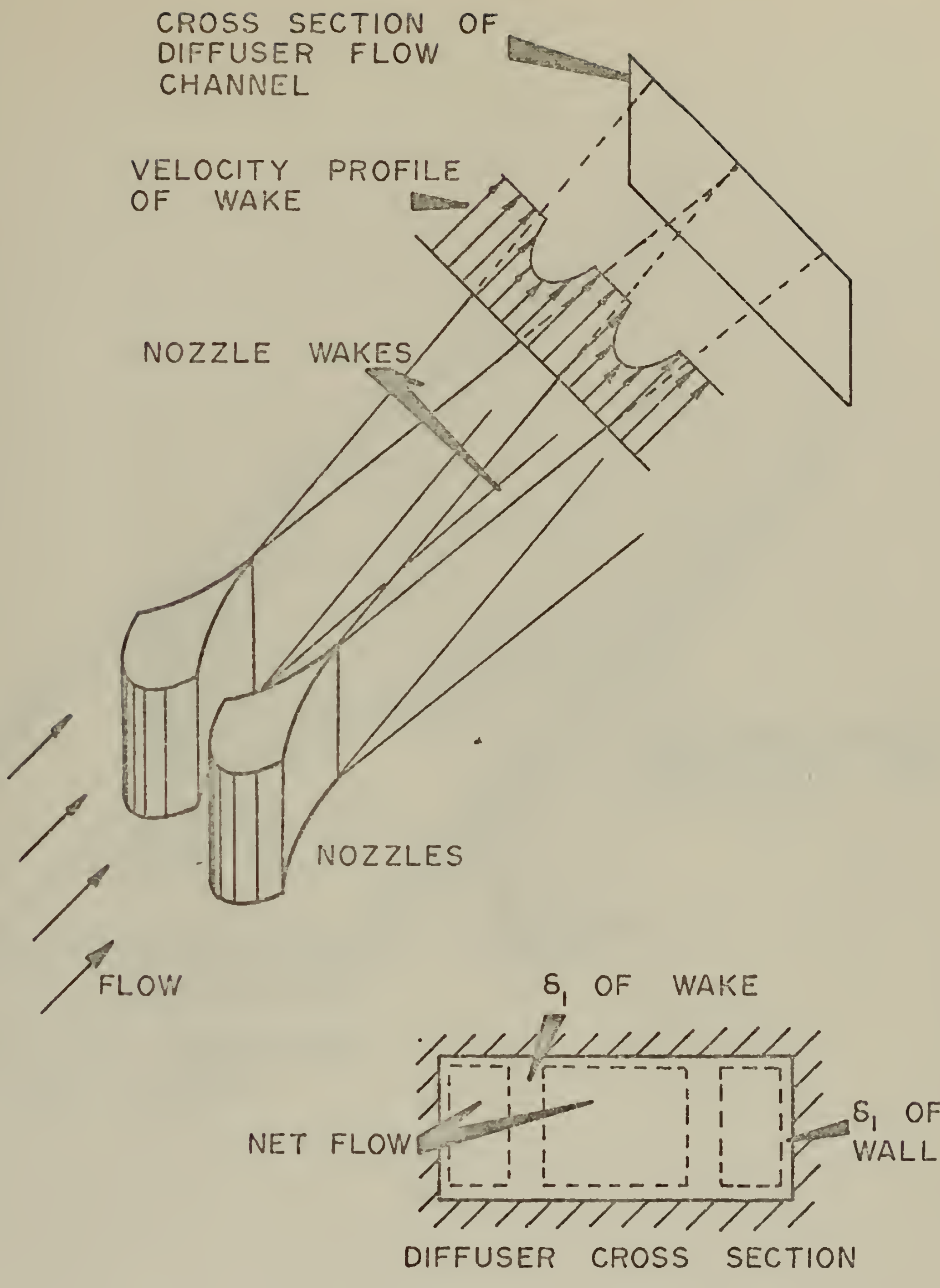

FIGURE (9) NOZZLE WAKE DISPLACEMENT THICKNESS

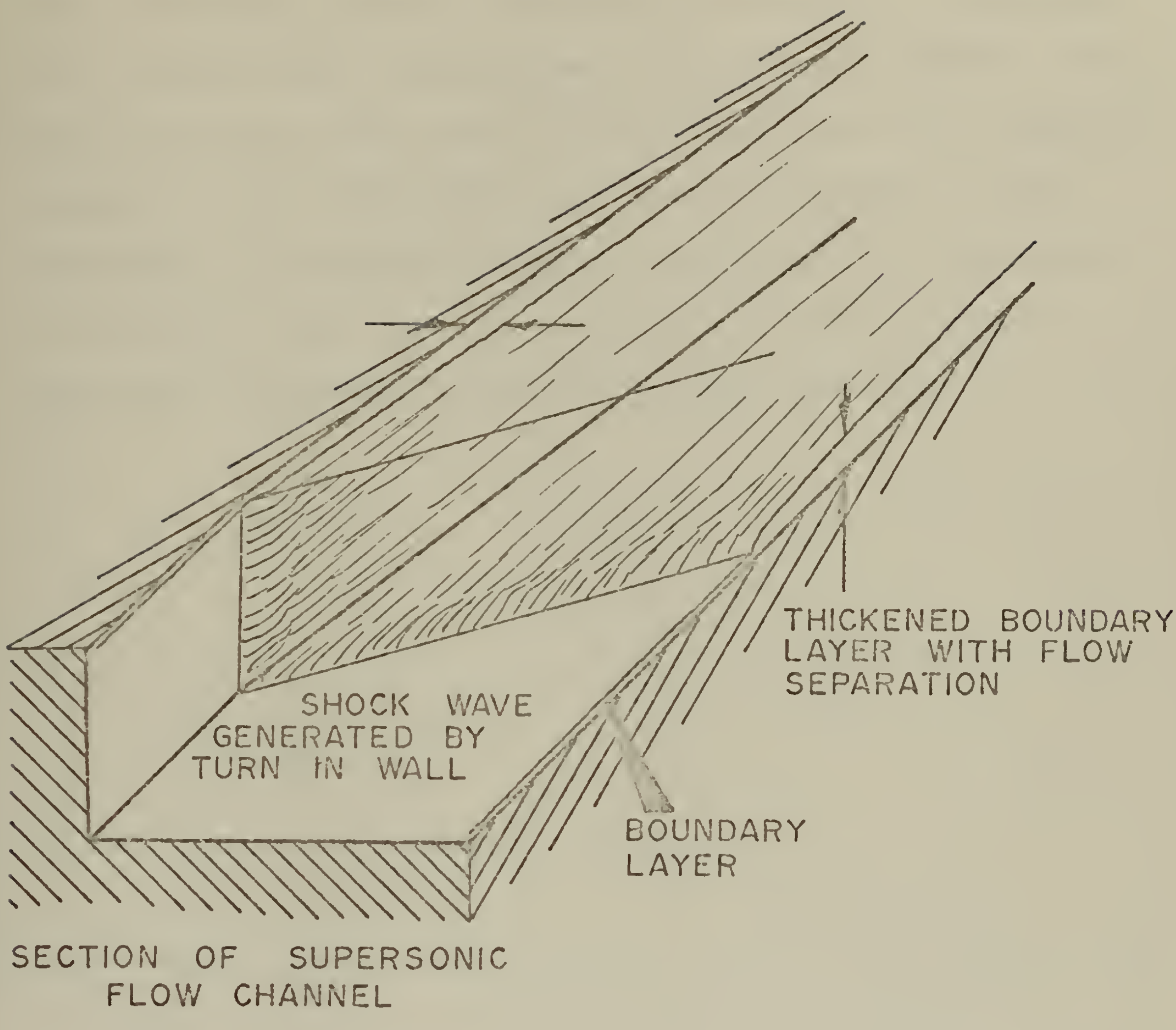

FIGURE (10) SHOCK WAVE AND BOUNDARY LAYER INTERACTION

E. NONEQUILIBRIUM EFFECTS

Lasers are inherently nonequilibrium devices. A population inversion is required for positive gain and light amplification. Figure (11) shows vibrational, rotational, and translational temperatures for a GDL and chemical laser. Nonequilibrium conditions as shown in Figure (11) generate entropy. It is well known and discussed in Ref. 6 that decreases in stagnation pressure are related to increases in entropy. This loss in stagnation pressure further decreases the overall efficiency of the laser.

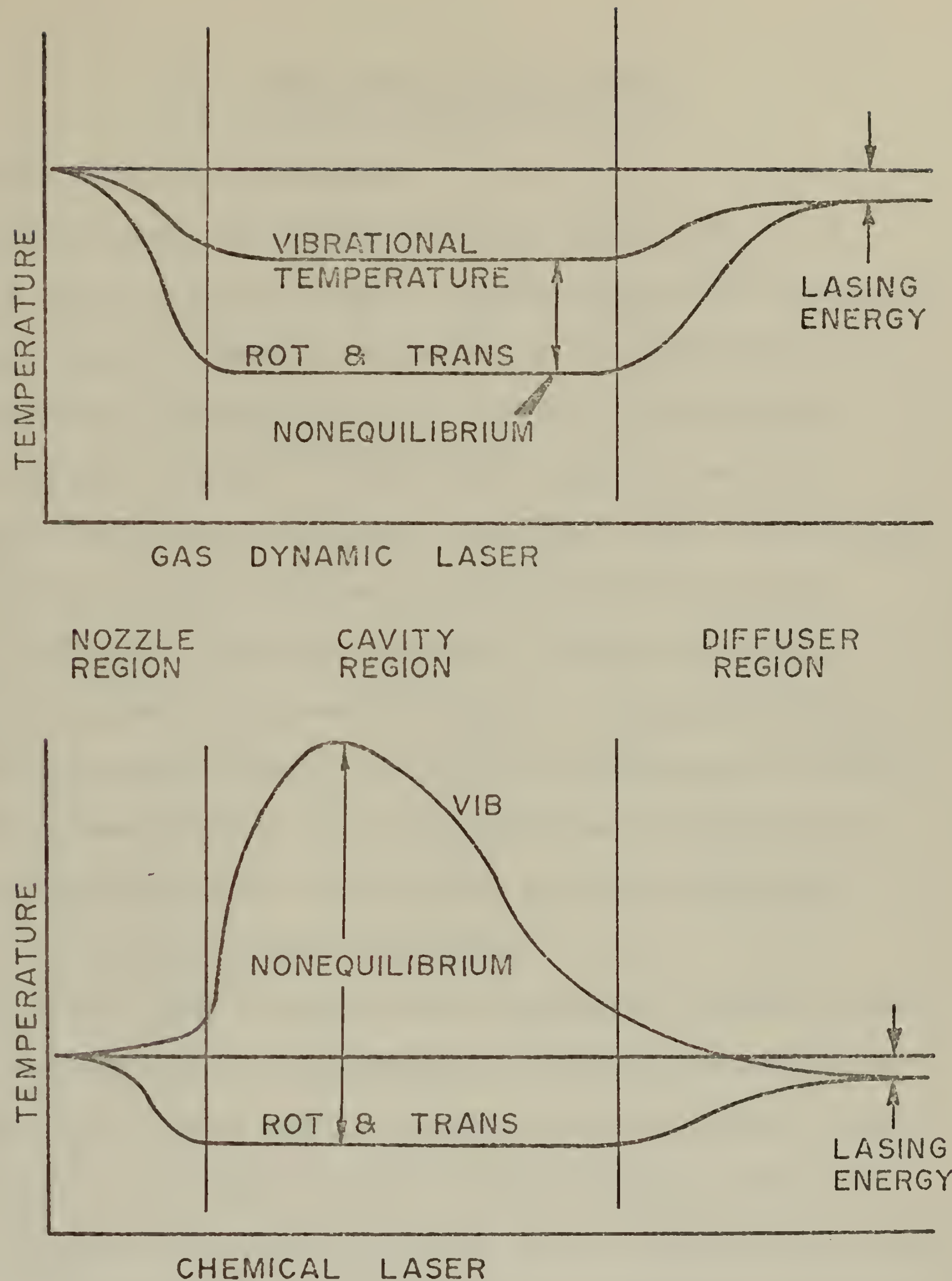

FIGURE (11) NONEQUILIBRIUM EFFECTS IN LASERS

III. EXPERIMENTAL DEVELOPMENT

A. DESCRIPTION OF EXPERIMENT

This research was conducted to study the effect of boundary layer bleed on a short length supersonic diffuser for a gas dynamic laser. Diffusion of the supersonic flow by an isentropic turn appeared to offer a flow passage with a smaller length to width ratio than a symmetric convergent supersonic diffuser. Boundary layer and separation control through the use of vacuum bleed slots and holes in the walls was incorporated to allow a greater pressure recovery in a shorter length. Design parameters and criteria were choosen to approach simulation of actual GDL flow parameters and allow the greatest latitude for physical alteration of the hardware and flow passages during the testing of the apparatus.

The actual flow passage would represent a narrow longitudinal element of a GDL diffuser as shown in drawing (b) of Figure (2). This design closely approximates two dimensionality in the layout of the diffuser passage and optimizes Schlieren flow visualization of the pressure gradients, shocks, and Mach lines produced in the flow by the diffuser geometry. Dimensional limitations of the high optical quality glass available for flow visualization and the size of the high pressure air discharge manifold on which the apparatus would be mounted limited the dimensions at the entrance of the diffuser passage to 1 inch by 2 inches. Plexiglass was chosen for fabrication of the flow passage because of its machinability and potential for easy modification.

The size of the entrance to the diffuser passage and the desire to attain flow speeds comparable to those found in the lasing cavity of a GDL dictated the area ratio and number of nozzles that could be placed at the entrance of the diffuser to generate the high speed flow. A nozzle array design with two throats and area ratios necessary for Mach 4 flow were chosen.

Boundary layer bleed was to be incorporated on all surfaces. The plexiglass walls of the diffuser passage would have slots perpendicular to the flow and the glass windows comprising the other walls of the diffuser would have rows of holes perpendicular to the flow. All of these bleed ports were to be connected through individual valves in parallel to a common manifold connected to a 200 cubic foot tank which was continuously excavated by a vacuum pump. Isolation of the boundary layer bleed into many regions of the diffuser with each region controlled by an individual valve would enable one to vary the amount and areas bled.

Analytical design was divided into two areas; layout of diffuser geometry by the method of characteristics and calculation of boundary layer bleed slots and holes using a computer program. Hardware was designed so that all parts could be made in the machine shop of the Aeronautical

Engineering Department of the Naval Postgraduate School, Monterey, California.

B. DIFFUSER DESIGN

Diffusion of the supersonic flow was accomplished by an isentropic turning of the flow. The geometry of the passage was such that Mach waves or weak oblique shocks generated by the turning of one wall would not be reflected by the opposite wall. Figure (12) illustrates this concept. The method of characteristics found in Ref. 1 was used to determine the contour of the diffuser's walls. The exact shape of the passage was laid out graphically and is shown on Drawing (19) in Appendix A. Tables were used which relate the Mach number, M, to the Prandtl-Meyer funcion, ν , and the wave angle, μ . Figure (13) illustrates the use of these tabulated values to lay out a section of the diffuser. Isentropic turning is approximated by making the turn of the diffuser wall in small increments of turning angle, $\Delta\theta$, thereby achieving an essentially smooth continuous turn. This diffuser was constructed using increments of 2 degrees for $\Delta\theta$ as shown in Figure (13). The master layout of the channel shown on Drawing (19) in Appendix A turns the flow through sixty degrees and theoretically slows the flow to a Mach number of 1.294. Appendix B is a table of the values of M, θ, ν, and μ used to construct the master layout of the channel. The initial diffuser blocks that were constructed out of plexiglass turned the flow through twenty degrees and decelerated

$M_1 > M_2 > M_3 > M_4$ MACH DECREASES

$P_1 < P_2 < P_3 < P_4$ PRESSURE INCREASES

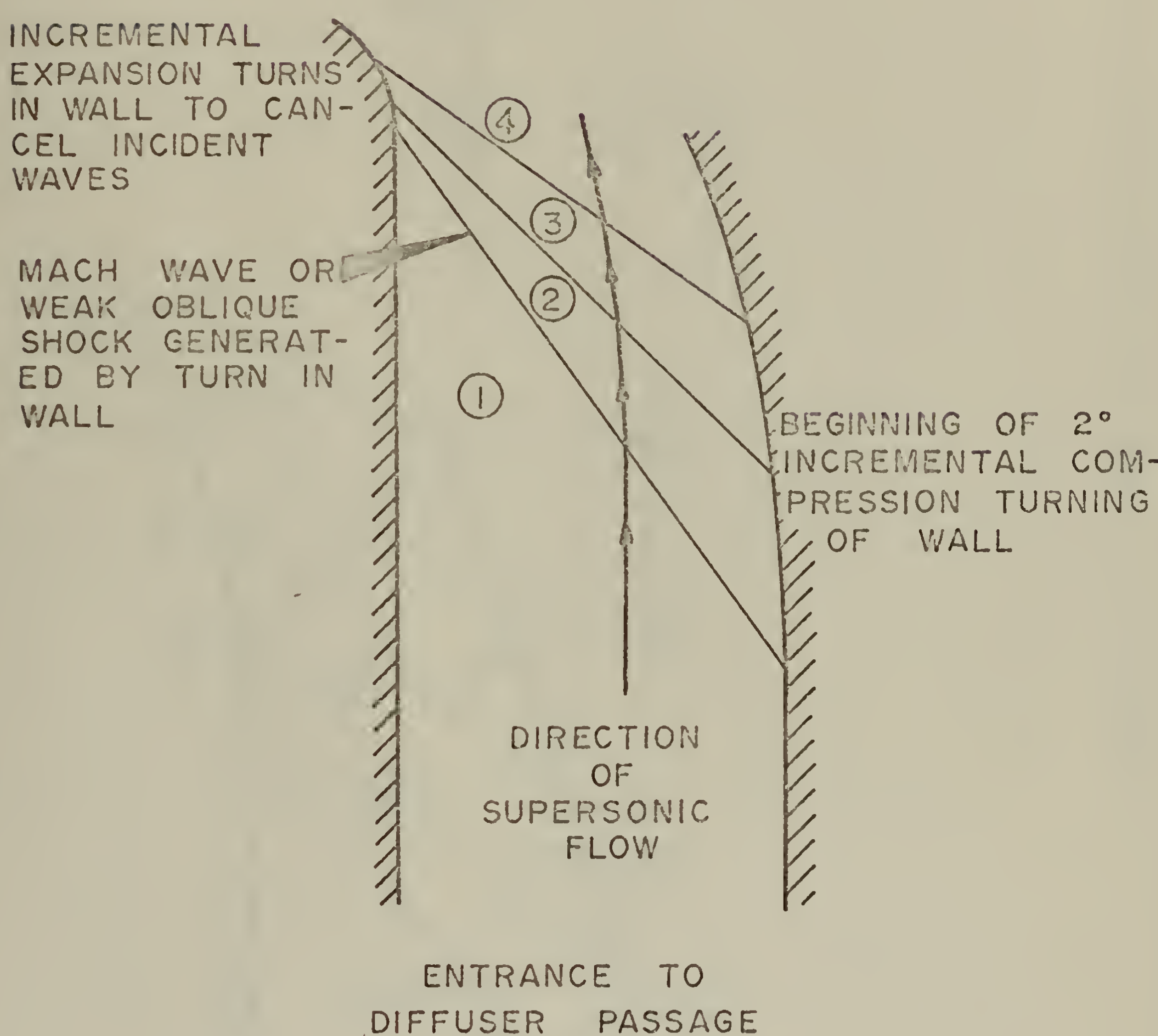

FIGURE (12) DIFFUSION BY ISENTROPIC TURN

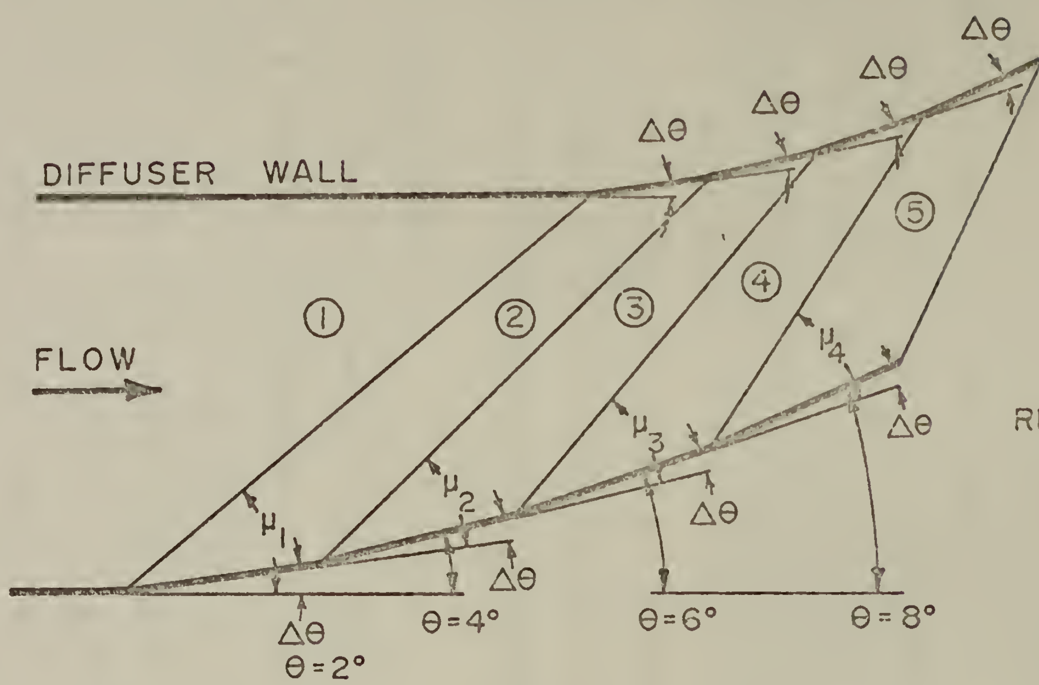

REGION	MACH NUMBER	TOTAL TURN ANGLE	WAVE ANGLE	PRANDTL-MEYER FUNCTION
	M	θ	μ	ν
1	4.016	0°	14.417°	66
2	3.868	2°	14.983°	64
3	3.728	4°	15.561°	62
4	3.594	6°	16.155°	60
5	3.467	8°	16.765°	58

FIGURE (13) GRAPHICAL CONSTRUCTION OF DIFFUSER it to a Mach number of 2.8. Drawing (16) in Appendix A shows the machine shop drawing of these diffuser blocks. The blocks are one inch thick and have a one inch wide by two inch long straight section of flow channel at the entrance prior to the initial turning of the compression wall. This section is analogous to the lasing cavity of a GDL. The existing channel or portion downstream of the narrowest part of the channel, the diffuser throat, has walls which each diverge one and one half degrees. The diffuser blocks were mounted in the apparatus so that the actual exit of the supersonic nozzles extended approximately one half inch into the parallel section of the diffuser channel entrance. This initial design had a contraction ratio, ψ , equal to 3.33. The contraction ratio is defined as the ratio of the diffuser entrance width divided by the diffuser throat or minimum area width. This first configuration had a two inch wide entrance and a six tenths of an inch wide throat. Figures (14) and (15) show this diffuser channel and plexiglass blocks.

C. NOZZLE DESIGN

A nozzle array based on theoretical calculations for Mach 4 flow was constructed. The size of the diffuser entrance, one inch by two inches, and the desire to produce a flow speed of Mach 4 determined the number and size of the nozzles. The width of the nozzles were one inch and two complete nozzles were fitted in the two inch dimension. The nozzles consisted of two half nozzle pieces along

DIFFUSER FLOW CHANNEL FOR CONTRACTION RATIO OF 3.33 ; SHOWING BOUNDARY LAYER BLEED PASSAGES AND VACUUM FITTINGS

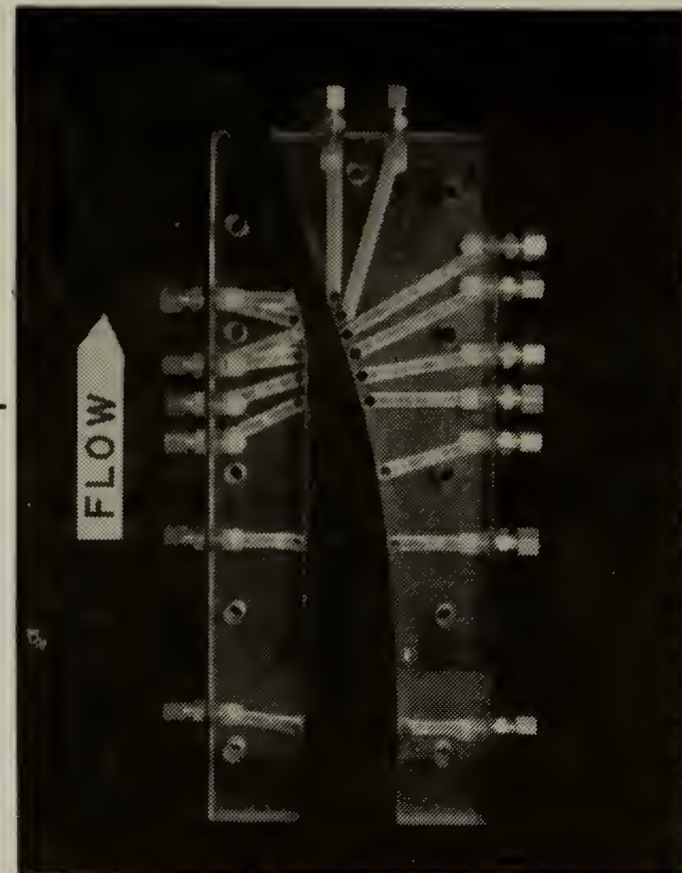

FIGURE (14) DIFFUSER BLOCKS, $\psi = 3.33$

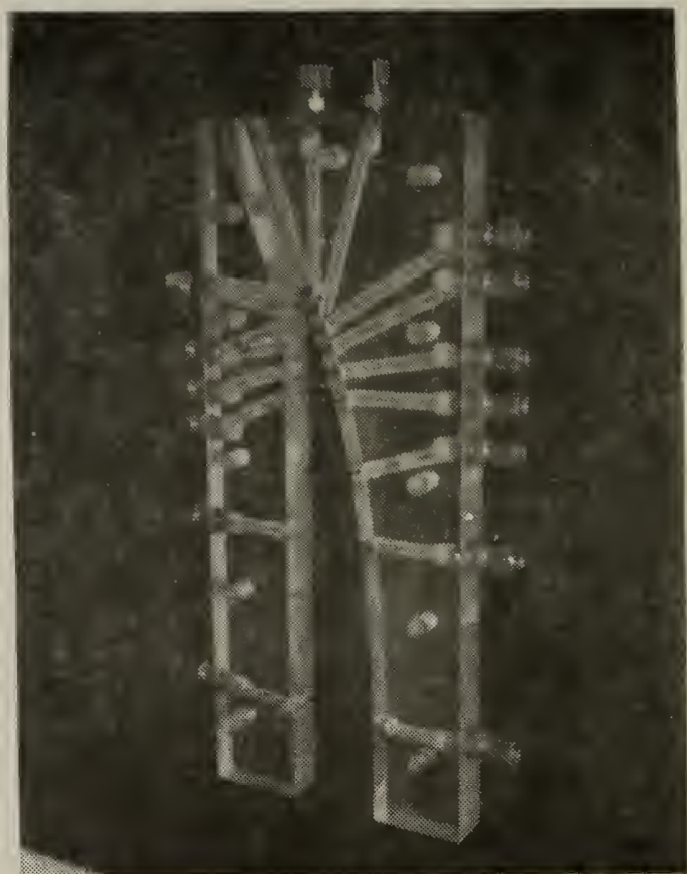

DIFFUSER BLOCKS

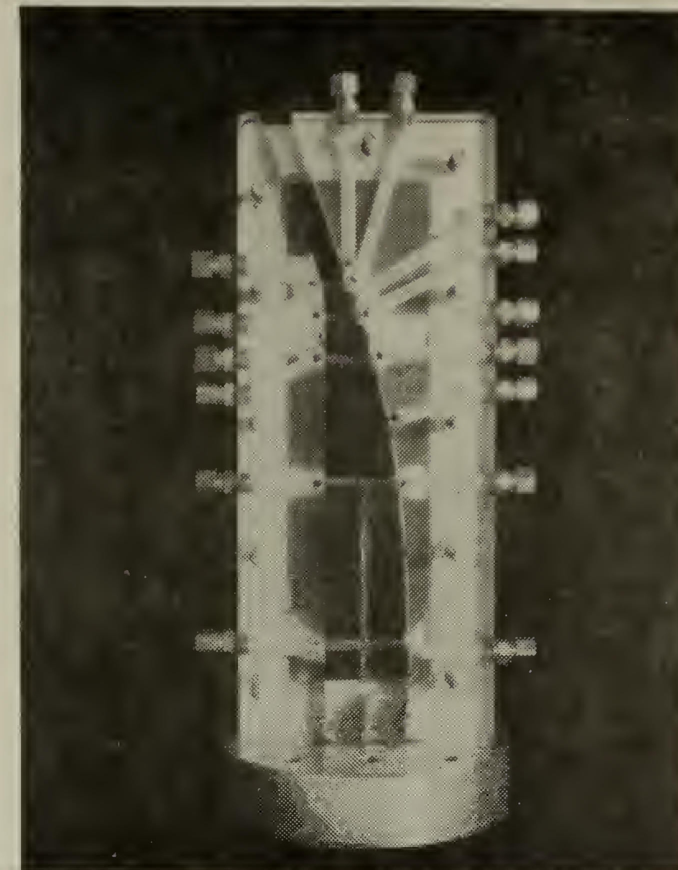

DIFFUSER BLOCKS MOUNTED ON WINDOW AND BASE PLATE

FIGURE (15) DETAILS OF DIFFUSER BLOCKS, $\psi = 3.33$

each wall and one symmetric nozzle piece mounted in between the two halves thus forming two throats. Calculations of the area ratio necessary to achieve a flow speed of Mach 4 were based on isentropic or ideal flow and expansion by the nozzles. Reference 3 contains tables which give flow parameters versus Mach number for supersonic flow. An area ratio, throat area divided by exit area, of 0.09329 corresponds to a Mach number of four. The finite thickness of the nozzle exit walls decreased the possible exit area from 2.0 square inches to 1.976 square inches. Based on the area ratio of 0.09329 the nozzles each had a throat area equal to 0.0922 square inches. The method of characteristics was not used to lay out the nozzle shapes but rather nozzle contours were laid out graphically using smooth continuous curves. Drawings (10), (11), (12), and (13) in Appendix A give the specifications for the nozzles. Drawings (1), (2), and (3), describe the assembly for holding the nozzles in the base plate which is described in Drawings (4) and (5). Figures (16), (17) and (18) are pictures of the above components.

D. BOUNDARY LAYER BLEED

The effects of the boundary layer on the operation of a diffuser were discussed in part D under Principles of Diffuser Operation. The purpose of this research was to study the effect of boundary layer bleed on the operation of a supersonic diffuser. To achieve these goals the diffuser was designed with the capability of bleeding the

IO TO I AREA RATIO
NOZZLES INSTALLED AT
ENTRANCE TO DIFFUSER
-GENERATED MACH = 3.5

FIGURE (16) SUPERSONIC NOZZLES

NOZZLE PROFILE

NOZZLES MOUNTED IN NOZZLE BLOCK

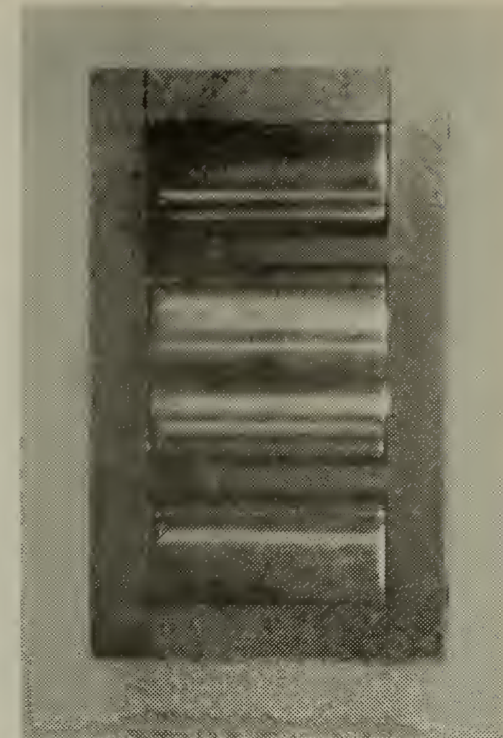

CLOSE UP VIEW OF NOZZLE THROATS

FIGURE (17) DETAILS OF NOZZLES

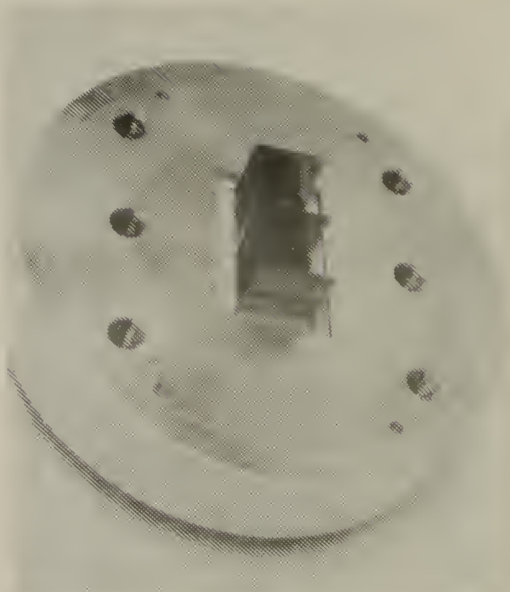

EXIT OF NOZZLES IN BLOCK
MOUNTED IN BASE PLATE

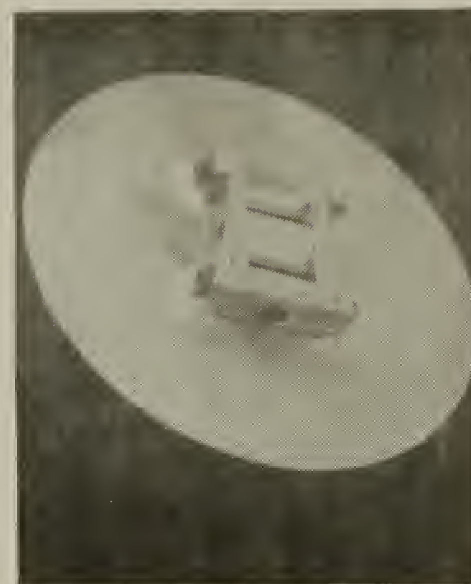

ENTRANCE TO NOZZLES IN
BLOCK MOUNTED IN BASE
PLATE

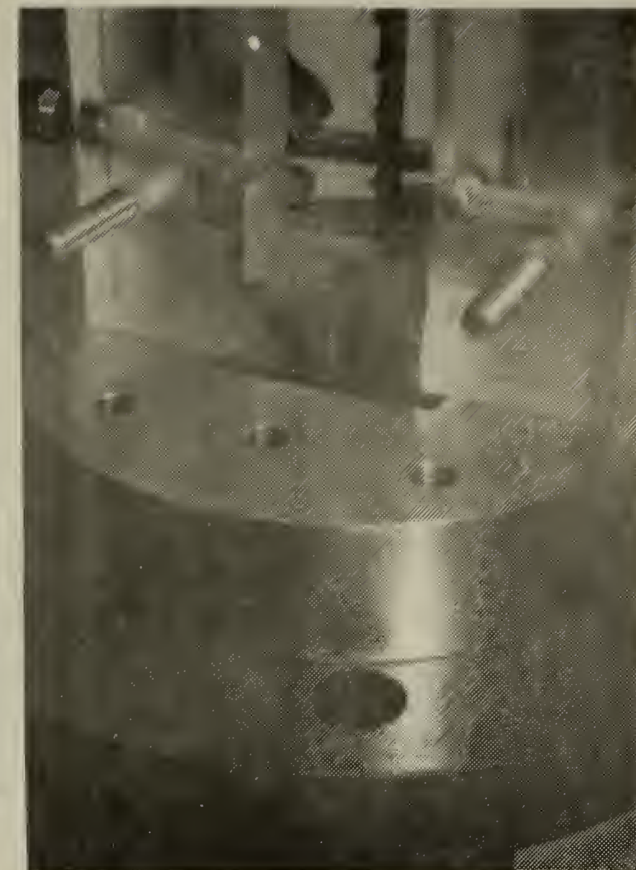

VIEW OF NOZZLES INSTALLED IN
DIFFUSER

FIGHRE (18) DETAILS OF NOZZLES IN BASE PLATE entire boundary layer at intervals along all flow surfaces. The various regions of bleed were individually connected to a common vacuum manifold through individual valves thus allowing many and varied configurations of bleed operation. Calculation of bleed hole and slot areas was based on methods and a computer program outlined in Ref. 4. This reference develops a model of the flow in a supersonic boundary layer and develops techniques to determine hole size and pressure ratio required to remove a certain fraction of the boundary layer.

1. Flow Model

A model fluid discussed by Stewartson (Ref. 5) was used in this development. The fluid is assumed to have a Prandtl number of unity and the viscosity is proportional to the static temperature so that $\mu\rho = \mu_1 \rho_1$, where subscript 1 denotes the reference condition. Assuming the fluid has a Blasius profile and that stagnation temperature is constant through the boundary layer, the incompressible profile was transformed to a compressible profile by the method described in Ref. 5.

For analytical ease, a Blasius profile was approximated by

$$u/U = \sin(A\eta)$$

where $A = 54^{\circ}$ and η is given by Ref. 5 as

$$\eta = X \quad 2/R_e \quad .$$

The reference length is denoted by X. The model shown in Figure (19) was used to describe the flow. By applying a

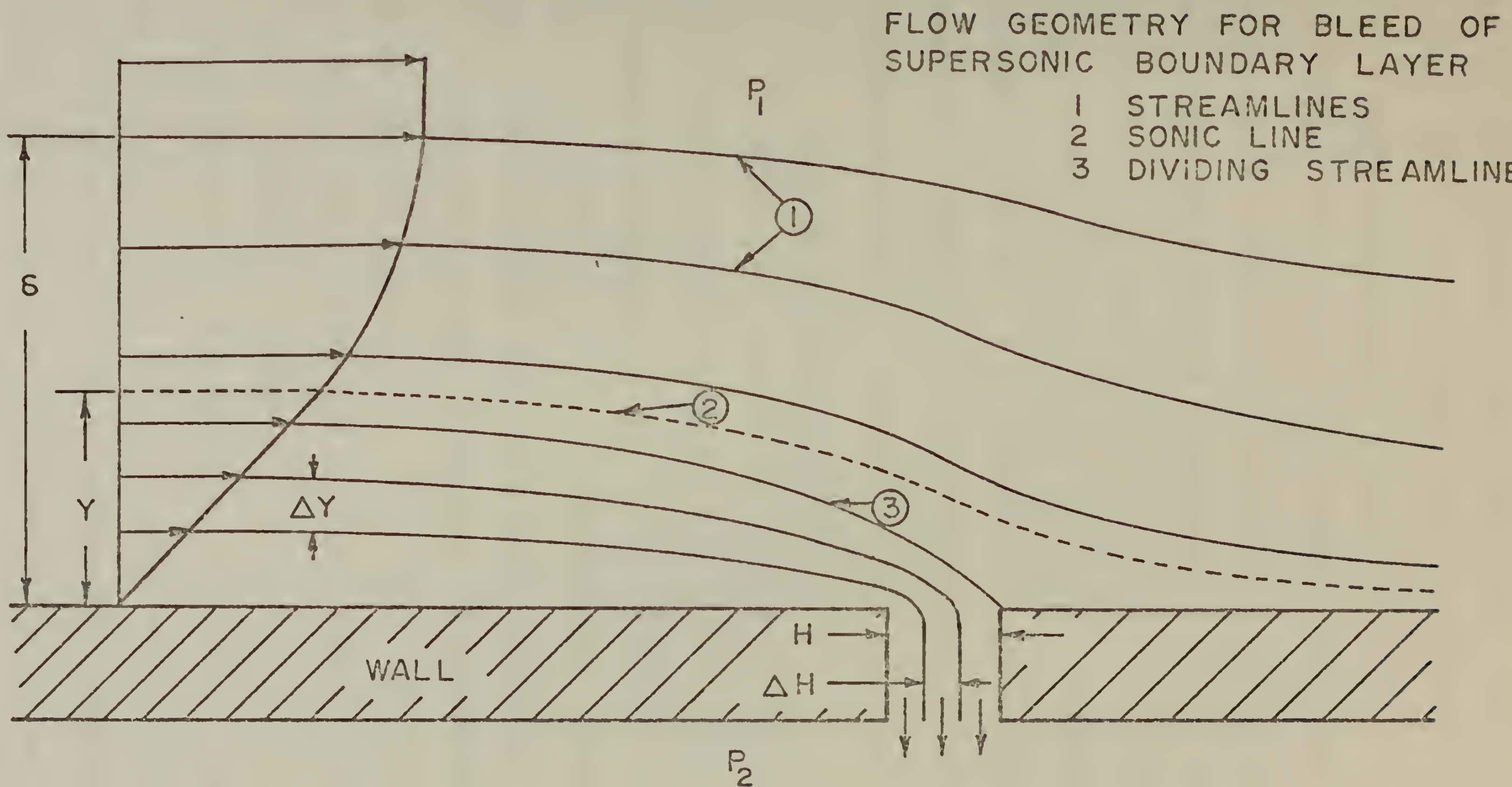

FIGURE (19) SUPERSONIC BOUNDARY LAYER MODEL bleed plenum pressure (P_2) lower than the freestream pressure (P_1), a streamline (4) is assumed to stagnate on the downstream edge of a slot of width H. All flow below this streamline goes through the slot, which is assumed long enough to have parallel streamlines at the slot exit. By assuming isentropic flow in each streamtube below (4), it is possible to calculate flow conditions at the slot exit by specifying (P_1/P_2). Using the continuity equation leads to a slot width, H. The complete set of equations programmed for the Hewlett Packard model 9830 computer is listed in Appendix C.

2. Results of Calculations

Figure (20) shows the diffuser flow channel divided into regions separated by Mach lines as laid out in Section B, Diffuser Design, and shows the intended location of boundary layer bleed slots or rows of holes. These locations were chosen so that the number and spacing of bleed holes is proportional to the magnitude of the pressure gradient in the decelerating flow. The least spacing occurs in the throat area where the highest adverse pressure gradient occurs. Table (1) gives the values of bleed area and mass flow generated by the computer program in Appendix C for the flow parameters listed at the beginning of the table and the local Mach number and static pressure. Holes were placed in the windows with cumulative areas in a given region of bleed equal to the slot area calculated and given in Table (1). Slots were cut in the walls of the diffuser

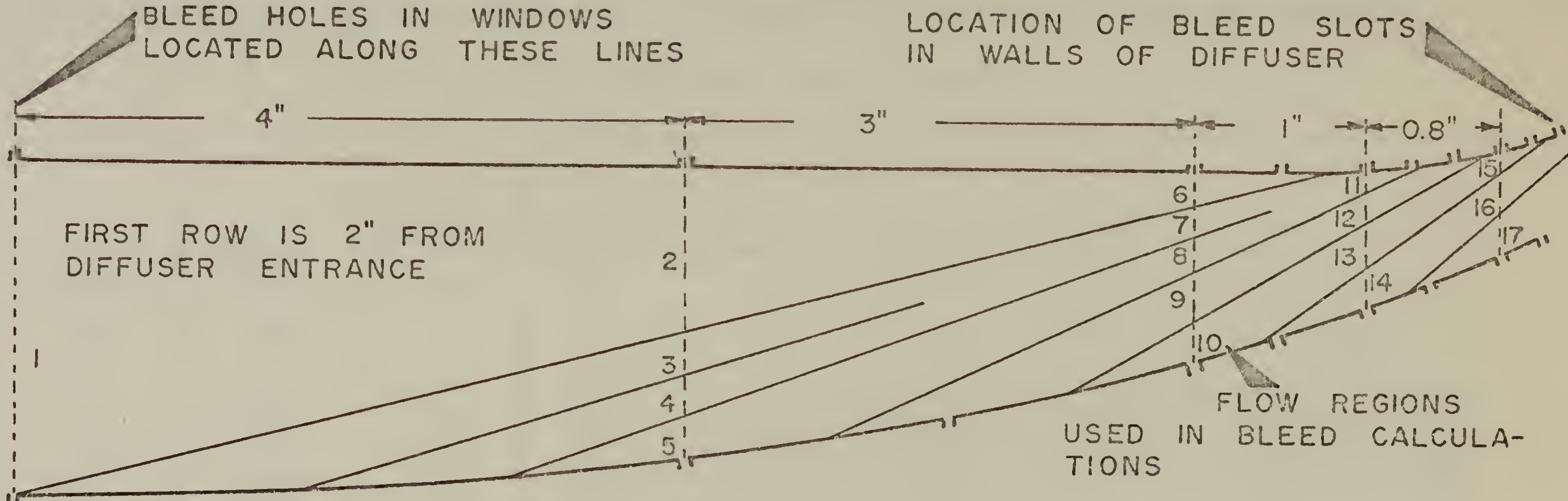

FIGURE (20) DIFFUSER FLOW REGIONS

TABLE 1 Boundary Layer Bleed Calculations

Flow conditions: P_0 = 165 psia, P_2 = 0.5 psia, η = 3.33 (total boundary layer)

T_0 = 70°F, γ = 1.4, a_0 = 1157 ft./sec.

Region	Mach Number	Reynolds Number X 10^4	Distance Parameter ft.	Static Pressure psia.	Flow Velocity ft./sec.	Slot Width in.	Slot Area sq. in.	Mass Flow slug/sec X 10^{-6}
#	M	V	X	P1	U8	H6		
1	4.01	237	.167	1.0	2260	.0175	.0350	.522
2	4.01	465	.33	1.0	2260	.0248	.0248	.368
3	3.87	459	.33	1.13	2230	.0252	.0063	.097
4	3.73	460	.33	1.49	2230	.0281	.0070	.124
5	3.59	452	.33	1.71	2190	.0291	.0073	.131
6	4.01	353	.25	1.0	2270	.0216	.0054	.082
7	3.59	343	.25	1.71	2190	.0253	.0051	.091
8	3.47	340	.25	2.05	2170	.0272	.0054	.104
9	3.26	333	.25	2.78	2130	.0307	.0092	.193
10	3.12	326	.25	3.41	2100	.0335	.0094	.207
11	3.47	112	.083	2.05	2170	.0157	.0024	.045
12	3.26	110	.083	2.78	2130	.0177	.0035	.074
13	3.01	107	.083	4.02	2080	.0207	.0062	.145
14	2.91	106	.083	4.68	2050	.0221	.0071	.170
15	3.01	87	.067	4.02	2080	.0186	.0028	.065
16	2.81	86	.067	5.44	2020	.0210	.0053	.130
17	2.63	82	.067	7.18	1970	.0240	.0067	.178

blocks with widths calculated by the computer program for their regions of flow. Additionally a row of holes were placed in the windows in the direction of flow downstream of the center nozzle body to bleed a portion of the nozzle wake. Figures (21), (22), (23), and (24) show these bleed slots in the diffuser walls and the bleed holes in the windows. Drawing (16) in Appendix A gives dimensions and locations of the slots in the diffuser blocks. Drawing (17) specifies the location and hole sizes for the windows. A vacuum manifold was designed and constructed to apply the vacuum to the window bleed holes with minimum visual obscuration of the flow. Drawing (18) in Appendix A as well as Figures (25), (26), and (27) shows this manifold and its details.

E. ASSEMBLED APPARATUS AND EXPERIMENTAL PROCEDURE

The assembled apparatus and its details are shown in Figures (28), (29), (30), and (31). Thirty five valves separate various regions of boundary layer bleed slots and holes from each other. Overall operation of the diffuser can be studied as a function of bleed from various regions of the diffuser. The common manifold, a section of two inch diameter pipe, was connected to a two-hundred-cubic-foot tank which was continuously evacuated by a vacuum pump. The high pressure air manifold was a section of four inch diameter pipe connected through a pressure regulator valve to a high pressure tank and air compressor.

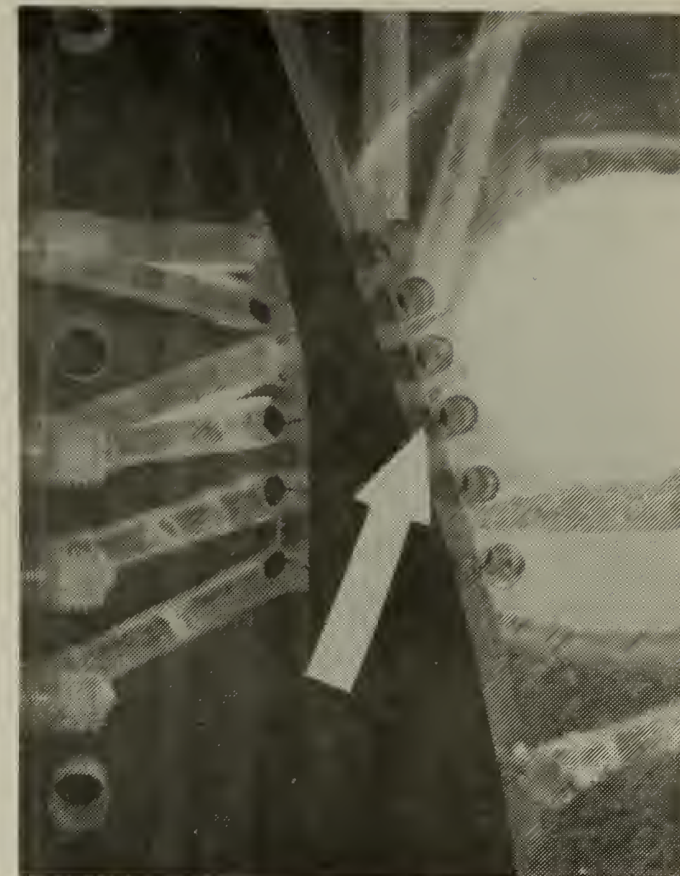

B.L. BLEED SLOTS IN
SIDE WALLS OF DIFFUSER

FIGURE (21) DIFFUSER WALL BLEED SLOTS

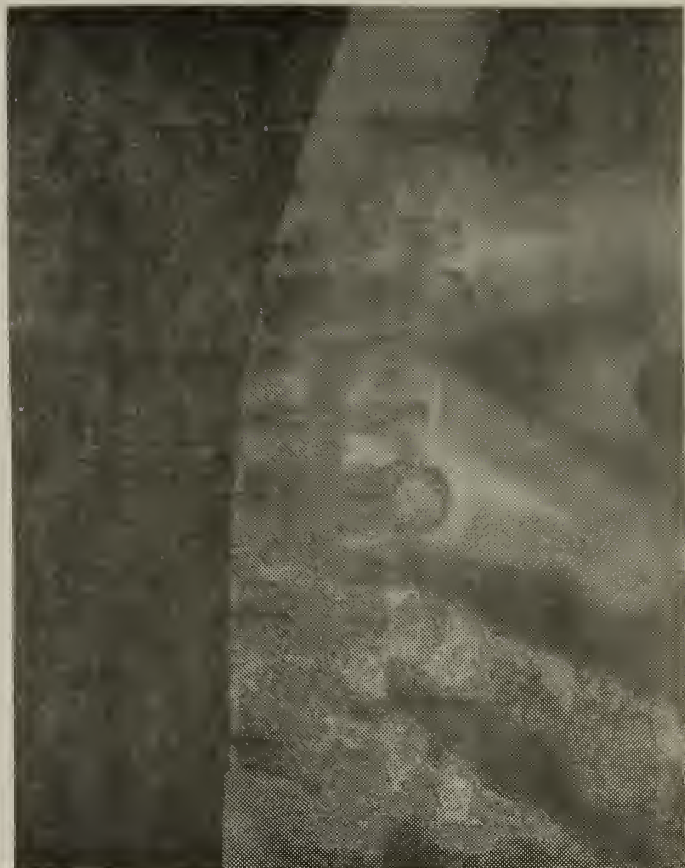

CLOSE UP VIEW OF BLEED SLOTS IN WALL
OF PLEXIGLASS DIFFUSER CHANNEL

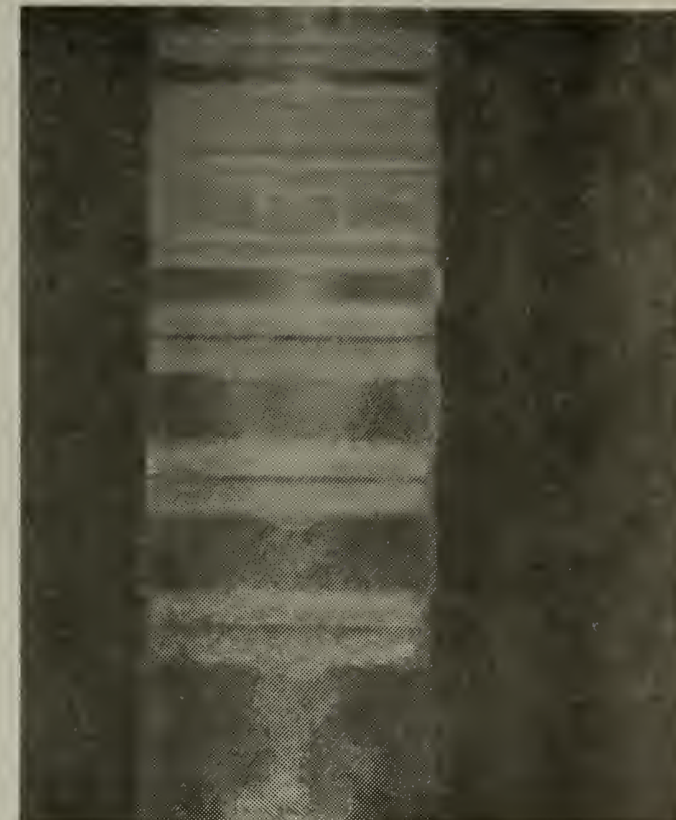

CLOSE UP VIEW OF BLEED SLOTS

FIGURE (22) DETAILS OF BLEED SLOTS

ONE OF TWO WINDOWS
THAT FORM TWO SIDES
OF DIFFUSER CHANNEL
-B.L. BLEED HOLES ARE
VISIBLE IN GLASS

FIGURE (23) DIFFUSER WINDOW

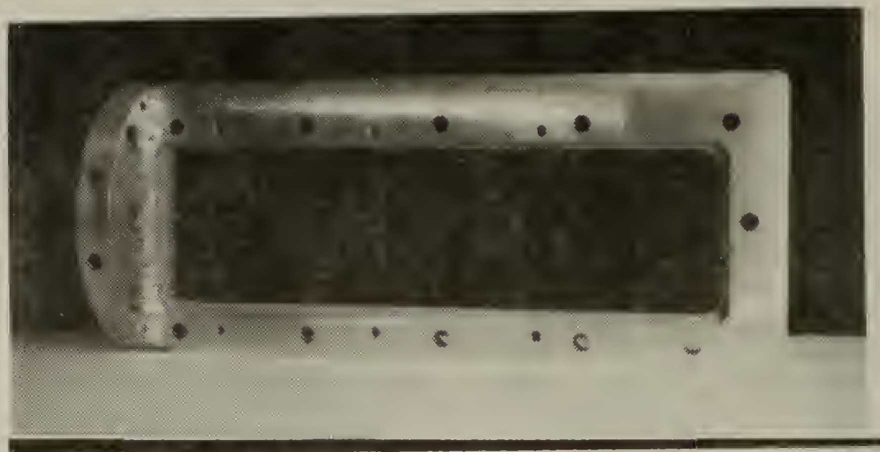

FRONT FACE OF WINDOW SHOWING B.L. BLEED HOLES

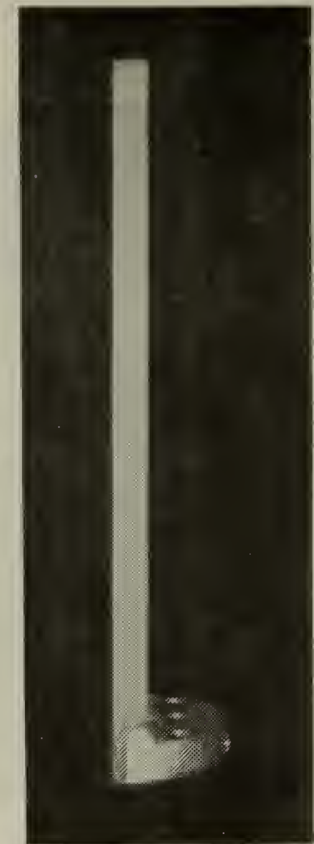

EDGE VIEW OF WINDOW

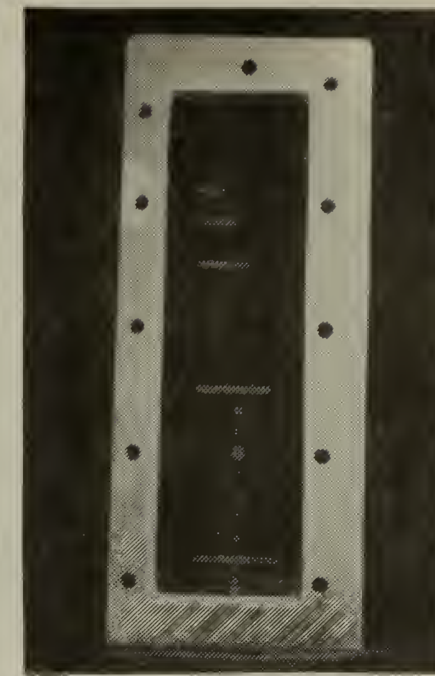

FLOW SIDE OF WINDOW

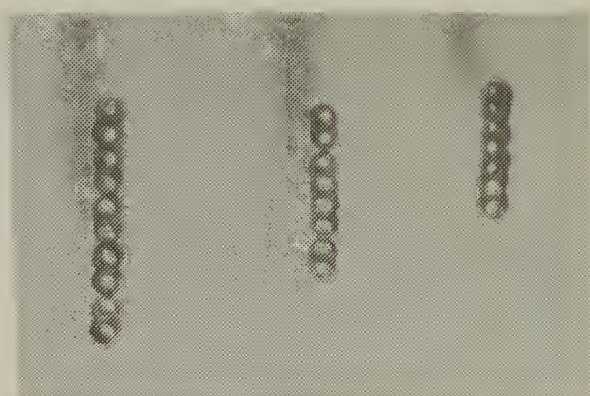

DETAILS OF B.L. BLEED HOLES

FIGURE (24) DETAILS OF DIFFUSER WINDOWS

ONE OF TWO VACUUM MANIFOLDS FOR B. L. BLEED ON WINDOWS

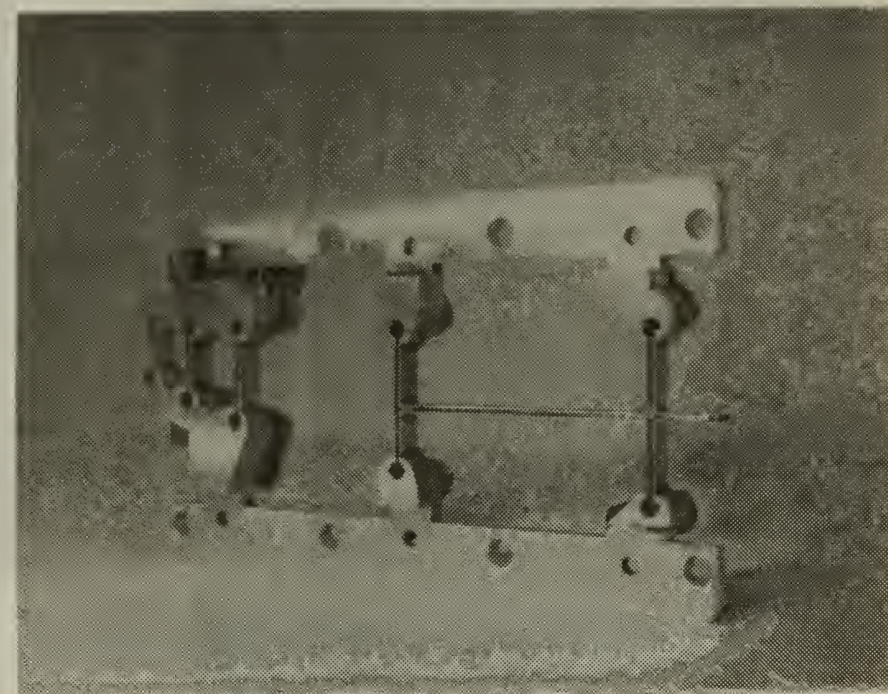

FIGURE (25) WINDOW VACUUM MANIFOLD

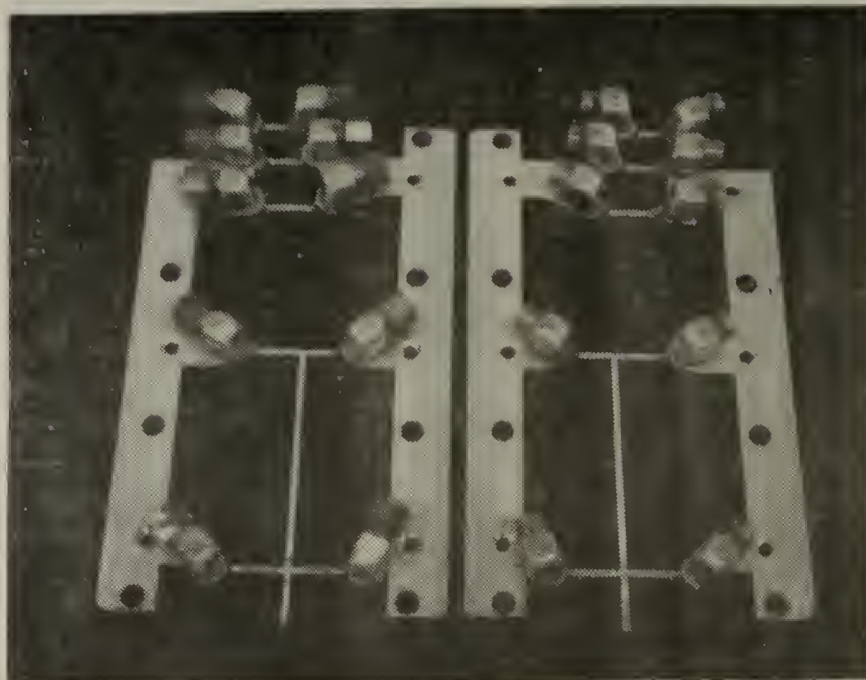

FRONT OF BOTH MANIFOLDS SHOWING VACUUM LINE FITTINGS

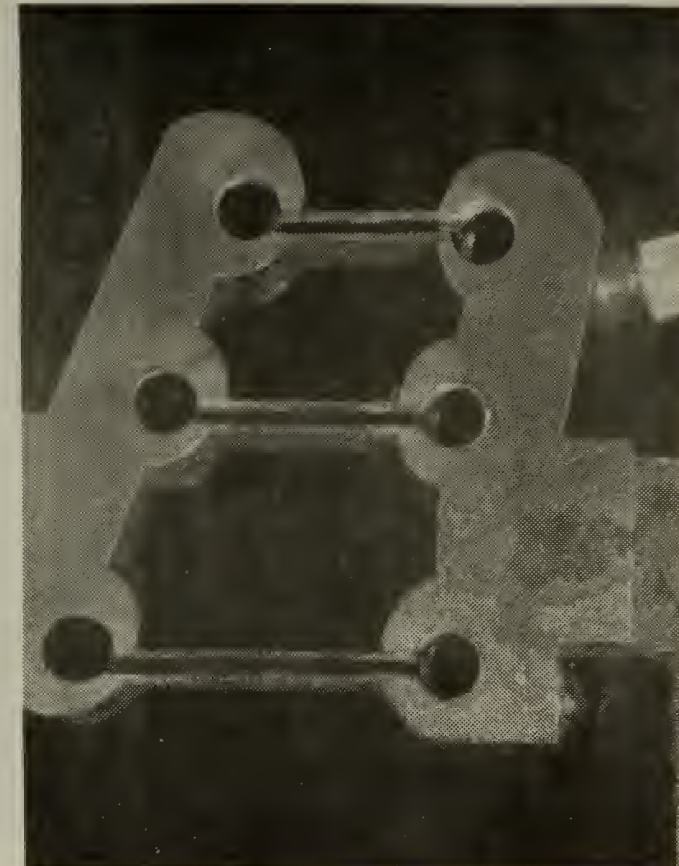

CLOSE UP VIEW OF VACUUM MANIFOLD SURFACE THAT IS SEALED TO WINDOW OVER B.L. BLEED HOLES

FIGURE (26) DETAILS OF WINDOW VACUUM MANIFOLD

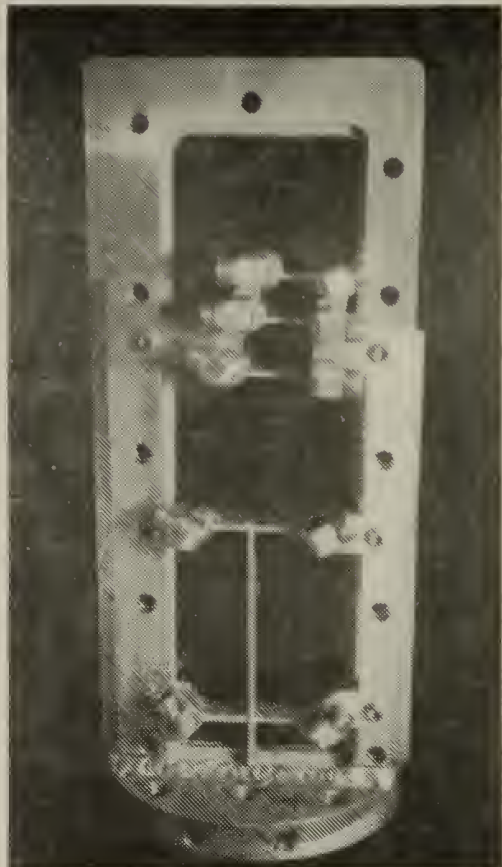

MANIFOLD MOUNTED ON A WINDOW

FLOW SURFACE OF WINDOW SHOWING MANIFOLD MOUNTED OVER B.L. BLEED HOLES

CLOSE UP VIEW THROUGH WINDOW OF MANIFOLD MOUNTED OVER B.L. BLEED HOLES

FIGURE (27) DETAILS OF MOUNTED WINDOW VACUUM MANIFOLD

ASSEMBLED DIFFUSER
WITH VACUUM LINES
ATTACHED

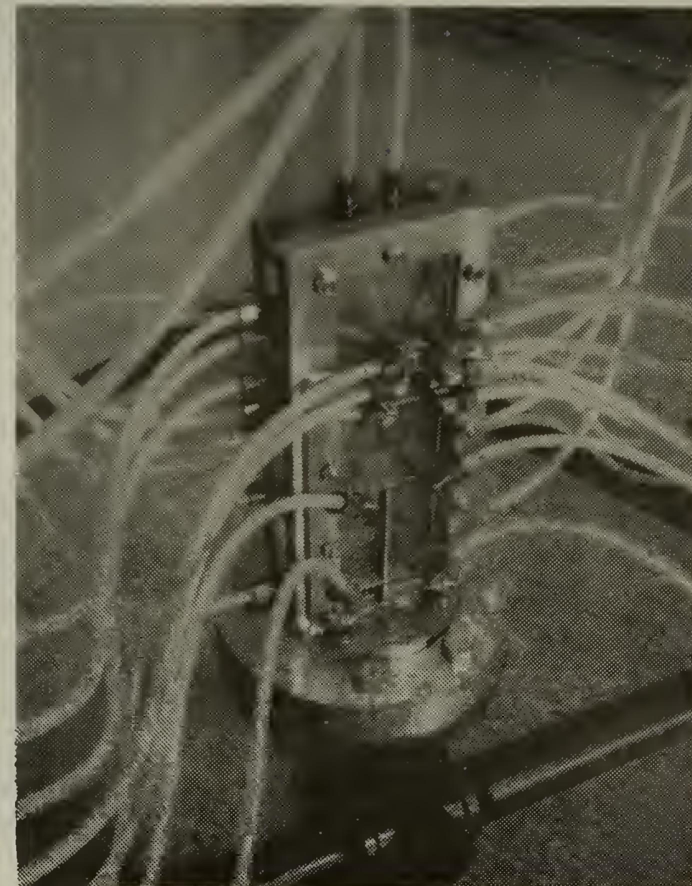

FIGURE (28) ASSEMBLED DIFFUSER

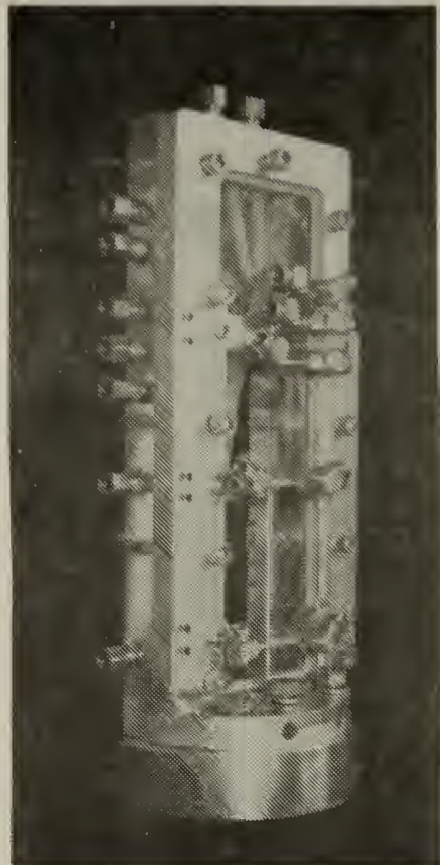

ONE WINDOW, VACUUM MANI-
FOLD, AND DIFFUSER
BLOCKS MOUNTED ON BASE
PLATE

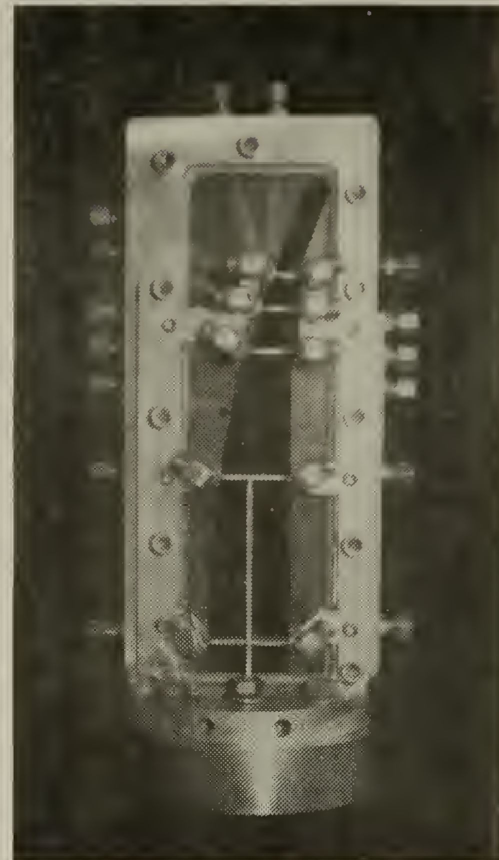

FRONT VIEW OF PARTIALLY
ASSEMBLED APPARATUS

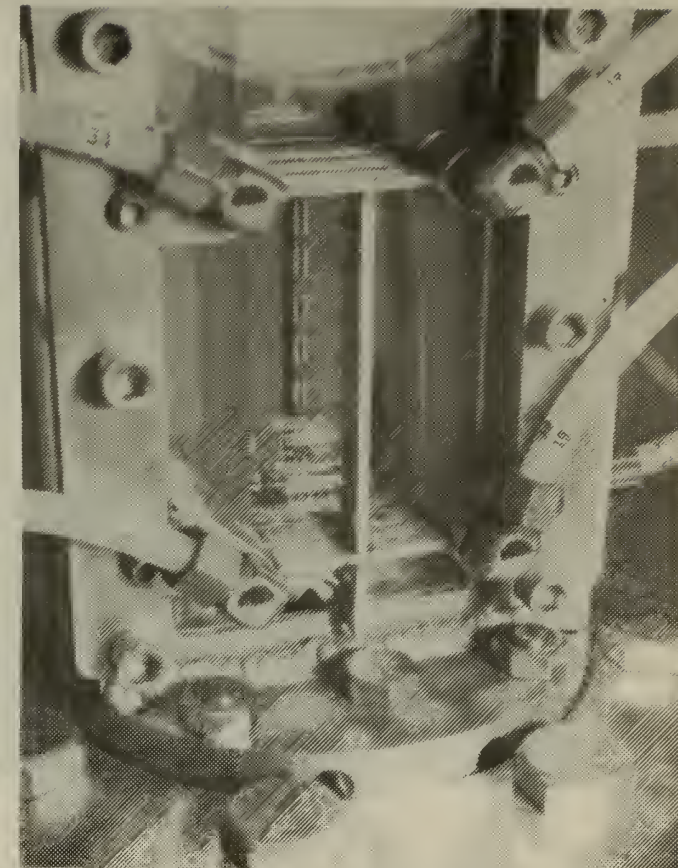

CLOSE UP VIEW OF ASSEMBLED APPARATUS
LOOK-THROUGH WINDOW INTO ENTRANCE OF
DIFFUSER PASSAGE

FIGURE (29) DETAILS OF ASSEMBLED DIFFUSER

DIFFUSER MOUNTED ON HIGH PRESSURE AIR STAND - DETAIL OF VACUUM LINES, VALVES, AND COMMON MANIFOLD

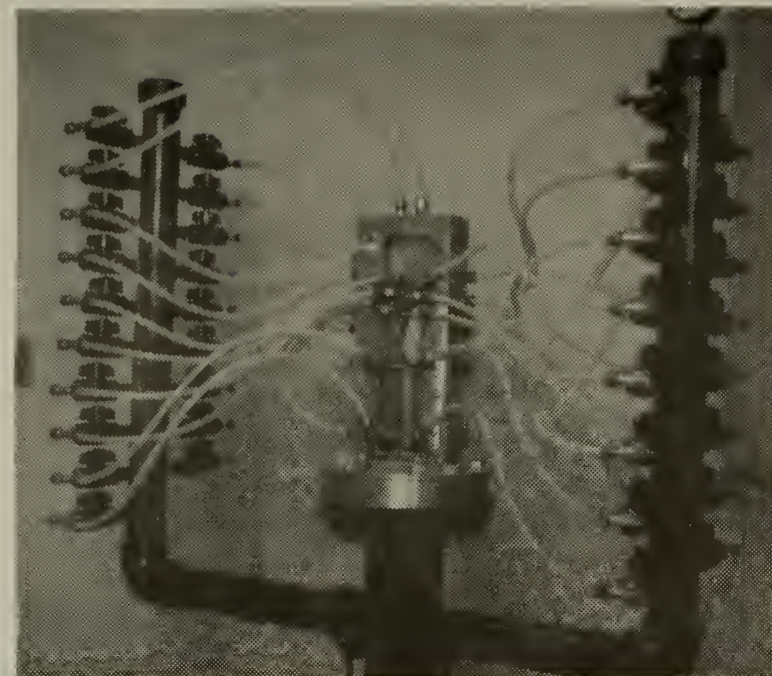

FIGURE (30) DIFFUSER AND VACUUM MANIFOLD

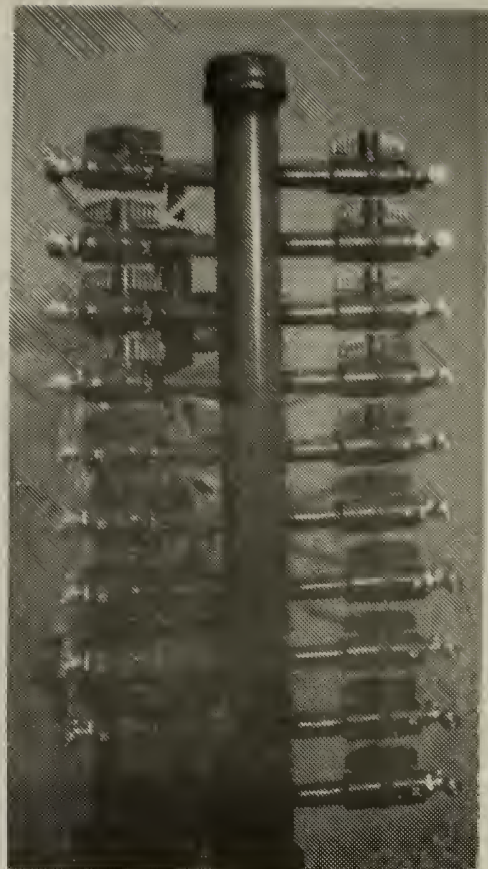

VALVES ON COMMON MANIFOLD CONNECTED TO VACUUM TANK

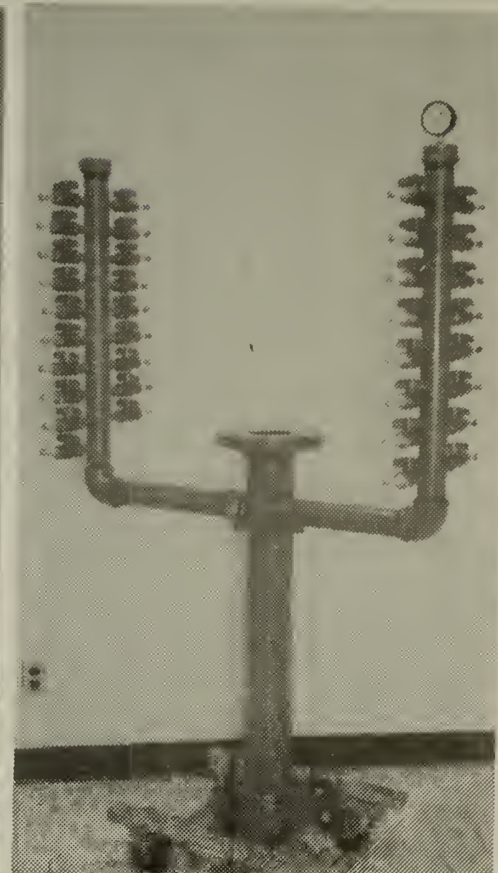

COMMON MANIFOLD AND 35 VALVES MOUNTED ON HIGH PRESSURE AIR STAND

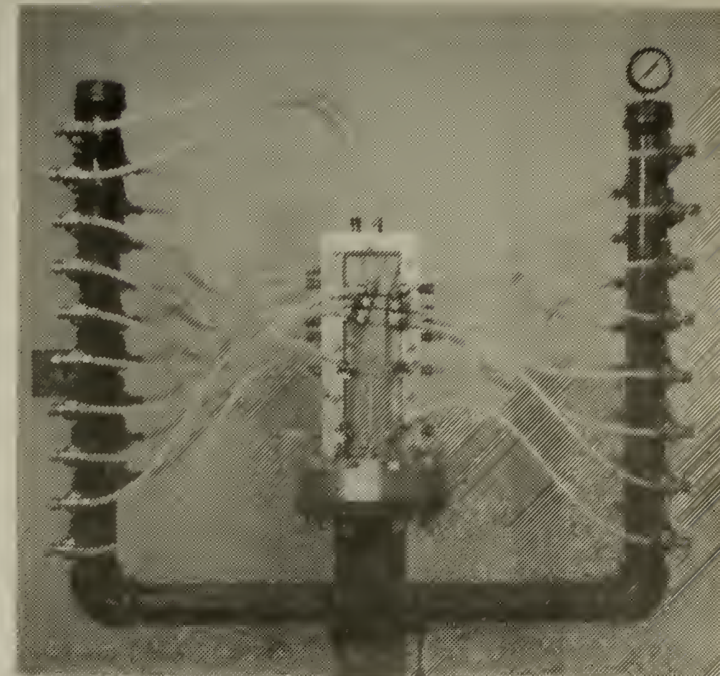

VIEW OF ASSEMBLED DIFFUSER, VACUUM LINES, VALVES, AND COMMON MANIFOLD MOUNTED ON HIGH PRESSURE AIR STAND

FIGURE (31) DETAILS OF VACUUM MANIFOLD

Many tests of the apparatus were conducted at various values of the contraction ratio, ψ , stagnation pressure, P_0, and boundary layer bleed configurations. Schlieren photographs of the flow were taken as well as static pressure readings in the diffuser by connecting pressure gages to isolated vacuum bleed lines. A typical run consisted of turning on the high pressure air flow and adjusting it to the desired stagnation pressure with the pressure regulator valve. The common vacuum manifold was connected to the vacuum tank through a valve. This valve was opened applying vacuum to the bleed lines after the valve for the high pressure air was opened. The stagnation pressure could be varied from atmospheric to a maximum pressure of 200 psig. The vacuum could initially be lowered to 0.5 psia in the vacuum tank which would increase to a steady state pressure of 3 to 4 psia during continuous bleeding. After several unsuccessful attempts to establish supersonic flow in the diffuser, which is the running condition, two alterations were made to the diffuser blocks to aid in starting the supersonic flow. The compression wall block was segmented as shown in Figure (32) to provide variable contraction ratio by assembling the diffuser blocks in the manner shown in Figure (33). One way check valves were installed in the lower portion of the diffuser blocks to remove high pressure air during starting. These valves provide mass bleed during starting. During the unfavorable starting conditions shown in Figure (3a) the shock wave

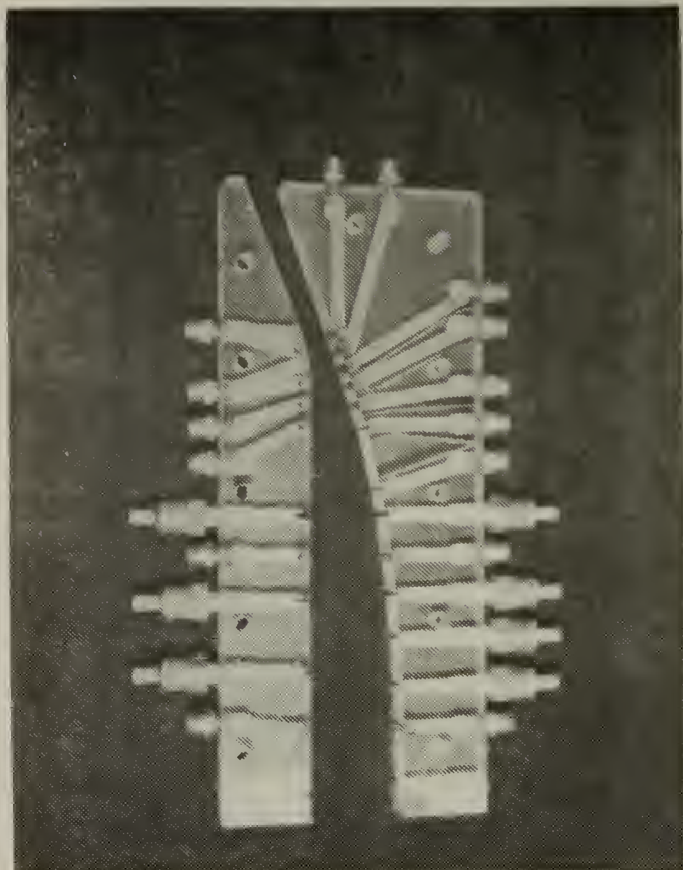

SEGMENTED DIFFUSER BLOCK SHOWING SEVEN BLOW OUT VALVES INSTALLED

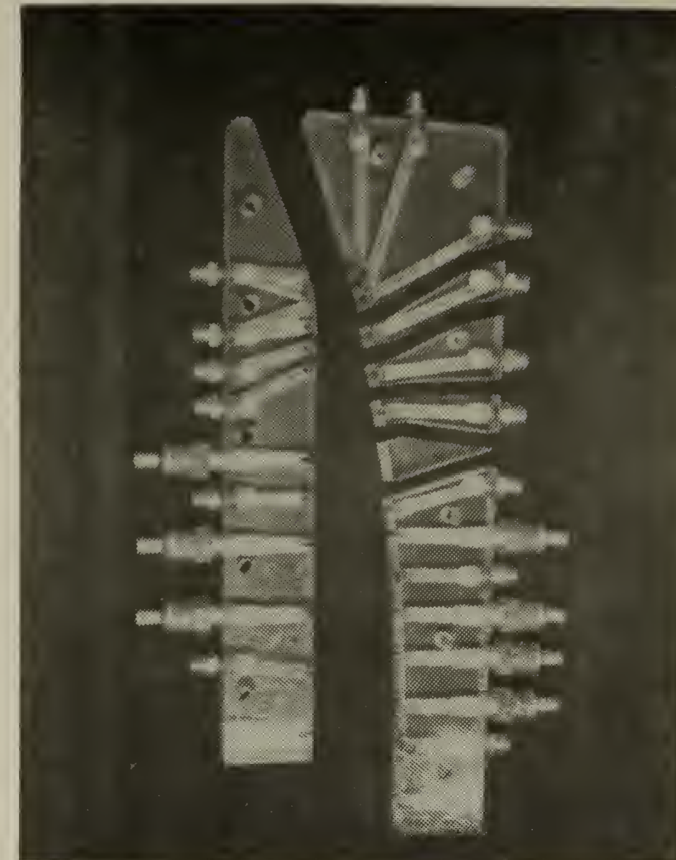

EXPLODED VIEW OF SEGMENTED DIFFUSER BLOCK

FIGURE (32) SEGMENTED DIFFUSER BLOCKS WITH BLOW OUT VALVES

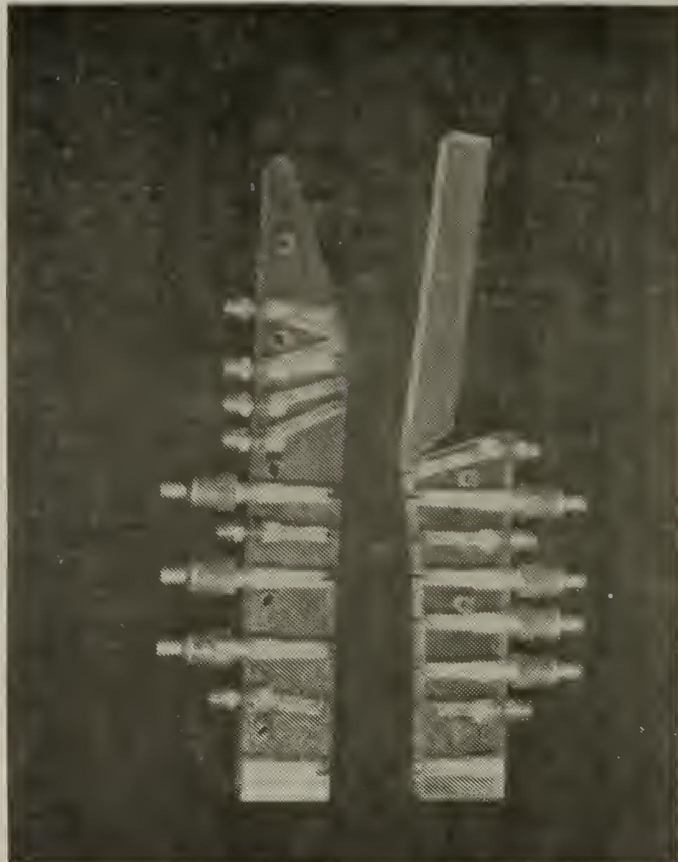

SEGMENTED DIFFUSER BLOCK FOR $\psi = 1.39$

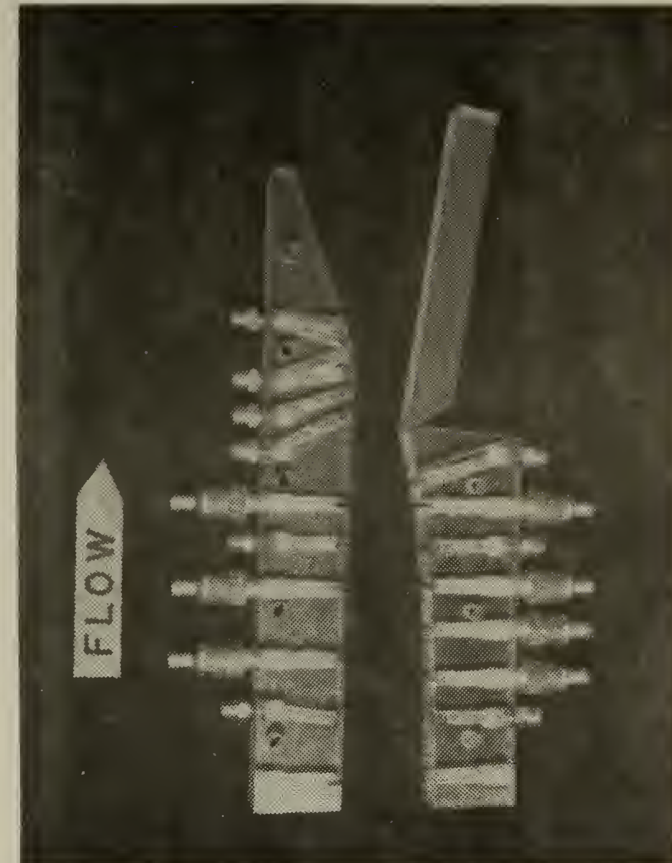

SEGMENTED DIFFUSER BLOCK FOR $\psi = 1.63$

FIGURE (33) SEGMENTED DIFFUSER BLOCKS

greatly increases static pressure. At the same time the stagnation pressure decreases across the shock wave requiring a larger diffuser throat to pass this quantity of flow, especially at high contraction ratios. The blow out valves discharge the excess mass flow upstream of the throat thus allowing the shock to pass through the diffuser and establish supersonic flow. The blow out valves are fast acting one way valves and close immediately upon sensing the extremely low static pressure of the supersonic flow. These valves are shown in Figure (32) and (33).

IV. RESULTS AND CONCLUSIONS

A. RESULTS

1. Contraction Ratio, 3.33

The initial configuration of the diffuser with a contraction of 3.33 would not start. Supersonic flow could not be established in the diffuser passage utilizing the maximum available stagnation pressure of 255 psia and the minimum vacuum attainable of 1.0 psia applied to all the boundary layer bleed passages. The analytically predicted contraction ratio for a Mach number of 4.0 and a diffuser without a bleed system is 1.44, so it was very optimistic to expect the initial geometry, even with extensive bleed, to start. This geometry had been picked as a design point for fabrication of the apparatus capable of accommodating any conceivable contraction ratio geometry. Since the throat and bleed system could not pass the necessary mass flow to start the diffuser, fast acting, one-way, blow-out valves were installed in the walls of the diffuser blocks to remove the excess flow. Nine of these valves were installed in the lower part of the passage and are shown in Figures (32) and (33). Pressure readings along the diffuser walls were taken for three configurations shown in Figure (34). From these data the relative effect of the vacuum boundary layer bleed and the blow-out valves on the pressures at given points in the diffuser could be

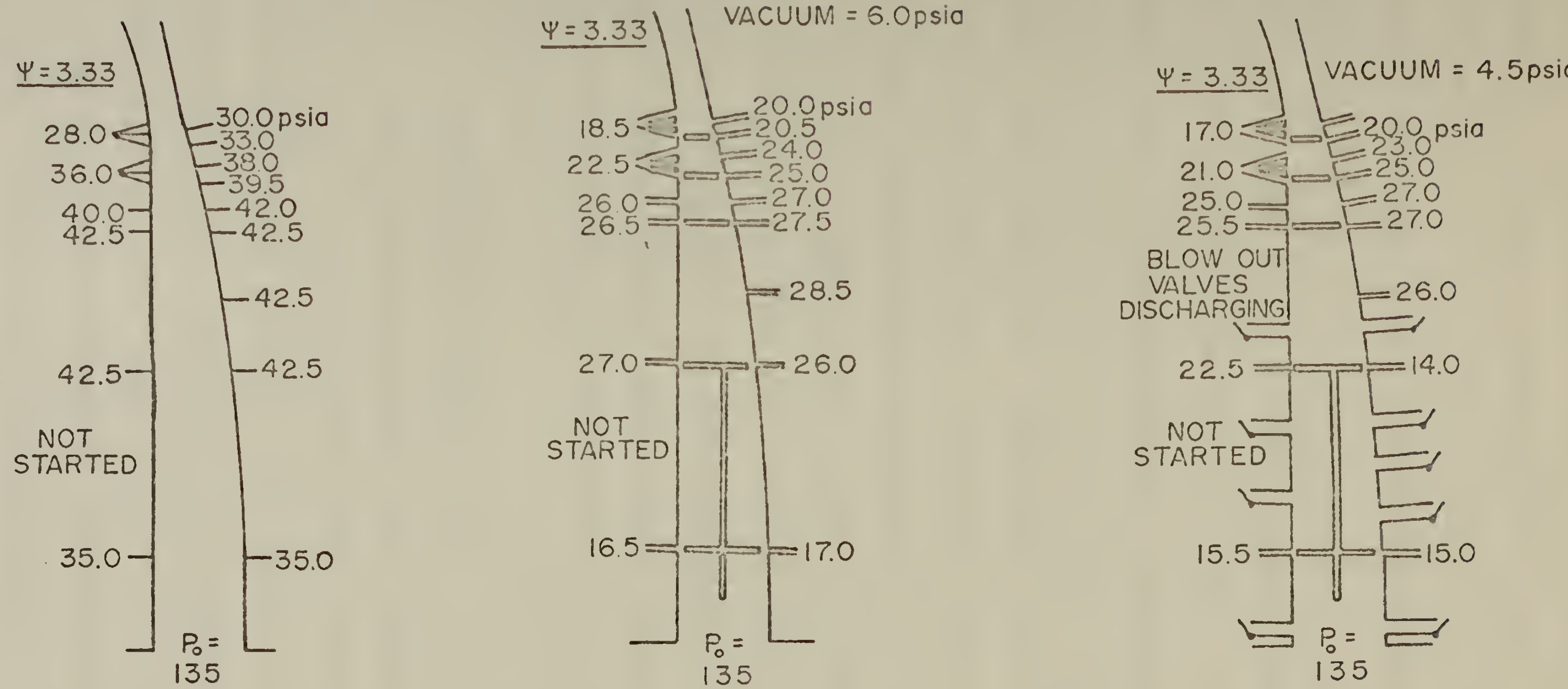

PRESSURE ALONG WALLS OF DIFFUSER WITH VACUUM OFF

PRESSURE ALONG WALLS OF DIFFUSER WITH VACUUM ON

PRESSURE ALONG WALLS OF DIFFUSER WITH VACUUM ON AND BLOW OUT VALVES DISCHARGING

FIGURE (34) EXPERIMENTAL DATA - WALL PRESSURES, $\Psi = 3.33$

studied. The boundary layer bleed lowered the starting pressures by approximately 38% and the discharge of the blow out valves lowered the pressures another 4%. The average pressure ratio across the boundary layer bleed system was 6.31 while the pressure ratio across the valves was 1.56. The area of the boundary layer bleed holes was 0.83 square inches and the area of the valve's bleed slots was 0.34 square inches. The above pressure ratios were sufficient to establish choked flow in the boundary layer bleed passages. The actual bleed hole areas were much greater than their effective flow areas. The boundary layer bleed system appeared to be ten times as effective as the bleed of the valves, but when one considers the lesser flow area and pressure ratio available to the valves, the product of area and pressure ratio is one-tenth that of the boundary layer bleed system, it appears that the two systems are equally effective, as in principle they should be.

2. Contraction Ratio, 1.39

The diffuser blocks were segmented as shown in Figure (32) to provide for lower and incrementally changeable contraction ratios. The lowest contraction ratio geometry of 1.39, equal to that predicted analytically in Figure (4) for starting, was tested next. Starting is defined as the establishment of supersonic flow in the diffuser. This configuration started without using boundary layer bleed or blow out valves. A sequence of Schlieren photographs of the flow in the diffuser for increasing stagnation pressures is shown in Figures (35) and (36). Mach lines which originate in the nozzle exits are visible at the bottom of each picture and Mach angles are used to determine the nozzle exit Mach numbers by the equation found in Ref. 3,

$$\mu = \sin^{-1} \frac{1}{M} \quad .$$

Static pressure measurements were made at several locations along the walls and are shown in Figures (35) and (36). These measurements were made by connecting a bourdon tube pressure gage with a range from 0 to 100 psia to individual isolated boundary layer bleed slots in the diffuser wall. Readings of pressures less than 5.0 psia were of doubtful accuracy because they were at the extreme low end of the gage's capabilities. This suspected inaccuracy is substantiated by the constant pressure reading obtained at a location just downstream of the nozzle exits even though the Mach angle and stagnation pressure were varied as in Figure (36).

3. Contraction Ratio, 1.63

A diffuser geometry with a contraction ratio of 1.63 as shown in Figure (33) was tried next and would start only with the blow out valves installed and the boundary layer bleed applied. Supersonic flow was established in the passage by first turning on and increasing the high pressure air to a sufficiently high stagnation pressure and then opening the main vacuum valve connecting the vacuum tank

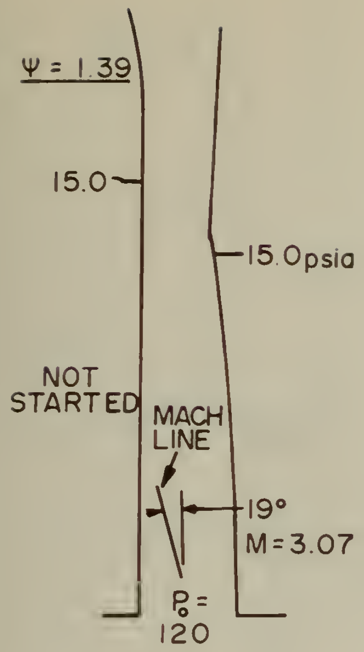

STARTING SEQUENCE
WITHOUT VACUUM BLEED
OR BLOW OUT VALVES,
P = 120

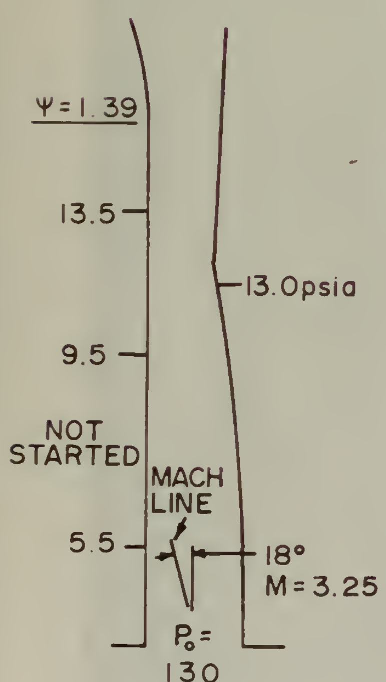

STARTING SEQUENCE
WITHOUT VACUUM BLEED
OR BLOW OUT VALVES,
P = 130

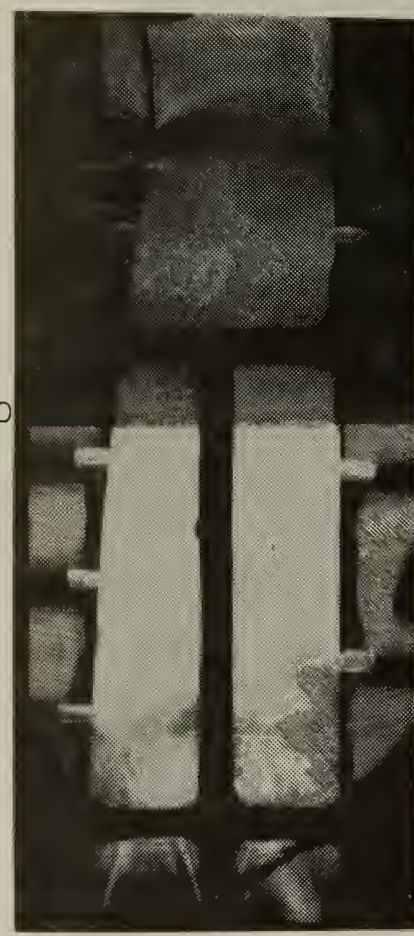

FIGURE (35) EXPERIMENTAL DATA - STARTING SEQUENCE $\Psi = 1.39$

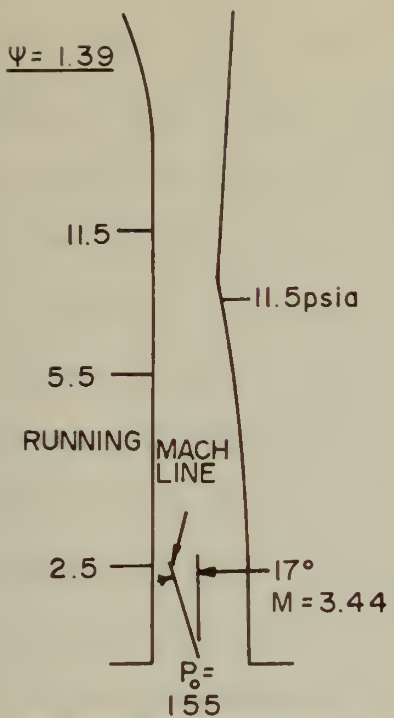

STARTING SEQUENCE
WITHOUT VACUUM BLEED
OR BLOW OUT VALVES,
P = 155

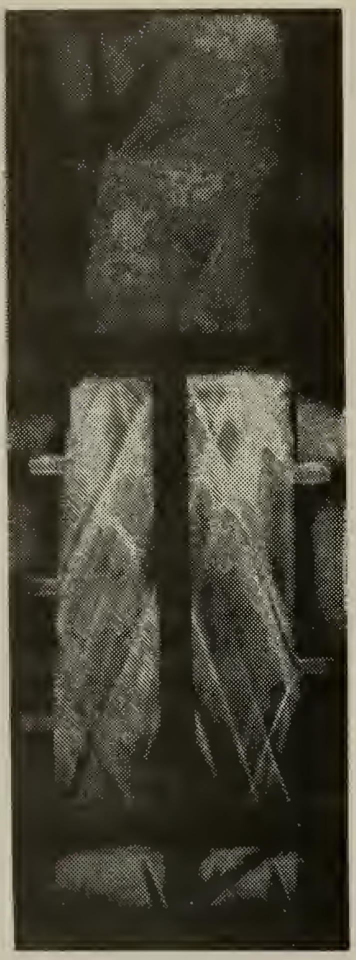

STARTING SEQUENCE
WITHOUT VACUUM BLEED
OR BLOW OUT VALVES,
P = 215

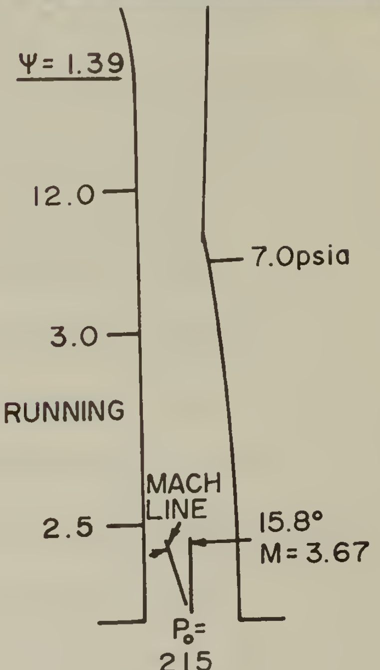

FIGURE (36) EXPERIMENTAL DATA - RUNNING SEQUENCE, $\Psi = 1.39$

to the common manifold, thereby applying vacuum to the boundary layer bleed system, until the diffuser started. With proper stagnation pressure, bleed area, and vacuum the diffuser would start in one to two seconds after the vacuum was applied. A larger contraction ratio of 2.16 was tried by adding the next segment of diffuser block, but this geometry was impossible to start by any means incorporated in the design of the diffuser. The maximum attainable contraction ratio was then assumed to lie between the values of 1.63 and 2.16. The diffuser was reconfigured back to a geometry with a contraction ratio of 1.63 and several tests were run yielding qualitative relationships between boundary layer vacuum bleed pressure versus stagnation pressure for intermittent and positive starts, Figure (37), and effective bleed area to throat area ratio versus starting stagnation pressure, Figures (38) and (39).

Figure (37) shows the experimental data points for seven combinations of boundary layer bleed vacuum and stagnation pressure and the resultant operation of the diffuser. The drawing in the right of the Figure shows the bleed configuration. The starts indicated by four of the data points were immediate upon application of the boundary layer bleed vacuum; supersonic flow was established in the passage and observed by means of Schlieren flow visualization. The two intermittent starts consisted of supersonic flow being established and observed for periods of one second or less followed by unstarting and intermittent

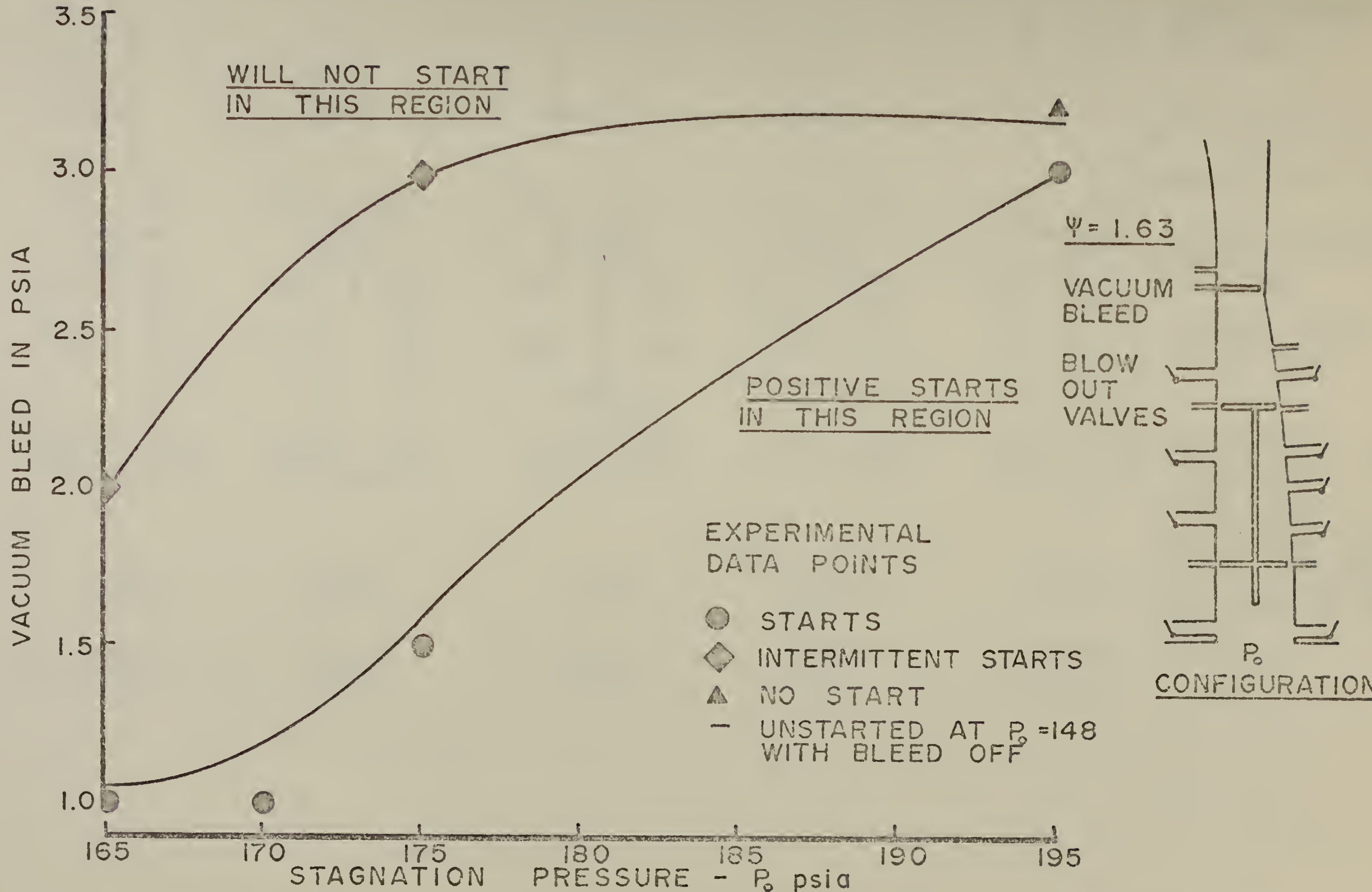

FIGURE (37) EXPERIMENTAL DATA - GRAPH OF OPERATING POINTS, $\psi = 1.63$

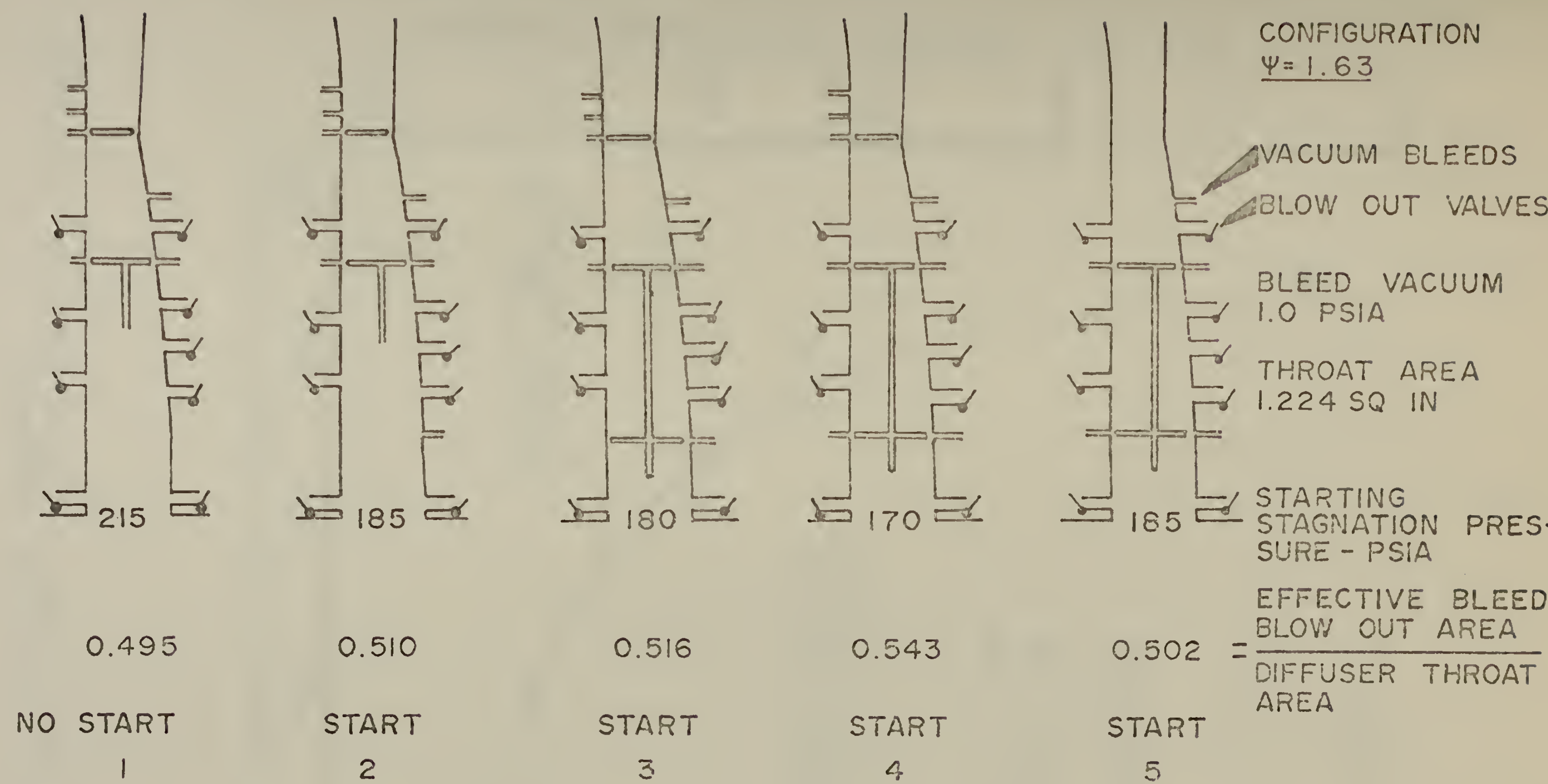

FIGURE (38) EXPERIMENTAL DATA - BLEED EFFECT ON STARTING, $\psi = 1.63$

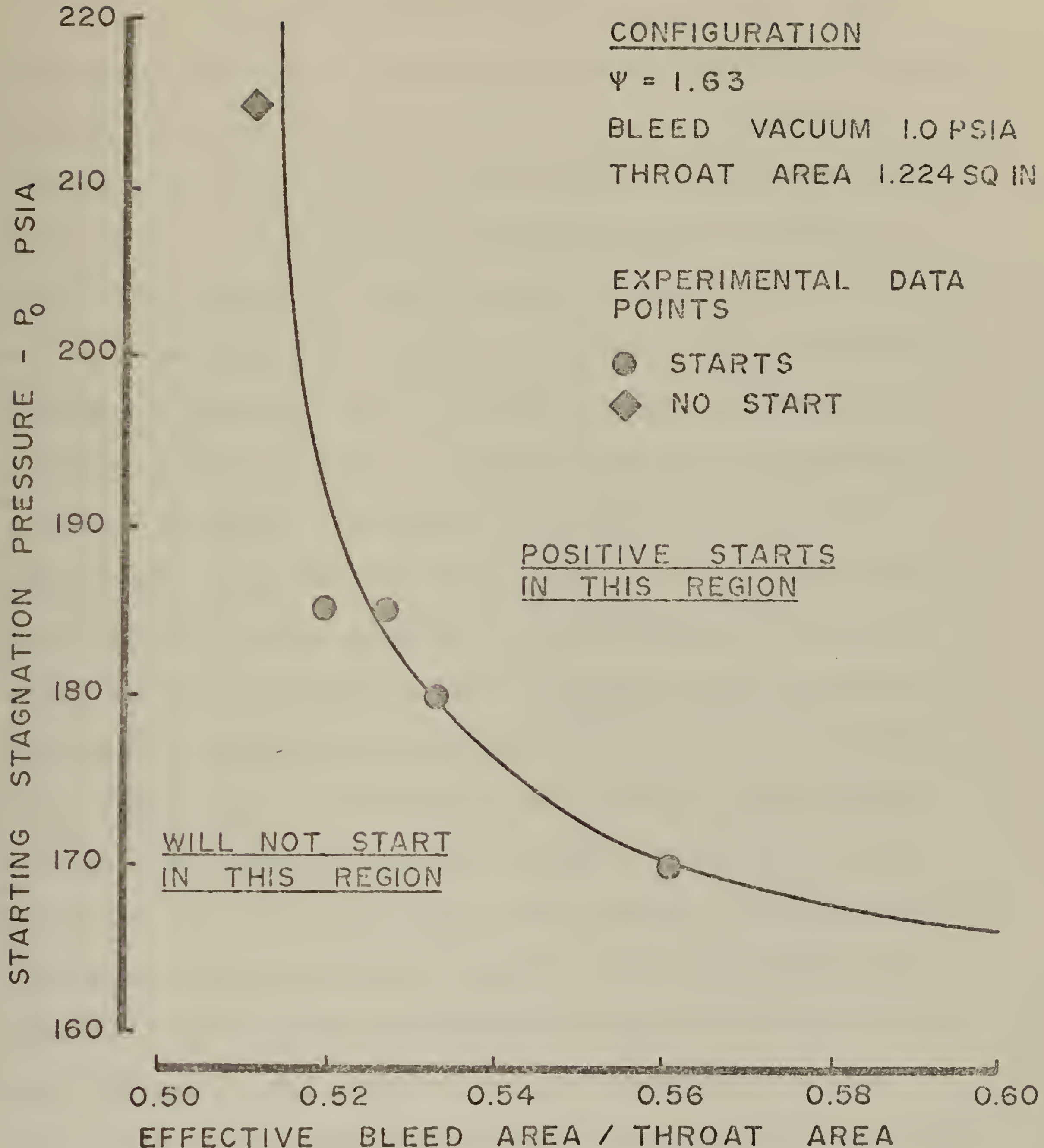

FIGURE (39) EXPERIMENTAL DATA - GRAPH OF BLEED EFFECT ON STARTING, $\psi = 1.63$

restarting. The diffuser would not start at the values of pressure and vacuum recorded by that data point on Figure (37). All of the data points were reproducible. The boundary layer bleed vacuum directly affected the starting stagnation pressure or vice versa until a stagnation pressure of 175 to 180 psia was reached. These pressures correspond to those predicted analytically by methods in Ref. 3 for choking of the nozzles installed in the diffuser. As expected once the nozzles were choked, increasing the stagnation pressure had no further effect on starting or running of the diffuser. Below the value of stagnation pressure to choke, the amount of boundary layer bleed vacuum necessary for starting appeared to vary directly with the stagnation pressure or vice versa. The static pressure in a diffuser before it starts, as described in Figure (3), increases directly with increases in stagnation pressure, so even though the boundary layer bleed vacuum was increased and the diffuser started one does not know the actual pressure ratio across the bleed system. The Mach number at which a shock occurs in a nozzle increases with increasing stagnation pressure up to design Mach number of the nozzle. As the shock Mach number increases the stagnation pressure losses across the shock also increase and then require a larger diffuser throat to pass the flow to start. It can be seen that higher bleed areas or pressure ratios would be required to start the diffuser at lower downstream stagnation pressures. For these reasons it is suspected that even though the bleed pressure was increased along with stagnation pressure the actual pressure ratio across the bleed system increased with the prenozzle stagnation pressure and the diffuser started. Figure (37) does depict regions of boundary layer bleed vacuum and stagnation pressure where the diffuser could not be started and regions where starting was a certainty for this diffuser.

Testing was done to study the effect of boundary layer bleed location and total area on the starting of the diffuser. Boundary layer bleed holes and slots were utilized starting first in the diffuser throat region and then adding more regions of bleed until the diffuser could be started. Figure (38) shows this sequence of testing and the configuration of the diffuser. The blow-out valves were used continuously. Boundary layer bleed applied to the upper regions of the diffuser with a total effective bleed ratio of 0.495 would not start the diffuser. The bleed ratio is the effective boundary layer bleed and blow-out valve area divided by the diffuser throat area. Increasing the bleed ratio by 3.1% to 0.510 allowed the system to start at 185 psia. An increase of bleed ratio by another 1.1% to 0.516 decreased the starting stagnation pressure by 2.7% to 180 psia. Further increasing the bleed ratio another 5.3% to 0.543 decreased the starting pressure 5.6% to 170 psia. These four runs had boundary layer bleed area progressively added to the system starting in the throat region and moving down the passage from run to run as shown in the configuration drawings in Figure (38). Run number five had almost the same bleed ratio as run number two except that the bleed areas were activated starting in the bottom of the diffuser passage and continuing upward until the bleed ratio of 0.502 was reached. This configuration started at the same stagnation pressure ratio as run two indicating that the bleed ratio and not location affects starting. Figure (39) shows a plot of stagnation pressure versus bleed ratio for starting. All of the data points are from the runs depicted in Figure (38) with a bleed vacuum of 1.0 psia. For this diffuser there appeared to be a definite minimum bleed ratio for this contraction ratio below which supersonic flow could not be established at any available stagnation pressure. The upper photograph in Figure (40) shows the flow established by the starting parameters of run five in Figure (38). A thick boundary layer on the glass surfaces obscures viewing of the interior flow and Mach lines. The thickening of the boundary layer can be seen to originate along a Mach line. Applying boundary layer bleed to the throat region caused the immediate disappearance of this region of thickened boundary layer. See the lower photograph in Figure (40).

4. Contraction Ratio, 1.69

The third piece of the segmented diffuser block was cut into four pieces which varied the contraction ratio from

SCHLIEREN PHOTOGRAPH OF FLOW AFTER STARTING WITH BLOW OUT VALVES AND LOWER B.L. BLEED ONLY. THICK BOUNDARY LAYER ON GLASS OBSCURES FLOW VISUALIZATION IN UPPER PART OF DIFFUSER PASSAGE. DRAWING (5) IN FIGURE (35) SHOWS THIS STARTING CONFIGURATION.

SCHLIEREN PHOTOGRAPH OF FLOW AFTER B.L. BLEED HAS BEEN APPLIED TO REGION OF THICK BOUNDARY LAYER SHOWN IN ABOVE PHOTOGRAPH. B.L. BLEED APPLIED TO THROAT REGION OF DIFFUSER PASSAGE ELIMINATES BOUNDARY LAYER BUILD UP IN THIS AREA.

FIGURE (40) EFFECT OF BOUNDARY LAYER BLEED IN DIFFUSER THROAT

1.63 to 2.16. Utilizing all available starting methods it was found that a contraction ratio of 1.69 was the maximum at which the diffuser would start. Tests were then conducted to determine the minimum starting stagnation pressure and the minimum running stagnation pressure for various bleed geometries. Figure (41) shows the minimum stagnation pressure starting configuration. All discharge valves and boundary layer bleed slots and holes were used. The bleed ratio was 0.561 with a throat area of 1.185 square inches. The minimum starting pressure was 155 psig. Starting was instant upon application of the bleed vacuum, but only at a vacuum of 0.5 psia.

The diffuser was configured as shown in Figure (42), i.e. with discharge valves closed and all bleed line valves closed; the minimum running stagnation pressure was 150 psig. This configuration represents a baseline geometry diffuser. Supersonic flow with a Mach number of 3.5 was maintained in the diffuser entrance with a stagnation to ambient pressure ratio of 11.22. Starting stagnation pressure was 3.0% above running.

The mode of operation shown in Figure (43) was discovered by this research and is extremely significant. It is called the self bleed mode of running and allows the diffuser to operate at a reduced stagnation pressure without the use of external vacuum tanks or pumps. Higher static pressure air from the boundary layer in the throat region is bleed through the common vacuum manifold into

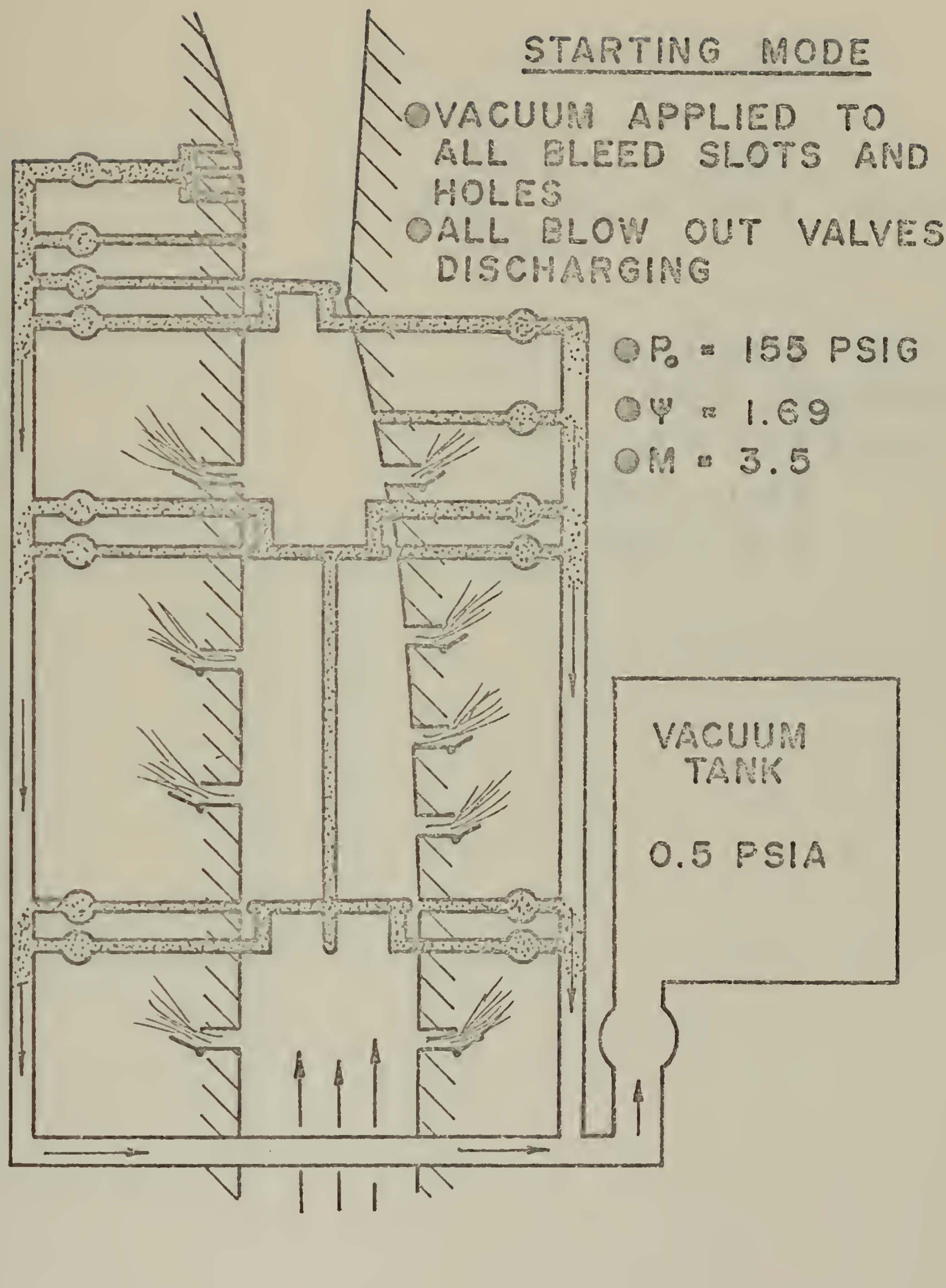

FIGURE (41) EXPERIMENTAL DATA - STARTING MODE, $\psi = 1.69$

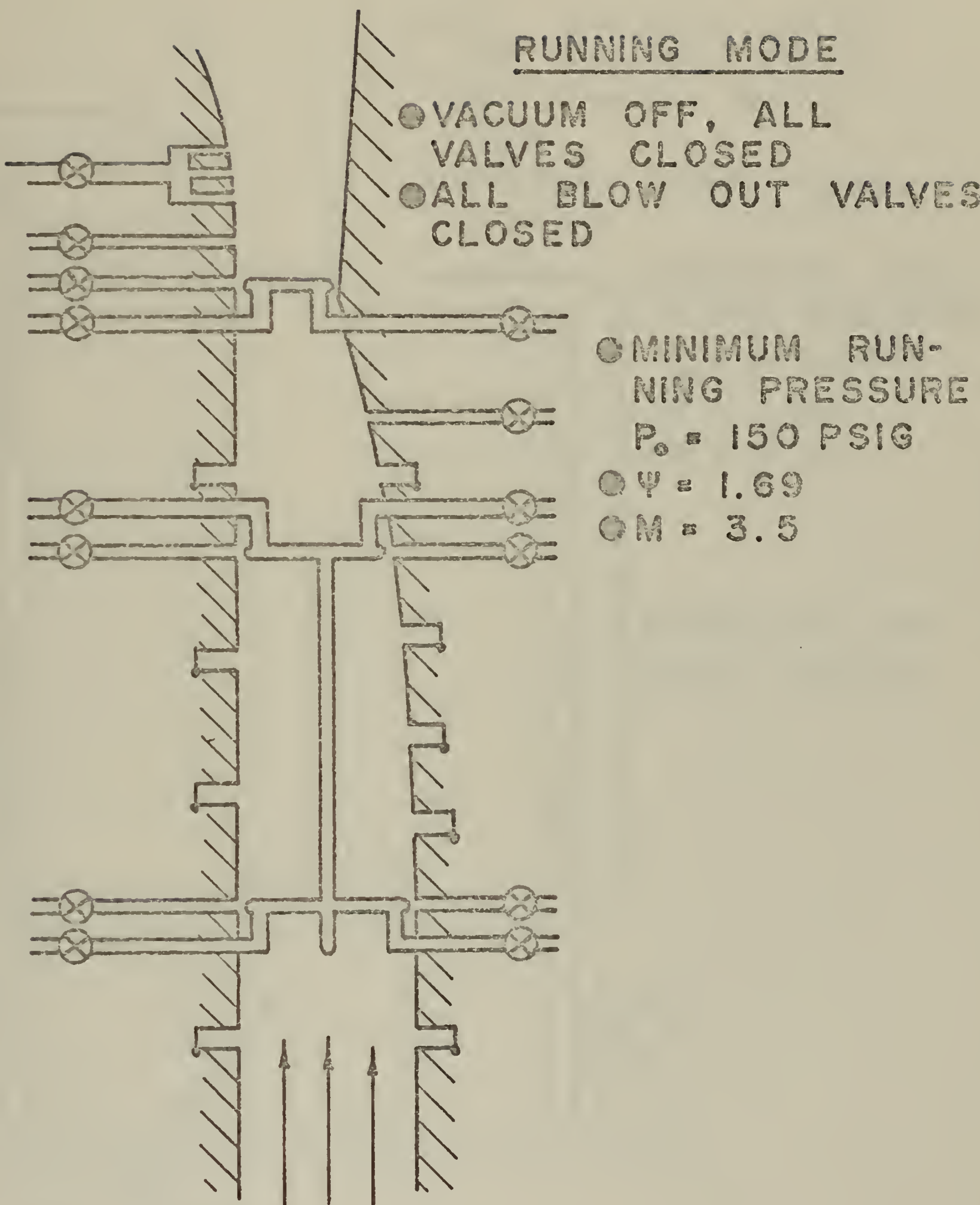

FIGURE (42) EXPERIMENTAL DATA - RUNNING MODE, $\psi = 1.69$

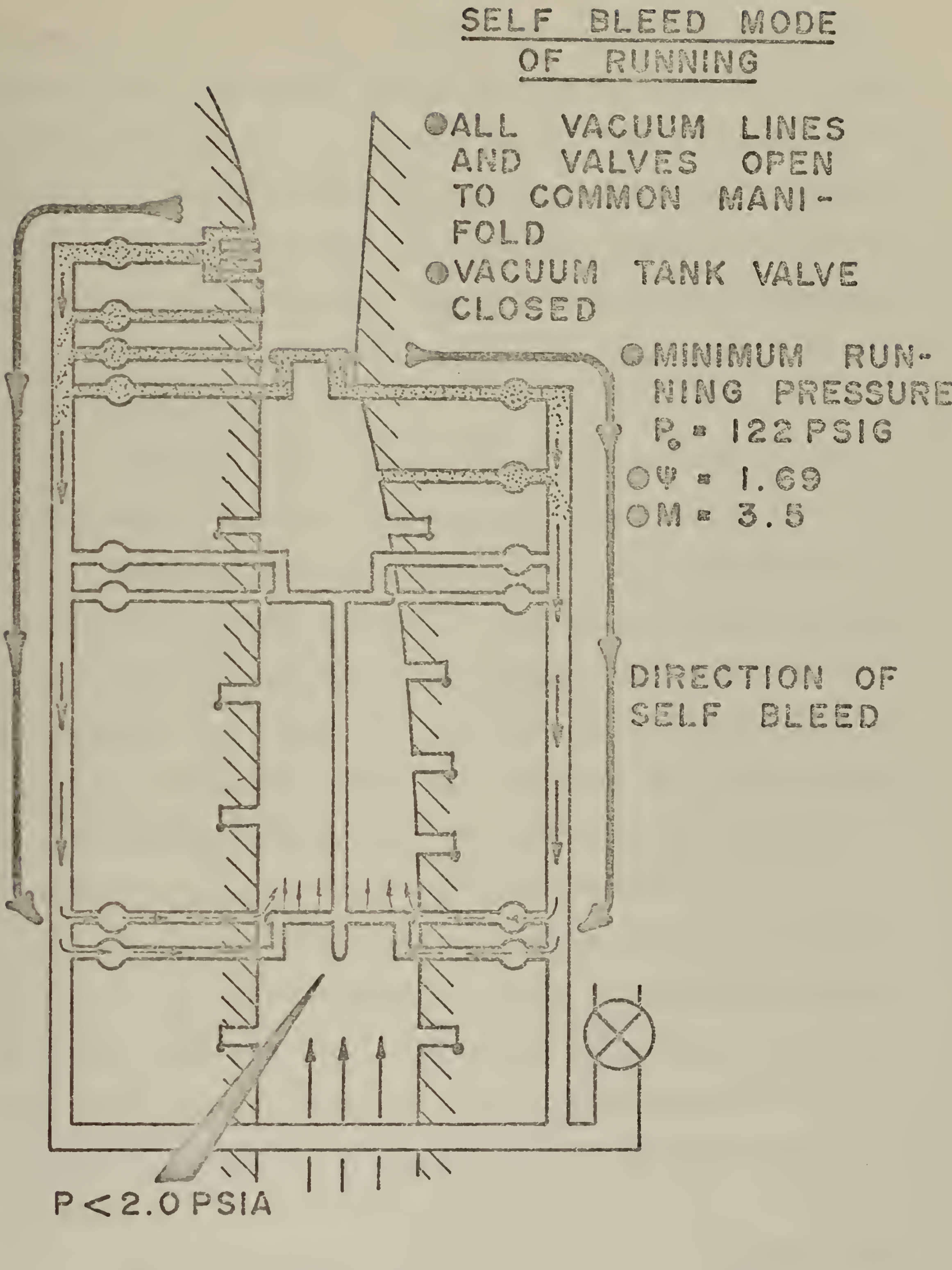

FIGURE (43) EXPERIMENTAL DATA - SELF BLEED MODE OF RUNNING, $\psi = 1.69$

the first portion of the diffuser by the lower static pressure of that region's flow. The operating stagnation pressure was reduced to 122 psig or a pressure ratio, as defined earlier, of 9.32. This is a 17.0% reduction of the stagnation pressure from the running mode shown in Figure (42). This method bleeds the boundary layer in the critical throat region, effectively decreasing the displacement thickness and allowing the diffuser to operate at its actual contraction ratio.

Boundary layer vacuum bleed was applied to the throat region of the diffuser only. See Figures (44) and (46a). The significant effect on diffuser operation of bleeding the boundary layer in the throat was demonstrated by this mode of running. The minimum running pressure was lowered 21.2% from the running mode of Figure (42) to 115 psig. This test shows that bleed in the throat region is the principal reason for the reduction in running pressure in the self bleed mode of operation.

A further reduction of minimum running stagnation pressure was attained with the bleed configuration shown in Figure (45) and (46b). This was called the vacuum and self bleed mode of running. The running pressure was lowered 28.5% below the running mode in Figure (42) to 103 psig.

The five modes of operation shown in Figures (41), (42), (43), (44), and (45) are the significant and principal results of this research. These findings were presented

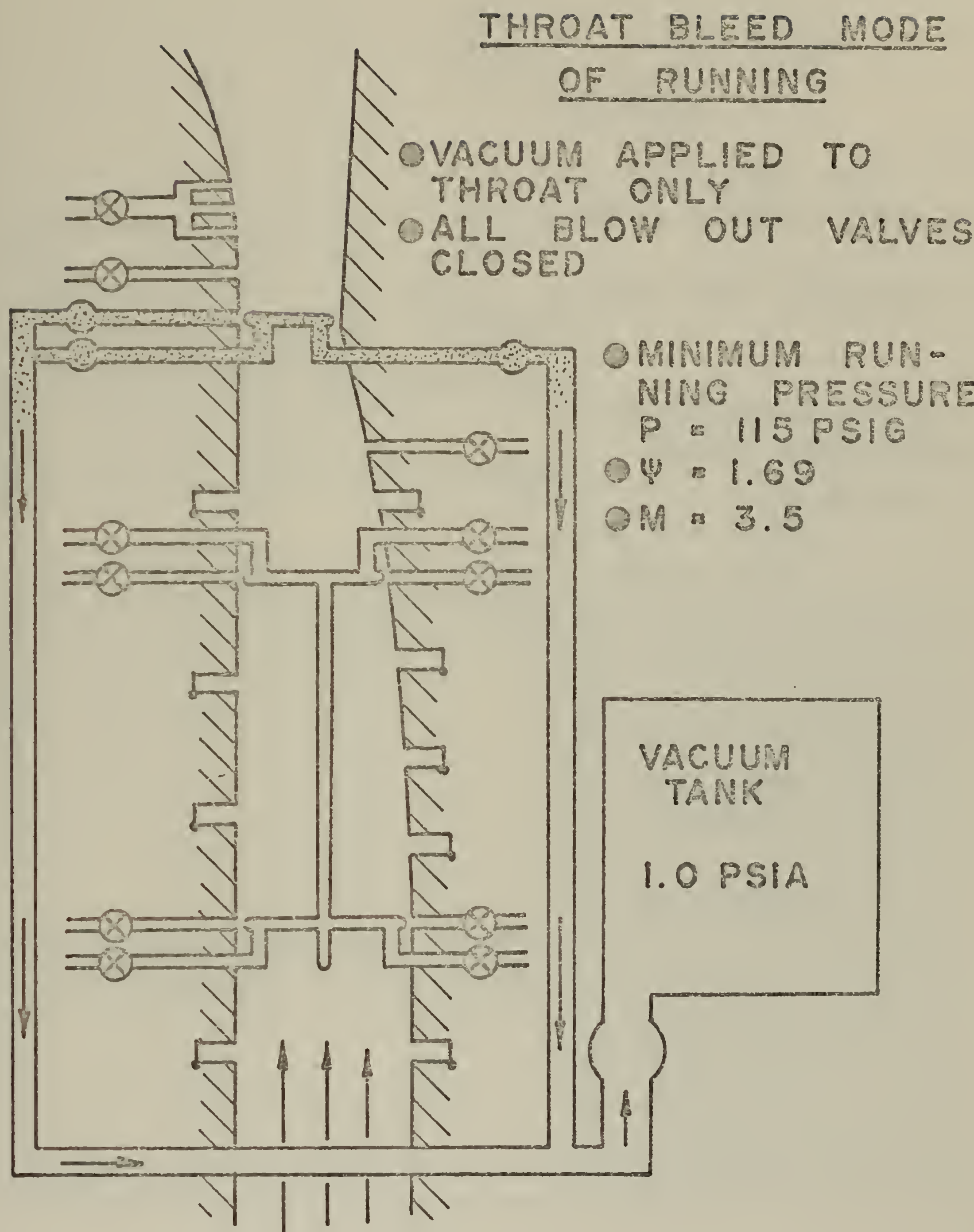

FIGURE (44) EXPERIMENTAL DATA - THROAT BLEED MODE OF RUNNING, $\psi = 1.69$

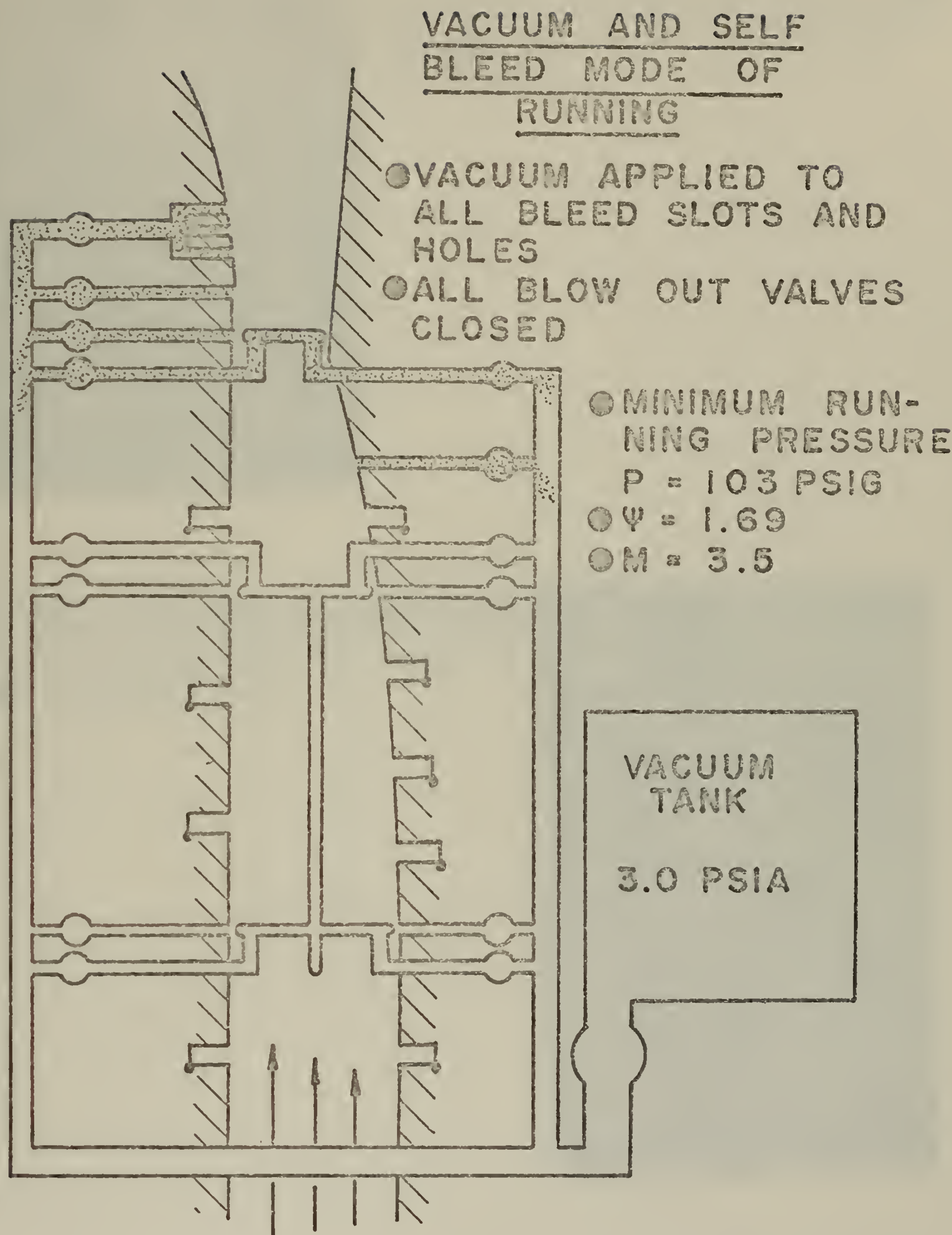

FIGURE (45) EXPERIMENTAL DATA - VACUUM AND SELF BLEED MODE OF RUNNING, $\psi = 1.69$

SCHLIEREN PHOTOGRAPH OF THROAT BLEED MODE OF RUNNING AT MINIMUM RUNNING PRESSURE, 115 PSIG, AS SHOWN IN FIGURE (41).

SCHLIEREN PHOTOGRAPH OF VACUUM AND SELF BLEED MODE OF RUNNING AT MINIMUM RUNNING PRESSURE, 103 PSIG, AS SHOWN IN FIGURE (42).

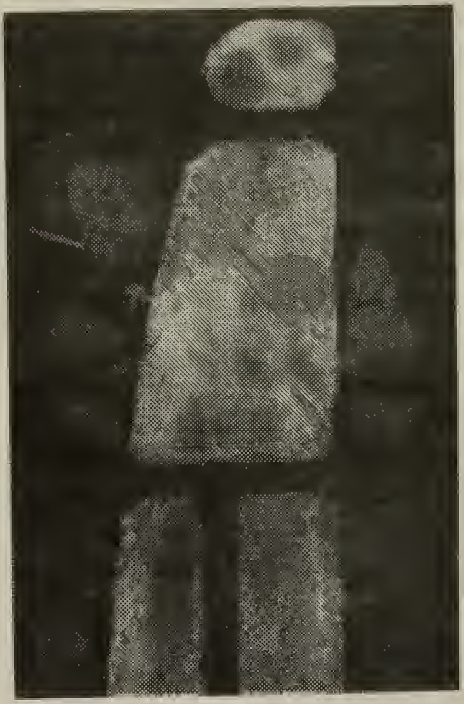

FIGURE (46) SCHLIEREN PHOTOGRAPHS OF FLOW, $\psi = 1.69$

in a lecture at the Tri Service Chemical Laser Symposium at the Air Force Weapons Laboratory, Albuquerque, New Mexico, 17 to 20 February, 1976. Figure (47) is a slide from this lecture which summarizes these results. The self bleed mode of operation is the most significant bleed configuration because it lowers the running stagnation pressure without the use of bulky or energy consuming external vacuum tanks or pumps.

B. CONCLUSIONS AND RECOMMENDATIONS

The low static pressure conditions at the entrance region of a supersonic diffuser can be used via suitable external ducting to bleed the boundary layer from the higher static pressure throat region of a diffuser. This is called self bleed. This method, which does not use vacuum tanks or pumps, lowered the minimum operating stagnation pressure 17% below that of a fixed geometry diffuser during the diffusion of Mach 3.5 flow. The minimum operating stagnation pressure was reduced 21.2% by using a vacuum tank and pump to bleed the boundary layer in the throat region of the diffuser. Utilizing both self bleed and vacuum-assisted boundary layer bleed throughout all regions of the diffuser reduced the minimum operating stagnation pressure by 28.5%.

Vacuum-assisted boundary layer bleed and the use of self-actuating, one-way valves in the diffuser walls to bleed excess flow during starting, i.e. establishment of supersonic flow, of the diffuser lowered the required

RESULTS

SOURCE PRESSURE PSIA	PERCENT REDUCTION	MODE OF OPERATION
165	BASELINE	RUNNING
170	-3.0%	STARTING
137	17.0%	SELF BLEED
130	21.2%	THROAT BLEED
118	28.5%	VACUUM AND SELF BLEED

FIGURE (47) EXPERIMENTAL RESULTS, $\psi = 1.69$

starting stagnation pressure of a fixed geometry diffuser. The maximum contraction ratio of the diffuser that could be started with these methods was found to be 1.69. This geometry, which diffused Mach 3.5 flow, could not otherwise be started.

The following recommendations are made for further research on this subject:

1. Conduct experiments to further quantify the parameters affecting the self bleed mode of diffuser operation, i.e. amount of bleed versus effectiveness in lowering running pressure.
2. Determine self bleed effectiveness on the operation of higher Mach number diffusers.
3. Apply self bleed technology to existing supersonic diffusers on wind tunnels and high energy lasers.

APPENDIX A

MACHINE DRAWINGS USED TO CONSTRUCT DIFFUSER COMPONENTS

DRAWING NUMBER	TITLE
1	NOZZLE HOLDER COMPONENTS
2	NOZZLE HOLDER
3	NOZZLE HOLDER TAB
4	BASE PLATE
5	BASE PLATE ASSEMBLY
6	DIFFUSER BASE PLATE
7	DIFFUSER FACE PLATE
8	DIFFUSER BACK PLATE
9	DIFFUSER ASSEMBLY
10	HALF NOZZLE BILLET
11	CENTER NOZZLE BILLET
12	HALF NOZZLE
13	CENTER NOZZLE
14	SPACER RING
15	DIFFUSER BLOCK BILLET
16	DIFFUSER BLOCKS
17	DRILL TEMPLATE
18	VACUUM MANIFOLD
19	SUPERSONIC DIFFUSER

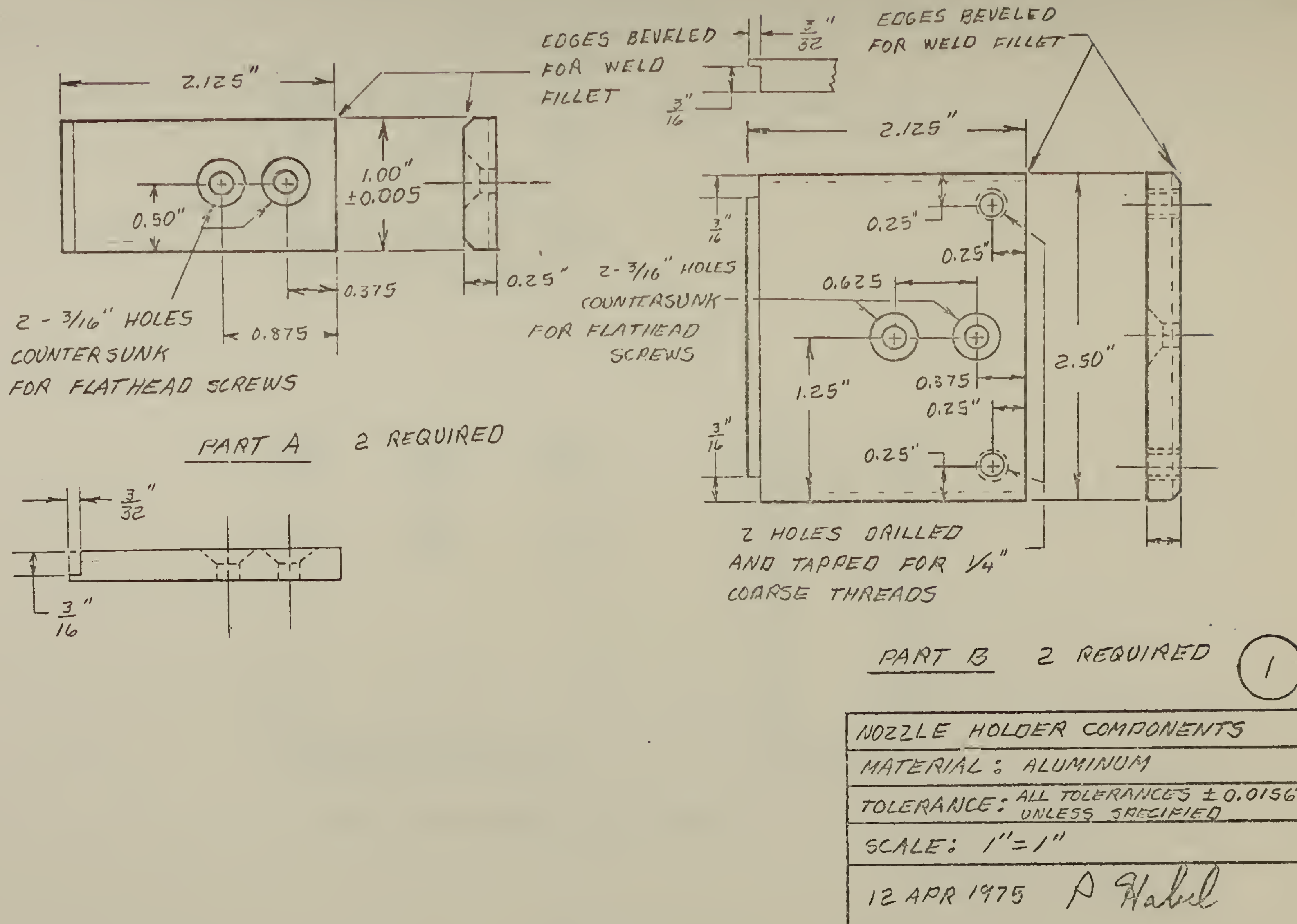

2.125"
EDGES BEVELED FOR WELD FILLET
1.00" ±0.005
0.50"
0.375
0.25"
0.875
2 - 3/16" HOLES COUNTERSUNK FOR FLATHEAD SCREWS
PART A 2 REQUIRED
3/32"
3/16"
EDGES BEVELED FOR WELD FILLET
2.125"
0.25"
0.25"
2-3/16" HOLES COUNTERSUNK FOR FLATHEAD SCREWS
0.625
1.25"
0.375
0.25"
0.25"
2.50"
2 HOLES DRILLED AND TAPPED FOR 1/4" COARSE THREADS
PART B 2 REQUIRED
1
NOZZLE HOLDER COMPONENTS
MATERIAL : ALUMINUM
TOLERANCE: ALL TOLERANCES ±0.0156" UNLESS SPECIFIED
SCALE: 1"=1"
12 APR 1975

DRAWING (1)

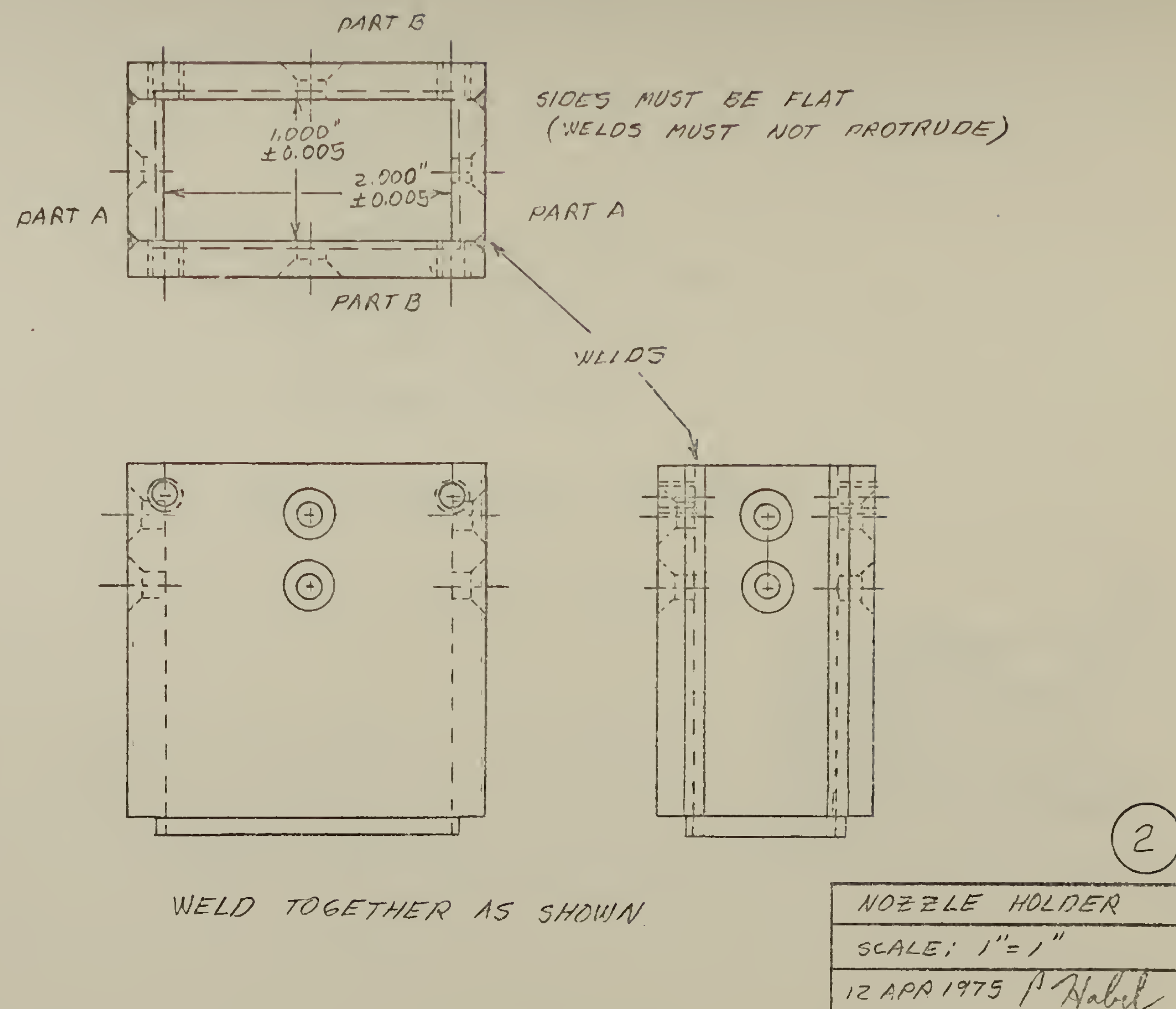

PART B
SIDES MUST BE FLAT
(WELDS MUST NOT PROTRUDE)
1.000" ±0.005
2.000" ±0.005
PART A
PART A
PART B
WELDS
WELD TOGETHER AS SHOWN
2
NOZZLE HOLDER
SCALE: 1"=1"
12 APR 1975

DRAWING (2)

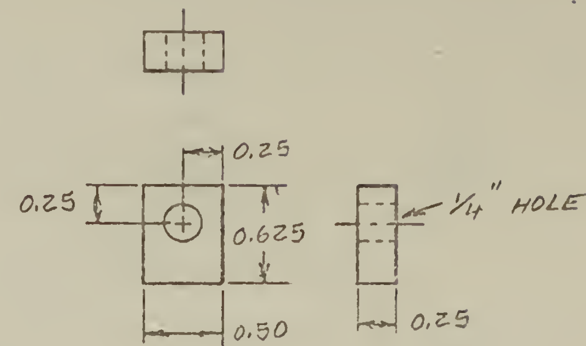

NOZZLE HOLDER TAB 4 REQUIRED

(3)

NOZZLE HOLDER TAB
MATERIAL: ALUMINUM
TOLERANCE: ± 0.0156
12 APR 1975 P Habel

DRAWING (3)

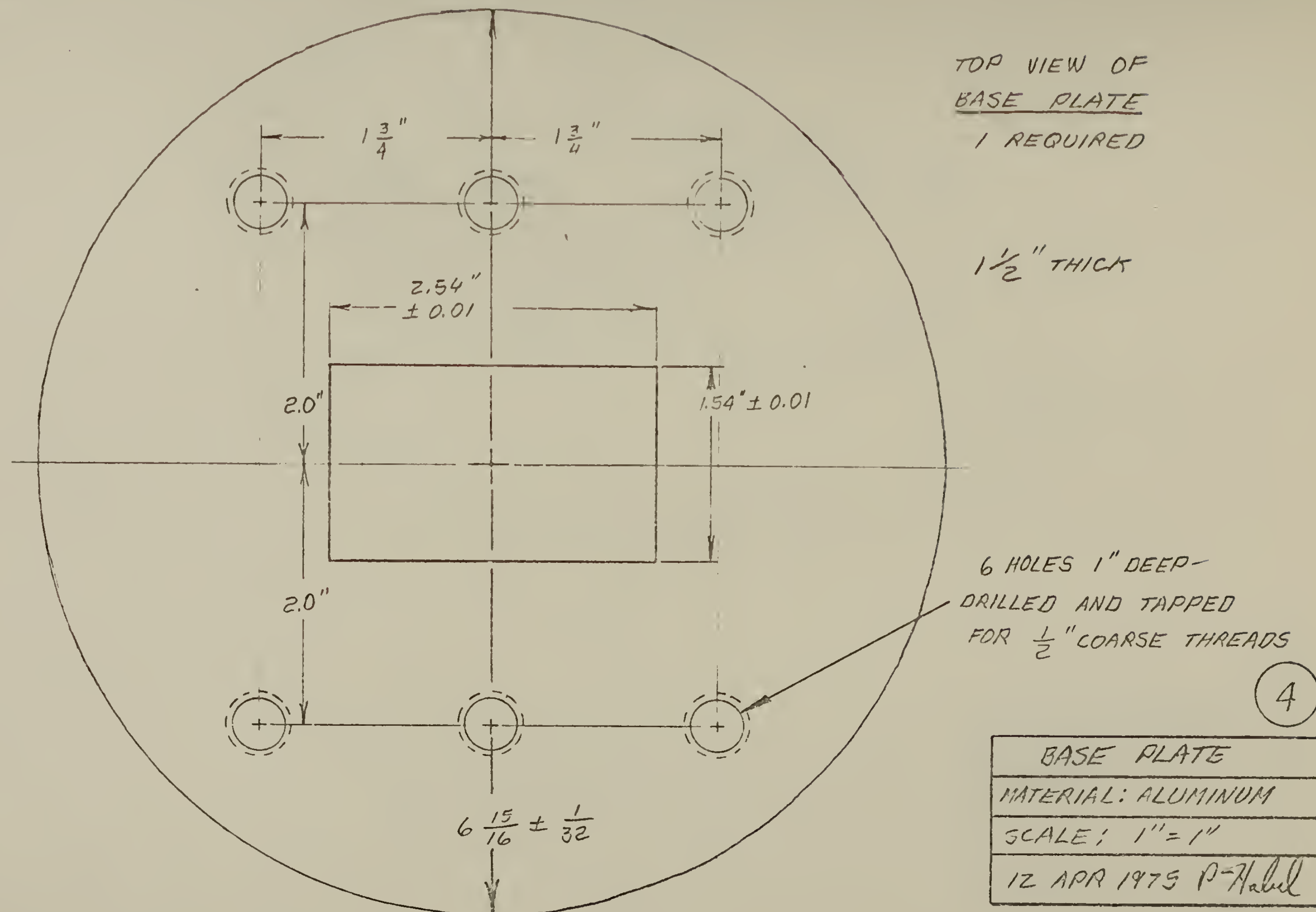
TOP VIEW OF
BASE PLATE
1 REQUIRED
1½" THICK
1 3/4"
1 3/4"
2.54" ± 0.01
1.54" ± 0.01
2.0"
2.0"
6 15/16 ± 1/32
6 HOLES 1" DEEP-
DRILLED AND TAPPED
FOR 1/2" COARSE THREADS
4
BASE PLATE
MATERIAL: ALUMINUM
SCALE: 1" = 1"
12 APR 1975

DRAWING (4)

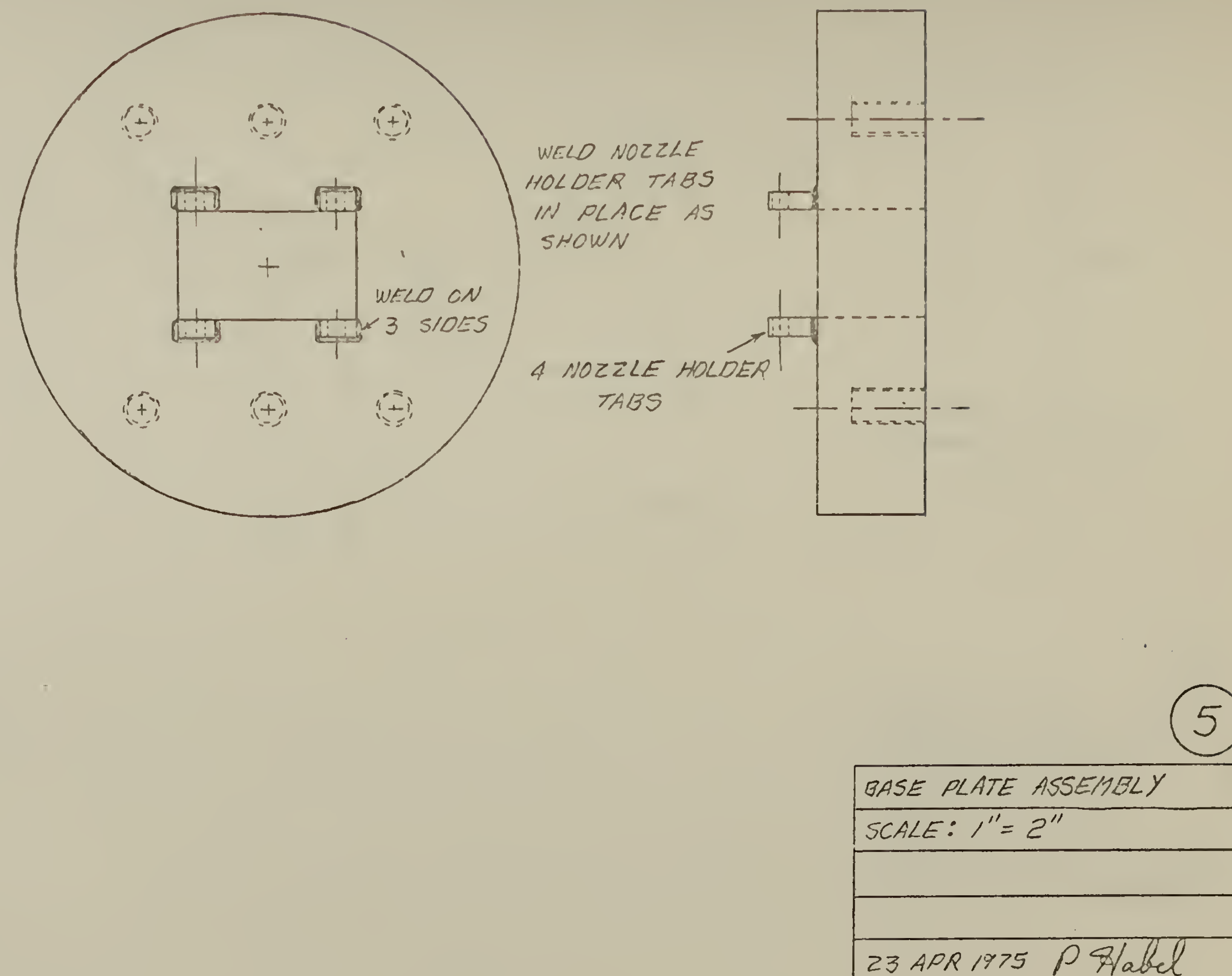
WELD NOZZLE HOLDER TABS IN PLACE AS SHOWN
WELD ON 3 SIDES
4 NOZZLE HOLDER TABS
5
BASE PLATE ASSEMBLY
SCALE: 1" = 2"
23 APR 1975 P Habel

DRAWING (5)

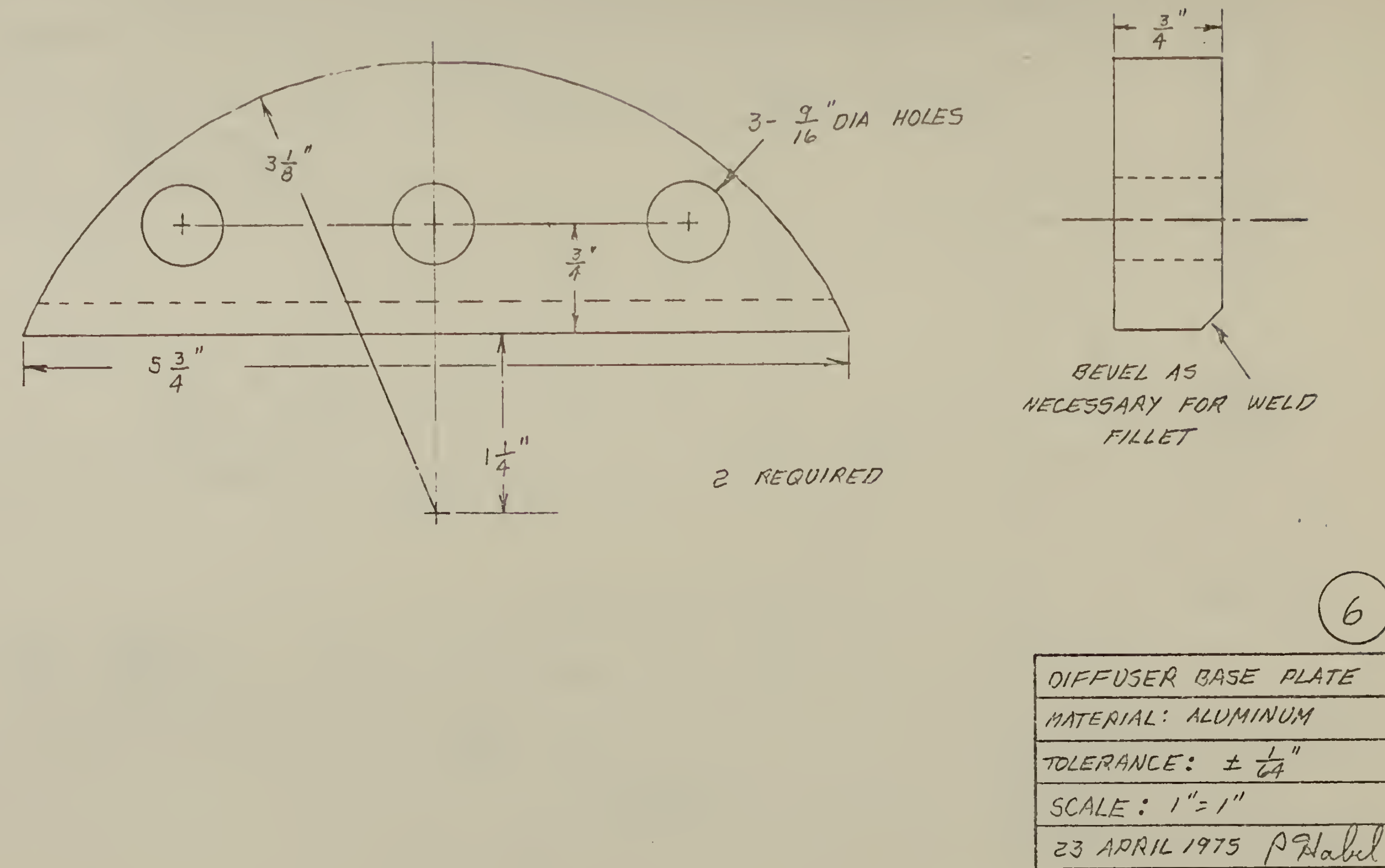
3- 9/16" DIA HOLES
3 1/8"
3/4"
5 3/4"
1 1/4"
2 REQUIRED
3/4"
BEVEL AS
NECESSARY FOR WELD
FILLET
6
DIFFUSER BASE PLATE
MATERIAL: ALUMINUM
TOLERANCE: ± 1/64"
SCALE: 1" = 1"
23 APRIL 1975

DRAWING (6)

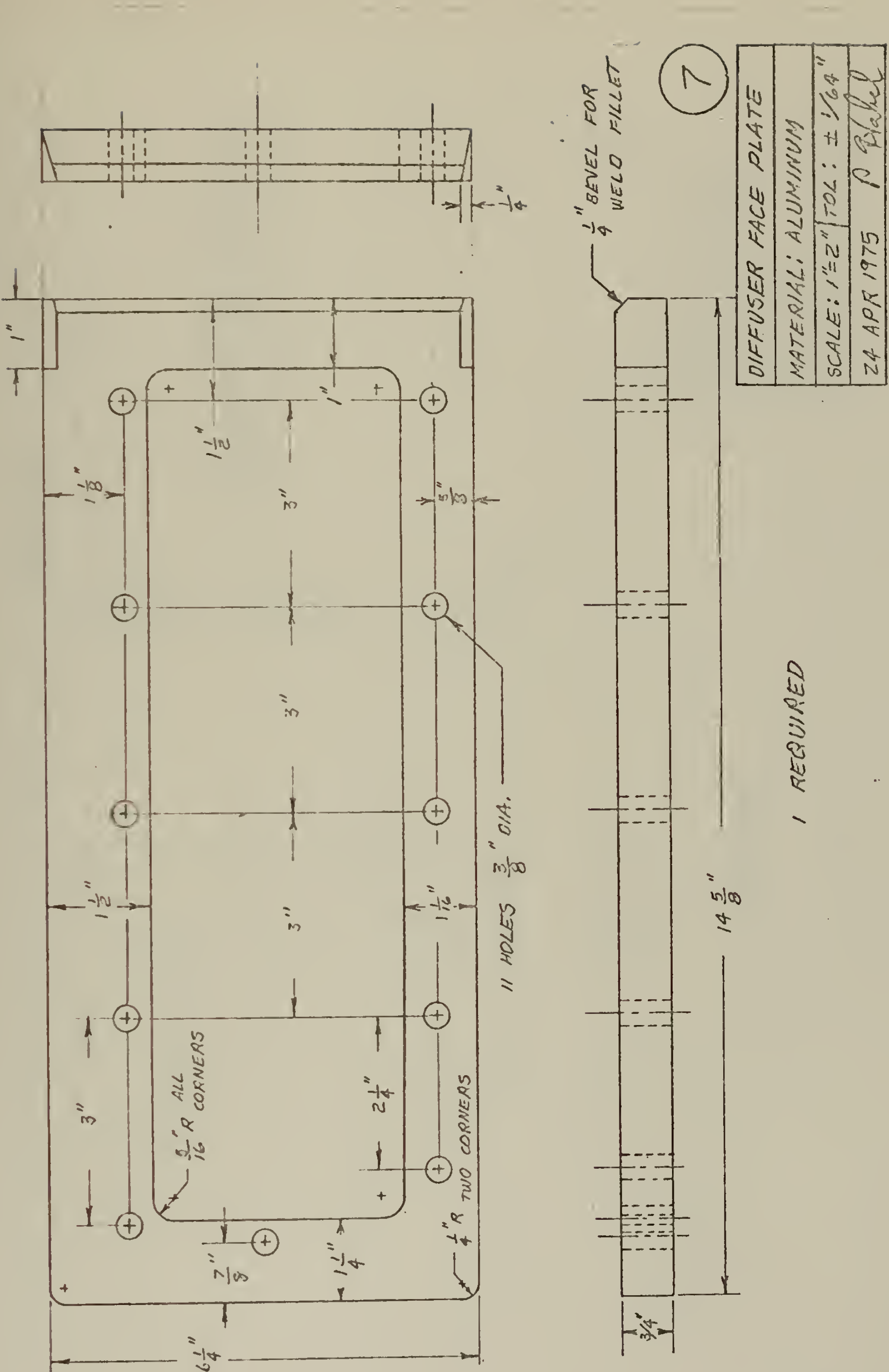
DIFFUSER FACE PLATE
MATERIAL: ALUMINUM
SCALE: 1"=2"
TOL: ± 1/64"
24 APR 1975
1 REQUIRED
11 HOLES 3/8" DIA.
1/4" BEVEL FOR WELD FILLET
TWO CORNERS
ALL CORNERS

DRAWING (7)

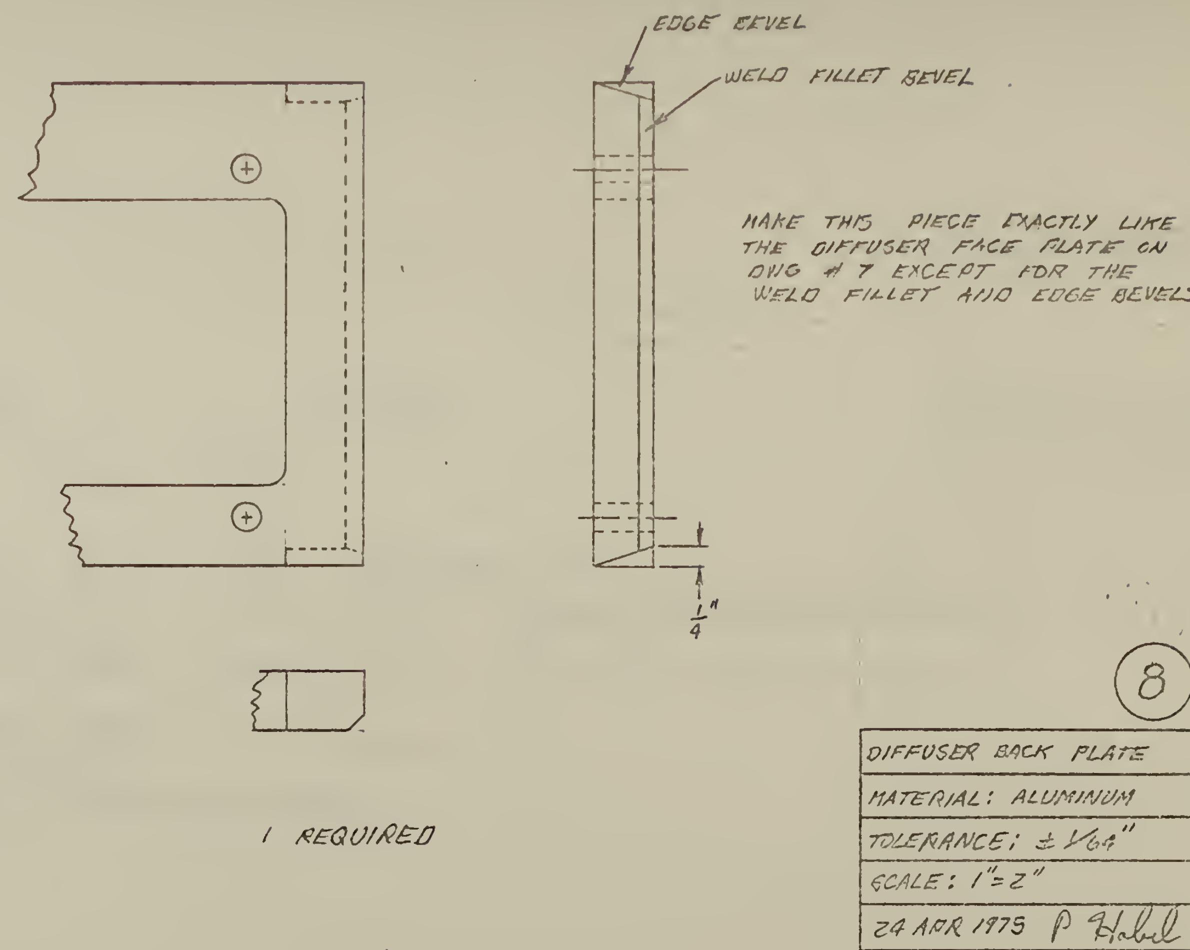
EDGE BEVEL
WELD FILLET BEVEL
MAKE THIS PIECE EXACTLY LIKE THE DIFFUSER FACE PLATE ON DWG # 7 EXCEPT FOR THE WELD FILLET AND EDGE BEVELS
1/4"
1 REQUIRED
8
DIFFUSER BACK PLATE
MATERIAL: ALUMINUM
TOLERANCE: ± 1/64"
SCALE: 1" = 2"
24 APR 1975

DRAWING (8)

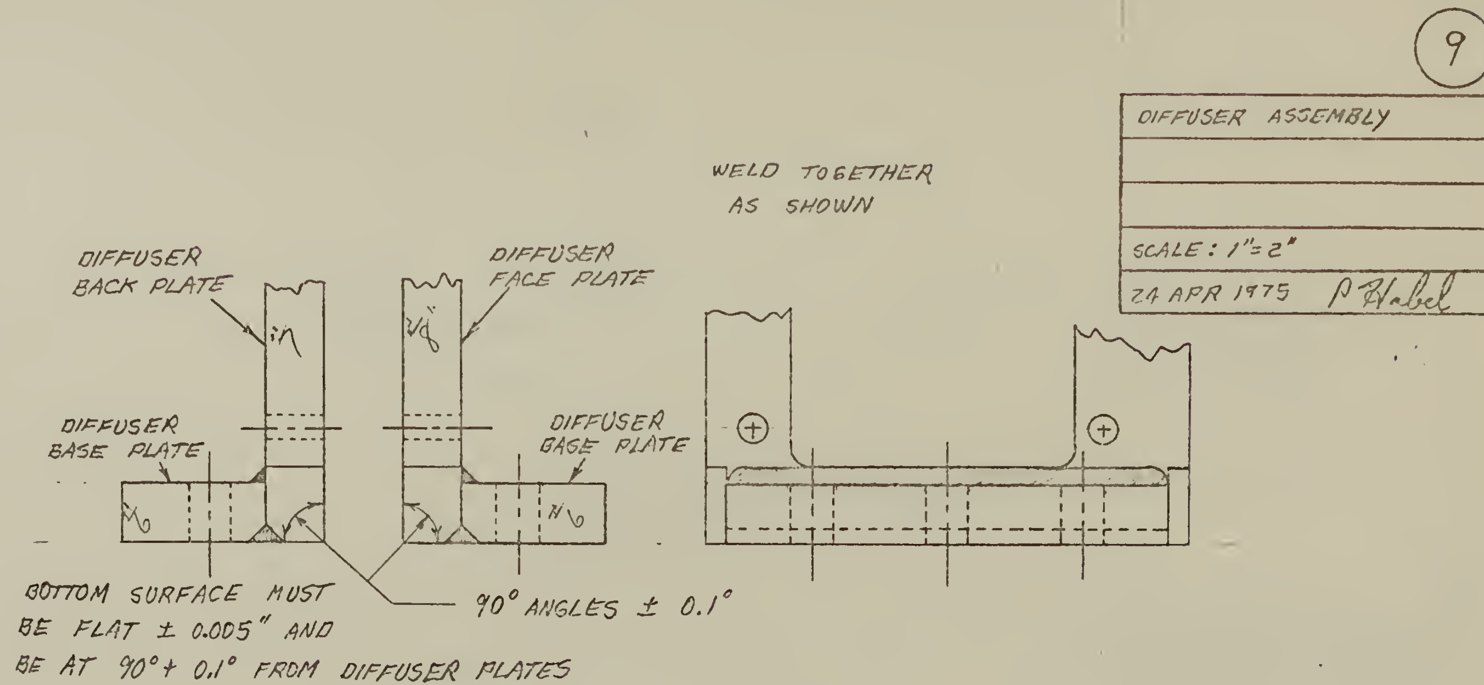

DIFFUSER ASSEMBLY
SCALE: 1" = 2"
24 APR 1975
9
WELD TOGETHER AS SHOWN
DIFFUSER BACK PLATE
DIFFUSER FACE PLATE
DIFFUSER BASE PLATE
DIFFUSER BASE PLATE
BOTTOM SURFACE MUST BE FLAT ± 0.005" AND BE AT 90° + 0.1° FROM DIFFUSER PLATES
90° ANGLES ± 0.1°

DRAWING (9)

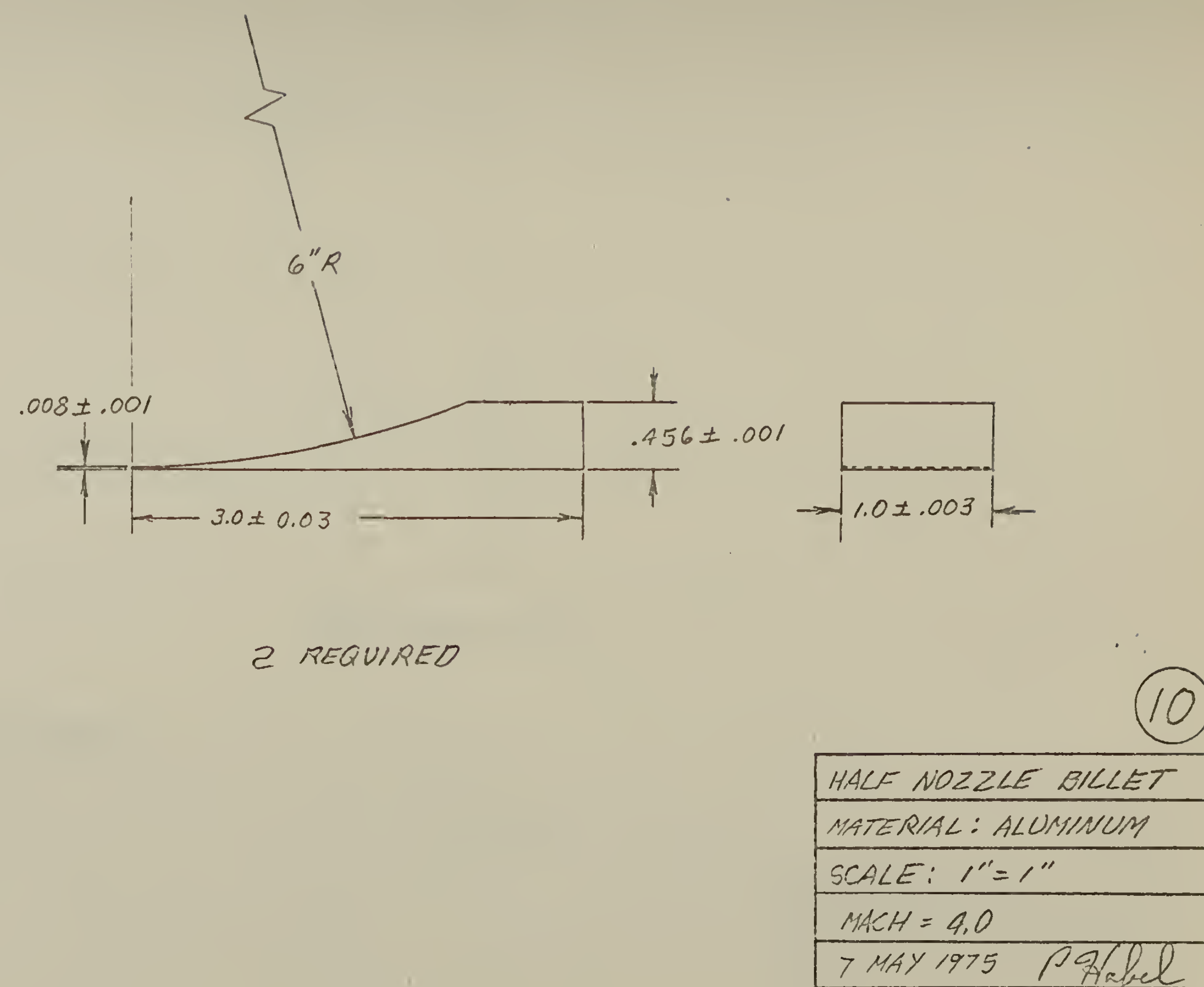
6"R
.008 ± .001
.456 ± .001
3.0 ± 0.03
1.0 ± .003
2 REQUIRED
10
HALF NOZZLE BILLET
MATERIAL : ALUMINUM
SCALE: 1" = 1"
MACH = 4.0
7 MAY 1975

DRAWING (10)

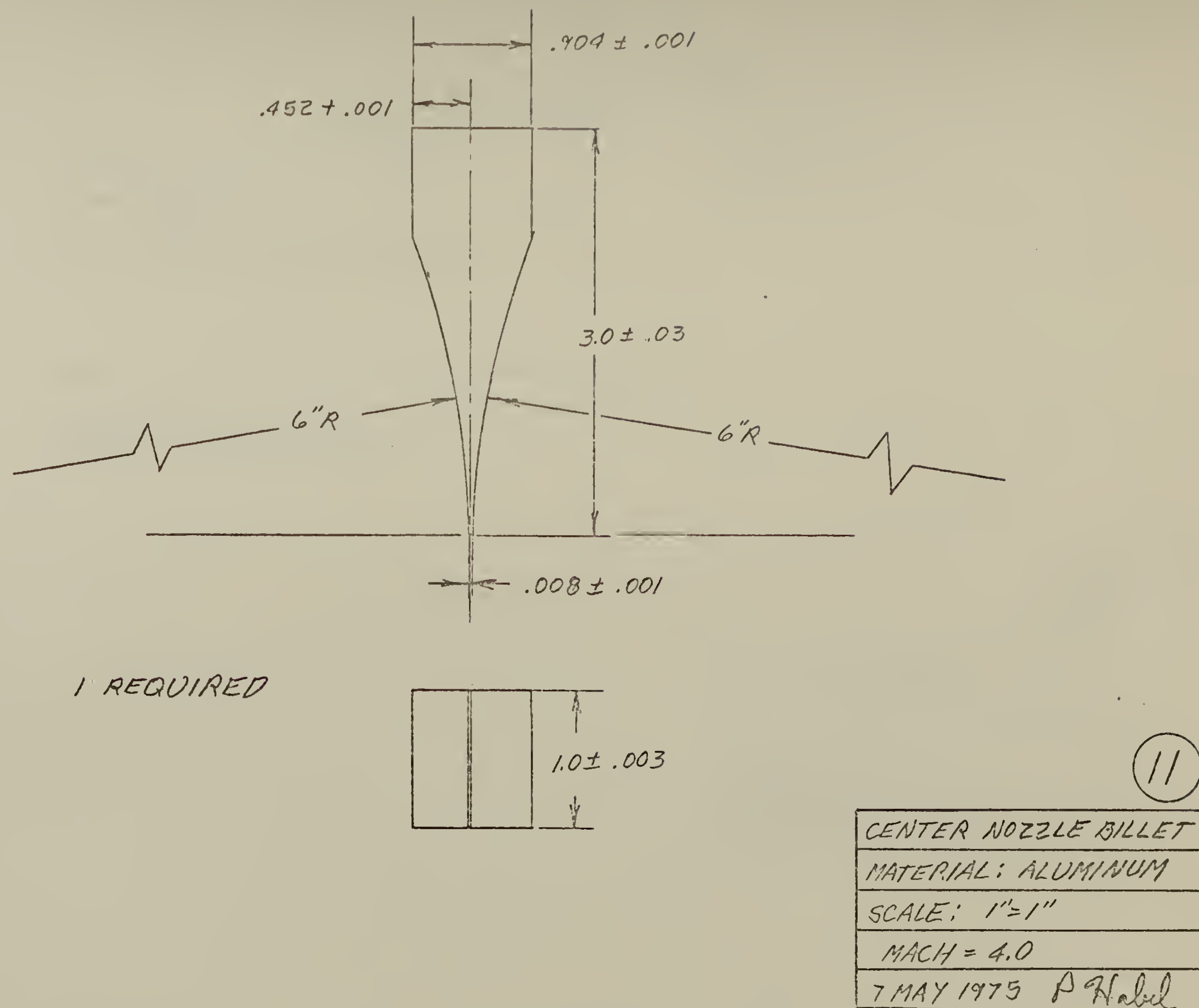
.704 ± .001
.452 + .001
3.0 ± .03
6"R
6"R
.008 ± .001
1 REQUIRED
1.0 ± .003
11
CENTER NOZZLE BILLET
MATERIAL: ALUMINUM
SCALE: 1"=1"
MACH = 4.0
7 MAY 1975

DRAWING (11)

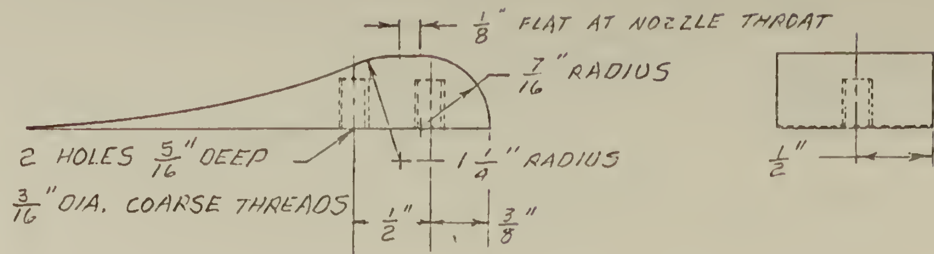

MAKE 2 FROM THE 2 HALF NOZZLE BILLETS ON DRAWING 10 ; ALL BUT FLAT SURFACES REQUIRE POLISHED FINISH

(12)

HALF NOZZLE
SCALE : 1" = 1"
TOLERANCE : ± 1/64"
19 MAY 1975 R Habel

DRAWING (12)

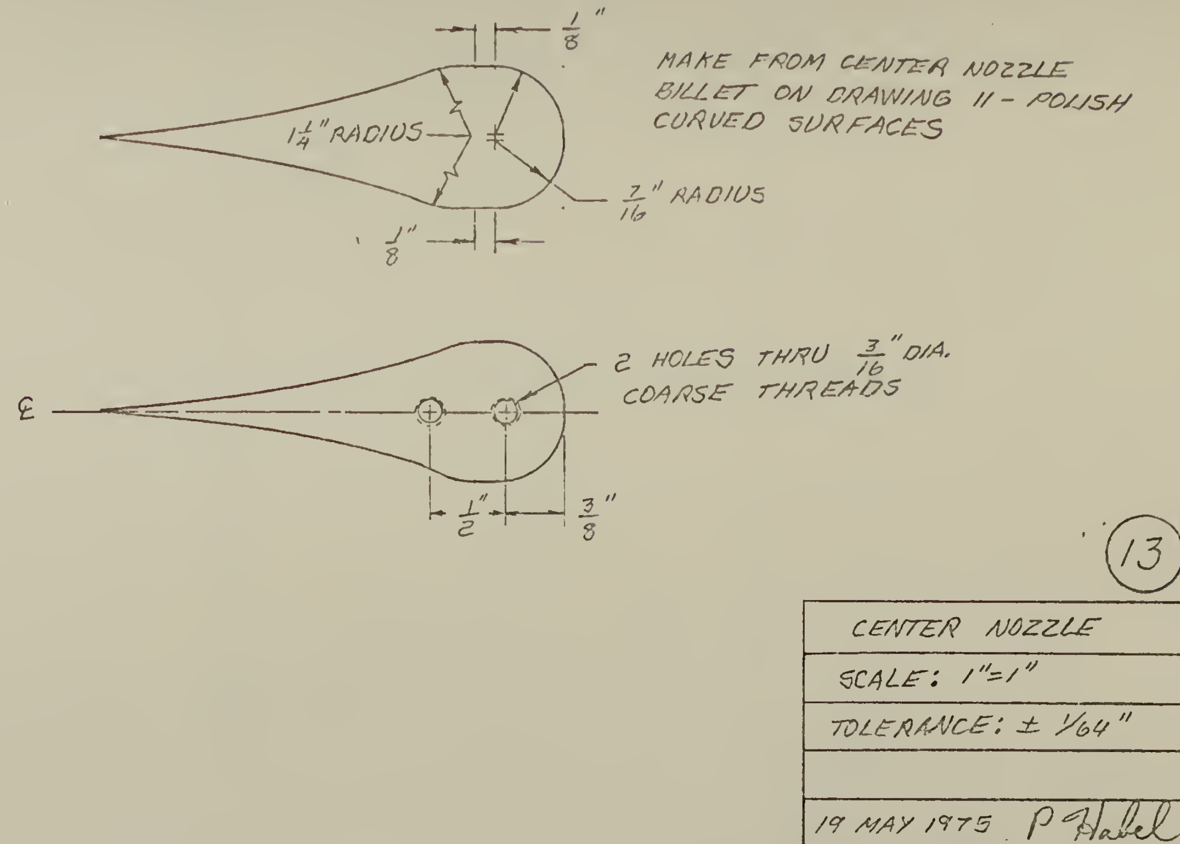

1/8"
MAKE FROM CENTER NOZZLE BILLET ON DRAWING 11 - POLISH CURVED SURFACES
1 1/4" RADIUS
7/16" RADIUS
1/8"
2 HOLES THRU 3/16" DIA. COARSE THREADS
1/2"
3/8"
13
CENTER NOZZLE
SCALE: 1"=1"
TOLERANCE: ± 1/64"
19 MAY 1975

DRAWING (13)

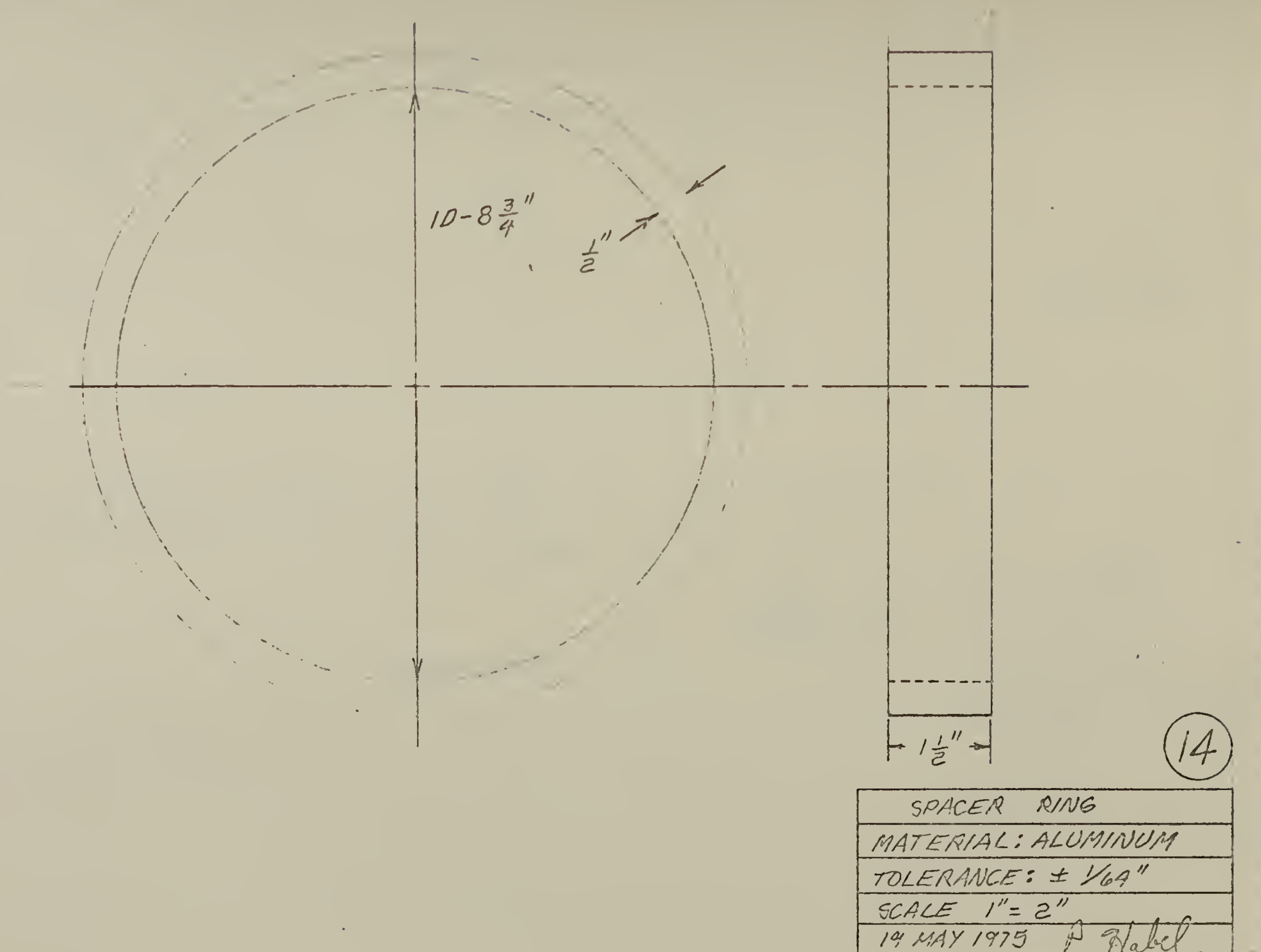
ID-8 3/4"
1/2"
1 1/2"
14
SPACER RING
MATERIAL: ALUMINUM
TOLERANCE: ± 1/64"
SCALE 1" = 2"
14 MAY 1975

DRAWING (14)

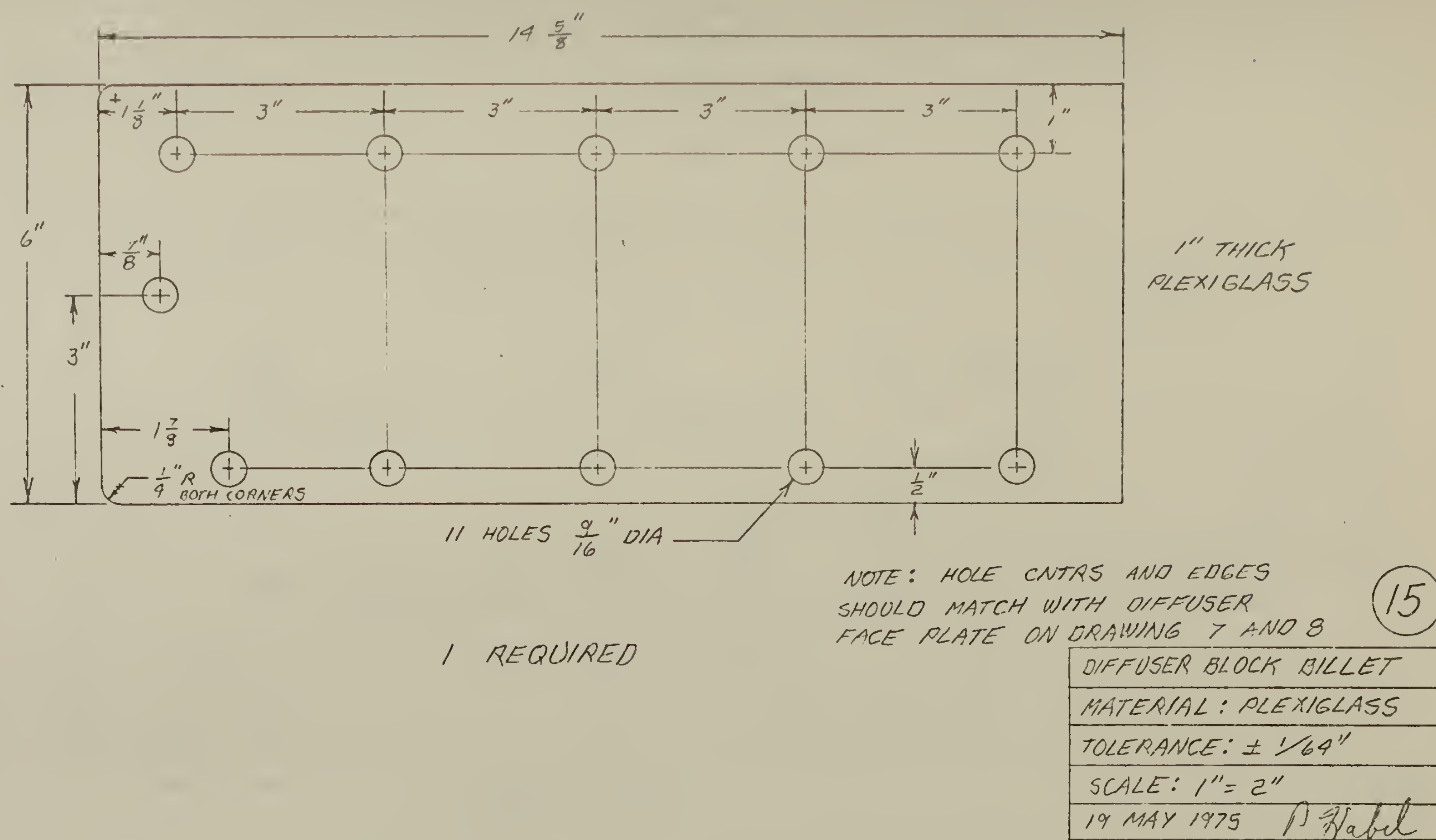
14 5/8"
1 1/8"
3"
3"
3"
3"
1"
6"
7/8"
3"
1 7/8
1/4"R BOTH CORNERS
1/2"
1" THICK PLEXIGLASS
11 HOLES 9/16" DIA
NOTE: HOLE CNTRS AND EDGES SHOULD MATCH WITH DIFFUSER FACE PLATE ON DRAWING 7 AND 8
1 REQUIRED
15
DIFFUSER BLOCK BILLET
MATERIAL: PLEXIGLASS
TOLERANCE: ± 1/64"
SCALE: 1" = 2"
19 MAY 1975

DRAWING (15)

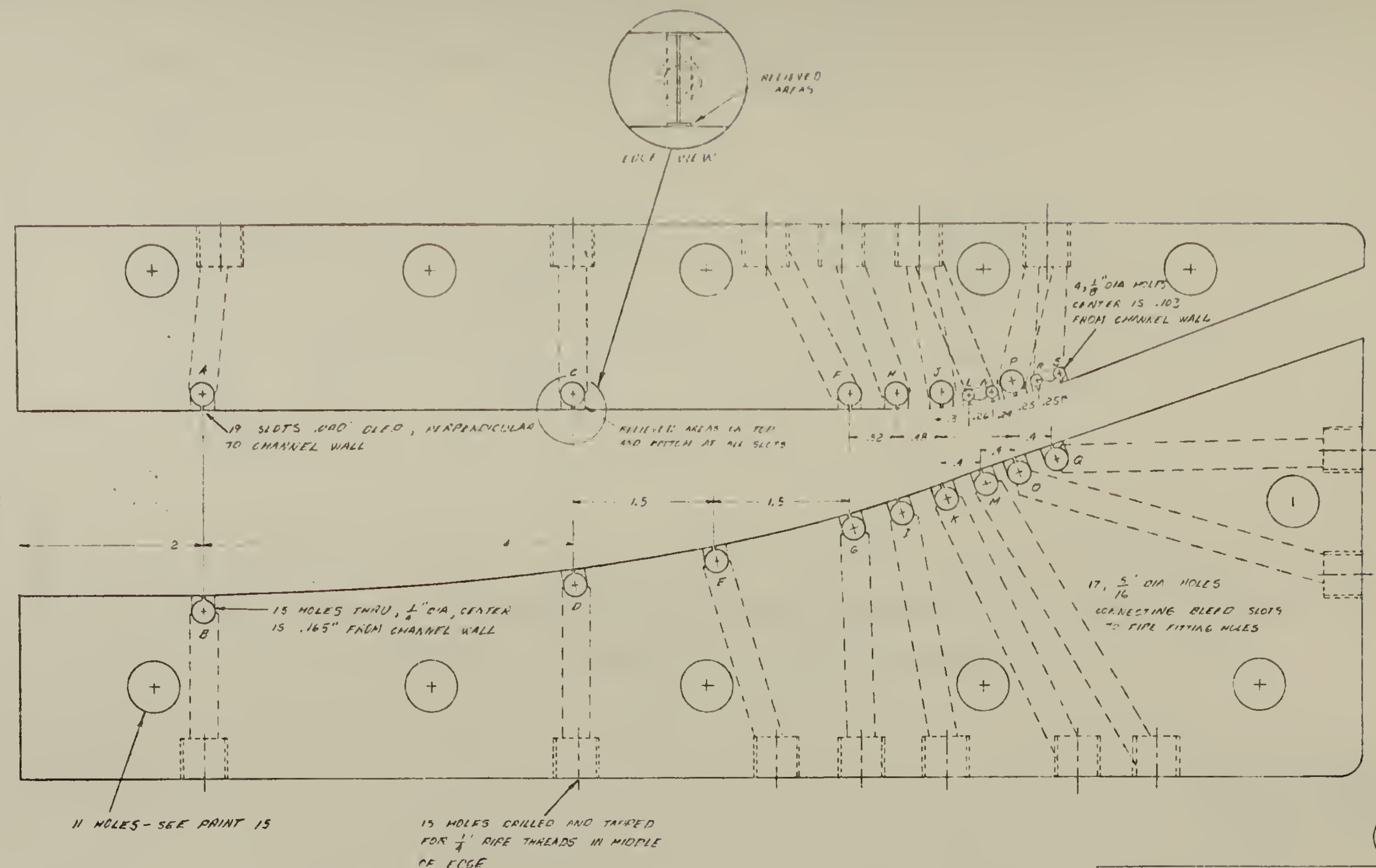

SLOT LOCATION	A	B	C	D	E	F	G	H	I	J	K	L	M	N	O	P	Q	R	S
WIDTH OF SLOT	.04	.04	.03	.04	.04	.03	.04	.02 →											.02
DEPT OF RELIEVED AREA	.04	.04	.04	.04	.04	.04	.04	.02 →											.02

(16)

DIFFUSER BLOCKS
MATERIAL: PLEXIGLASS
TOLERANCE: ——
SCALE: 1" = 1"
13 JUN 1975

DRAWING (16)

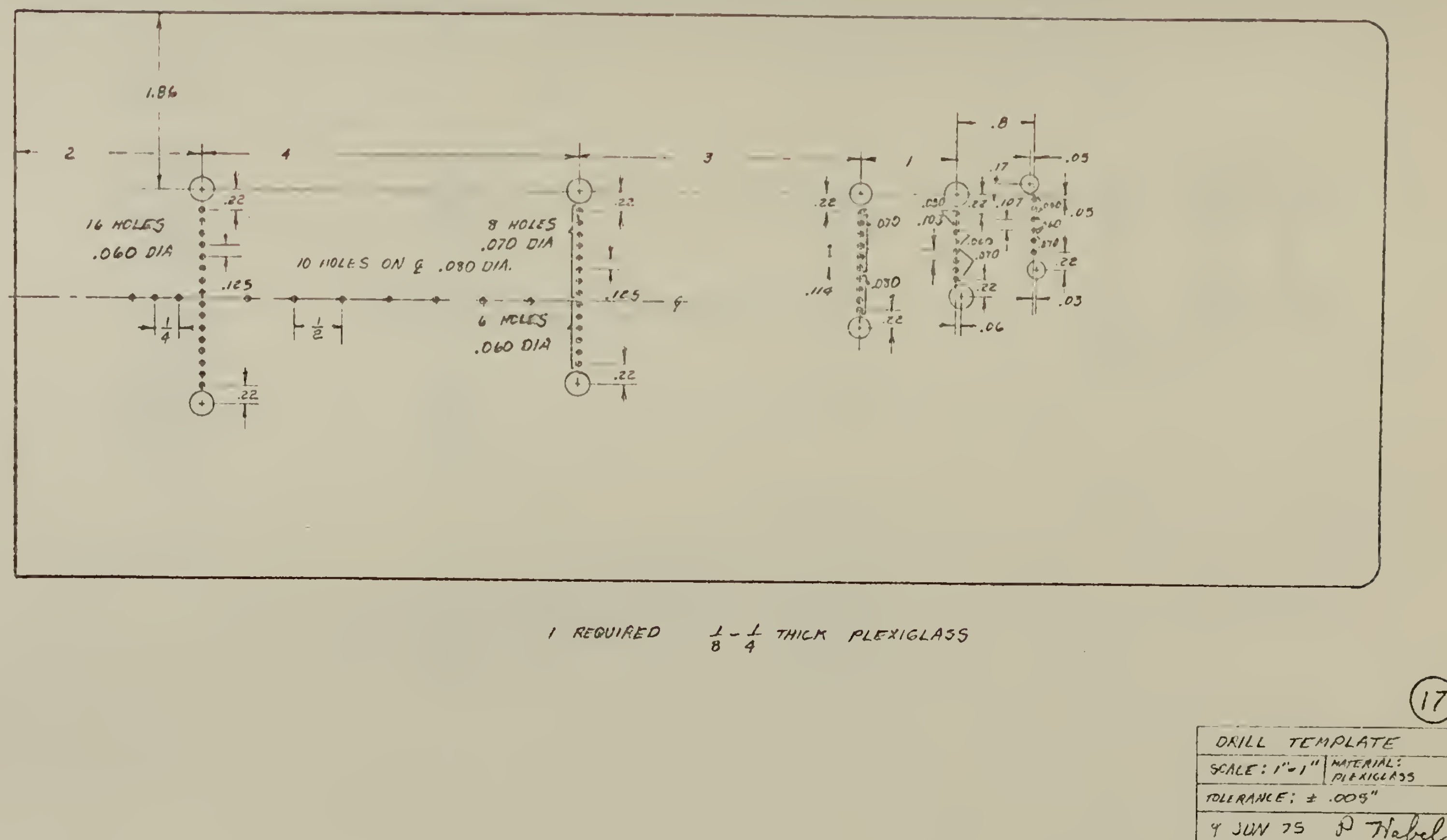

1.86
2
4
3
1
.8
16 HOLES
.060 DIA
10 HOLES ON ℄ .080 DIA.
8 HOLES
.070 DIA
6 HOLES
.060 DIA
.125
.22
.114
.030
.070
.17
.107
.05
.03
.06
1 REQUIRED 1/8 - 1/4 THICK PLEXIGLASS
17
DRILL TEMPLATE
SCALE: 1"=1"
MATERIAL: PLEXIGLASS
TOLERANCE: ± .005"
4 JUN 75

DRAWING (17)

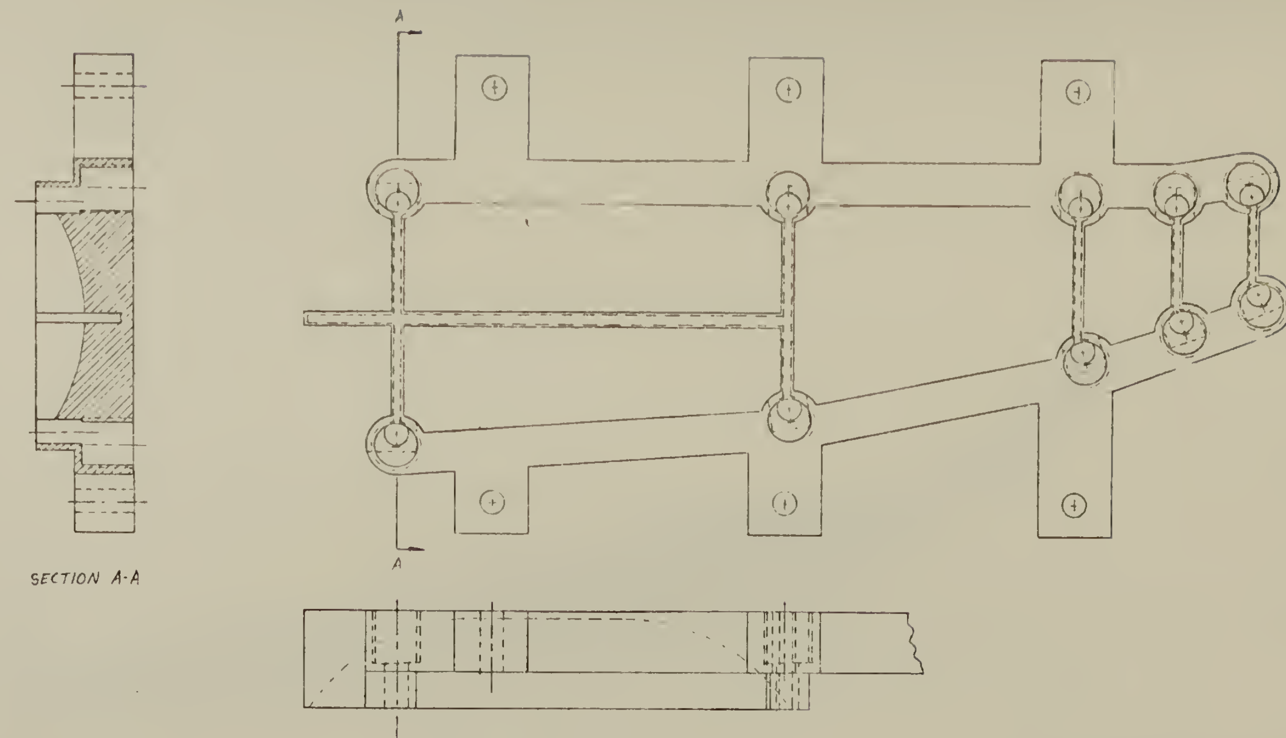

DRAWING (18) VACUUM MANIFOLD FOR WINDOWS

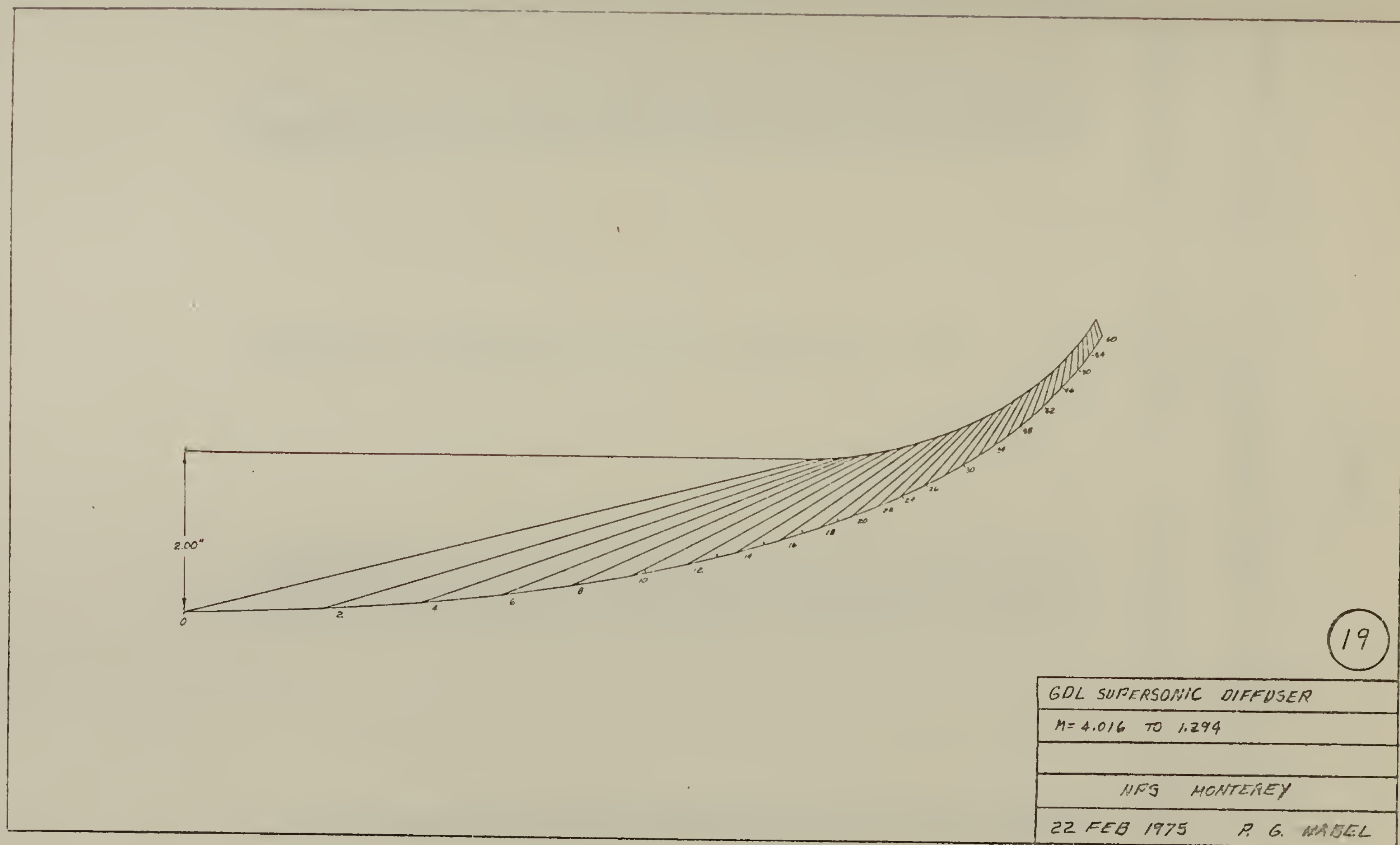
2.00"
GDL SUPERSONIC DIFFUSER
M= 4.016 TO 1.294
NPS MONTEREY
22 FEB 1975 P. G. NABEL
19

DRAWING (19)

APPENDIX B

CHARACTERISTIC FUNCTIONS FOR TWO-DIMENSIONAL, ISENTROPIC, SUPERSONIC FLOW, K = 1.4

MACH NUMBER M	TOTAL TURN ANGLE θ	WAVE ANGLE μ	PRANDTL-MEYER FUNCTION ν
4.016	0	14.417	66
3.868	2	14.983	64
3.728	4	15.561	62
3.594	6	16.155	60
3.467	8	16.765	58
3.346	10	17.391	56
3.258	12	17.873	54
3.119	14	18.701	52
3.013	16	19.386	50
2.910	18	20.096	48
2.812	20	20.830	46
2.718	22	21.591	44
2.626	24	22.382	42
2.538	26	23.206	40
2.452	28	24.066	38
2.369	30	24.965	36
2.289	32	25.908	34
2.210	34	26.899	32
2.134	36	27.945	30
2.059	38	29.052	28
1.986	40	30.229	26
1.915	42	31.486	24
1.844	44	32.834	22
1.775	46	34.290	20
1.706	48	35.874	18
1.639	50	37.611	16
1.571	52	39.537	14
1.503	54	41.701	12
1.435	56	44.177	10
1.366	58	47.082	8
1.294	60	50.619	6

APPENDIX C

LISTING OF BOUNDARY LAYER BLEED COMPUTER PROGRAM

```
10 [illegible]
20 PRINT [illegible]
30 PRINT [illegible]
40 PRINT [illegible]
50 INPUT M5
60 PRINT "M5=";M5
70 C1=[illegible]
80 [illegible]
90 N5=PI/(2*A)
100 D=N5*C1*X*SQR(1/V)
110 PRINT "N5=";N5;" D=";D
120 Q7=P1/P2
130 PRINT "PRESSURE RATIO =";Q7
140 G1=(G-1)/G
150 Q6=Q7↑G1
160 G2=2/(G-1)
170 G3=1/G2
180 G4=(G+1)/(2*(G-1))
190 PRINT "C1=";C1;"C2=";C2 [illegible]
200 DIM N[6],B[6],Y[5],U[5] [illegible]
210 FOR I=1 TO 5
220 N[I]=0.2*I*N5
230 B[I]=N[I]*X*SQR(1/V)
240 Y[I]=2[I]*C1*(C2*B[I]+[illegible])/N[I]
250 U[I]=SIN(A*N[I])
260 NEXT I
270 PRINT "N4=";N[4];"B4=";B[4];"Y4=";Y[4];"U4=";U[4]
280 PRINT "Y1=";Y[1];"Y2=";Y[2];"Y3=";Y[3];"Y4=";Y[4];"Y5=";Y[5]
```

LISTING OF BOUNDARY LAYER BLEED PROGRAM (Continued)

```
290 W[1]=0.5*U[1]
300 W[2]=0.5*(U[1]+U[2])
310 W[ ]=0.5*(U[ ]+U[ ])
320 W[3]=0.5*(U[2]+U[3])
330 W[4]=0.5*(U[3]+U[4])
340 W[5]=0.5*(U[4]+U[5])
350 J[1]=Y[1]
360 J[2]=Y[2]-Y[1]
370 J[3]=Y[3]-Y[2]
380 J[4]=Y[4]-Y[3]
390 J[5]=Y[5]-Y[4]
400 FOR I=1 TO 5
410 M[I]=SQR((W[I]^[illegible]
420 R[I]=G*P1*(1+((G-1)/2)*(M[I]^[illegible]
430 F[I]=U8*R[I]*J[I]*W[I]
440 Z[I]=SQR(G2*((Q0^(1-G)[illegible]
450 S[I]=(1/G3*Z[I]^2)[illegible]
460 H[I]=[illegible]
470 NEXT I
480 H=H[1]+H[2]+H[3]+H[4]+H[5]
490 H6=12*H
500 H7=H/D
510 D[5]=Y[5]/D
520 F=F[1]+F[2]+F[3]+F[4]+F[5]
530 PRINT "W1=";W[1];"W2=";W[2];"W3=";W[3];"W4=";W[4];"W5=";W[5]
540 PRINT "D=";D;"J1=";J[1];"J2=";J[2];"J3=";J[3];"J4=";J[4];"J5=";J[5]
550 PRINT "D5=";D[5]
560 PRINT "M1=";M[1];"M2=";M[2];"M3=";M[3];"M4=";M[4];"M5=";M[5]
570 PRINT "R1=";R[1];"R2=";R[2];"R3=";R[3];"R4=";R[4];"R5=";R[5]
580 PRINT "F1=";F[1];"F2=";F[2];"F3=";F[3];"F4=";F[4];"F5=";F[5]
590 PRINT "Z1=";Z[1];"Z2=";Z[2];"Z3=";Z[3];"Z4=";Z[4];"Z5=";Z[5]
600 PRINT "MASS FLOW INTO BLEED HOLE IS";F;"SLUGS/SEC"
610 PRINT "H1=";H[1];"H2=";H[2];"H3=";H[3];"H4=";H[4];"H5=";H[5]
620 PRINT "PRESSURE RATIO IS";[illegible]"BLEED HOLE HEIGHT IS";H;"FEET OR";[illegible]
630 PRINT "RATIO OF BLEED HOLE HEIGHT TO BOUNDARY LAYER THICKNESS IS";H7
640 PRINT "FRACTION OF BOUNDARY [illegible] IS";D[5]
650 END
```

LIST OF REFERENCES

1. Shapiro, A. H., The Dynamics and Thermodynamics of Compressible Fluid Flow, v. 1, Ronald Press, 1953.

2. Christiansen, W. H., Hertzberg, A., and Russell, D. A., Gasdynamic Laser, Theory and Practice, lecture notes from AIAA short course, 1973.

3. Liepmann, A. H., and Roshko, A., Elements of Gasdynamics, John Wiley & Sons, 1957.

4. Donoghue, D. R., An Experimental Analysis of a Cylindrical Shock Wave for Use in a Cylindrical Gas Dynamic Laser, thesis done at Naval Postgraduate School, 1975.

5. Stewertson, K., The Theory of Laminar Boundary Layers in Compressible Fluids, Oxford at the Clarendon Press, 1972.

6. Vincenti, W. G., and Kruger, C. H., Introduction to Physical Gas Dynamics, John Wiley & Sons, 1965.

INITIAL DISTRIBUTION LIST

		No. Copies
1.	Defense Documentation Center Cameron Station Alexandria, Virginia 22314	2
2.	Library, Code 0212 Naval Postgraduate School Monterey, California 93940	2
3.	Dr. R. W. Bell Chairman, Department of Aeronautics Naval Postgraduate School Monterey, California 93940	1
4.	Dr. A. E. Fuhs Chairman, Department of Mechanical Engineering Naval Postgraduate School Monterey, California 93940	6
5.	Willaim Volz Code 320 Naval Air Systems Command Washington, D. C. 20360	1
6.	Ronald Dettling Naval Weapons Center China Lake, Ca. 93555	3
7.	Dr. Jim Ortwerth AFWL Kirkland AFB, N. M. 87117	1
8.	Captain Alfred Skolnik PMS-405 Naval Sea Systems Command Washington, D. C. 20360	1
9.	Mr. Richard Wasneski Code 350 Naval Air Systems Command Washington, D. C. 20360	1
10.	Dr. W. R. Warren Director, Aerodynamic and Propulsion Laboratory Aerospace Corporation Los Angeles, California 92045	1

11. Professor O. Biblarz 1
Department of Aeronautics
Naval Postgraduate School
Monterey, California 93940

12. Dr. George Sutton 1
AVCO Everett Research Laboratory
2385 Revere Beach Parkway
Everett, Massachusetts 02149

13. Dr. Edward A. Pinsley 1
Chief Laser Engineering
Pratt and Whitney Aircraft
P.O. Box 2691
West Palm Beach, Florida 33402

14. Mr. Earl C. Watson 1
Mail Stop 227-8
NASA Ames Research Center
Moffett Field, California 94035

15. Dr. Gary Ratekin 1
Advanced Programs
Rocketdyne Division
Rockwell International Corp.
Canoga Park Ave.
Canoga Park, California 91303

16. Lt. P. G. Habel 1
234 Tryon
Middletown, Connecticut 06457